Climate change and long-term fluctuations of commercial catches

The possibility of forecasting

FAO FISHERIES TECHNICAL PAPER

410

Food and Agriculture Organization of the United Nations

PREPARATION OF THIS DOCUMENT

This document presents the results of a study undertaken under contract to FAO by Professor Leonid B. Klyashtorin of the Federal Institute for Fisheries and Oceanography, Moscow, Russian Federation (e-mail: Klyashtorin@mtu-net.ru) . The study was inspired by discussions with FAO staff following a seminar given by Professor Klyashtorin in Rome in which he presented the results of previous work. Several people contributed to improvement of the document in various ways, including Dr Gary D. Sharp of the Center for Climate/Ocean Resources Study, Monterey, California, USA and Dr Paul Medley and Dr Gudrun Gaudian of Alne, Yorkshire, UK.

Distribution:

All FAO Members and Associate Members
FAO Fisheries Department
FAO Regional Fishery Officers
Directors of Fisheries
Regional and International Organizations

Klyashtorin, L.B.
Climate change and long-term fluctuations of commercial catches: the possibility of forecasting.
FAO Fisheries Technical Paper. No. 410. Rome, FAO. 2001. 86p.

ABSTRACT

The main objective of the study was to develop a predictive model based on the observable correlation between well-known climate indices and fish production, and forecast the dynamics of the main commercial fish stocks for 5–15 years ahead.

Populations of the most commercially important Atlantic and Pacific fish species - Atlantic and Pacific herring, Atlantic cod, European, South African, Peruvian, Japanese and Californian sardine, South African and Peruvian anchovy, Pacific salmon, Alaska pollock, Chilean jack mackerel and some others - undergo long-term simultaneous oscillations. Total catch of these species accounts for about 50% of total fish harvest over Atlantic and Pacific.

It was found that the dynamics of global air surface temperature anomaly (dT), although in correlation with the long-term dynamics of marine fish production, is of poor predictive significance because of high inter-annual variability and a long-term trend. The Atmospheric Circulation Index (ACI), characterizing the dominant direction of air mass transport, is less variable and in closer correlation with the long-term fluctuations of the main commercial stocks (r = 0.70-0.90).

Spectral analysis of the time series of dT, ACI and Length Of Day (LOD) estimated from direct observations (110-150 years) showed a clear 55-65 year periodicity. Spectral analysis of the reconstructed time series of the air surface temperatures for the last 1500 years suggested the similar (55-60 year) periodicity. Analysis of 1600 years long reconstructed time series of sardine and anchovy biomass in Californian upwelling also revealed a regular 50-70 years fluctuation. Spectral analysis of the catch statistics of main commercial species for the last 50-100 years also showed cyclical fluctuations of about 55-years.

These relationships were used as a basis for a stochastic model intended to forecast the long-term fluctuations of catches of the 12 major commercial species for up to 30 years ahead. According to model calculations, the total catch of Atlantic and Pacific herring, Atlantic cod, South African sardine, and Peruvian and Japanese anchovy for the period 2000–2015 will increase by approximately two million tons, and then decrease. During the same period, the total catch of Japanese, Peruvian, Californian and European sardine, Pacific salmon, Alaska pollock and Chilean jack mackerel is predicted to decrease by about four million tons, and then increase. In the next 15 years, total catch of main commercial species in the North Pacific is predicted to decline by 1.5 –2 million tons, while in the North Atlantic it is predicted to increase by about 1.7 –2 million tons. The probable scenario of climate and biota changes for next 50-60 years is considered.

Key words: Global climate change, Stock fluctuations, Climate-production cycles, Pacific, Atlantic.

TABLE OF CONTENTS

1. BACKGROUND

Marine fish populations show evidence of significant long-term fluctuations in abundance, which have implications for medium and long term forecasting of fish catches. The relationship between these fluctuations and large-scale climate changes is an important scientific and economic concern.

Simultaneous outbursts of sardine and anchovy populations in both North and South Hemispheres suggest that the fish populations are governed by the same global climatic events (Lluch-Belda *et al.* 1989, 1993; Kawasaki 1992a, b; Shwartzlose *et al*. 1999). An even more interesting phenomenon, pointed out in a number of publications, is regular synchronous outbursts of Japanese, Californian, and Peruvian sardine catches in different regions of the world ocean.

A reliable correlation between the long-term stock fluctuations and global climate characteristics has been ignored until recently, and the mechanisms that initiate, sustain and terminate such outbursts are still unclear. Beginning from the early 1990s, several attempts have been made to correlate regular fluctuations of sardine and anchovy stock with the dynamics of global and regional climatic indices. Kawasaki (1994) first applied the concept of cyclic climate changes (Shlesinger and Ramankutti 1993) to explain regular changes in the Japanese sardine catches for the last 350 years.

There are a number of new data sets on long-term climatic changes influencing gross production of zooplankton and nekton in North Pacific (Brodeur and Ware 1995). Synchronous changes in some climatic indices and abundance of crustaceans, fishes[1], and sea mammals were reported to occur in the tropical Pacific (Polovina *et al*. 1994).

A special issue of the journal *Fisheries* (1990) was dedicated to the synchronous character of climatic changes and populations of sea and fresh-water fish species. Francis (1990) analysed climate changes in relation to the fluctuations of the world commercial catches. Regier and Meisner (1990) estimated probable changes in the population of some species of fresh-water species as a possible consequence of global warming. Glanz (1990) tried to forecast the impact of expected climate changes on the world fishery. In spite of challenging titles, all these papers consider the fish stock fluctuations in response to various scenarios of "global warming" only.

The topical workshop *Cod and Climate* (1994) comprised a range of papers dedicated to the long-term dynamics of commercial stock and considered most important fish species in the North Atlantic in the context of global climate change. Jonsson (1994) carried out a statistical analysis on the reconstructed time series of Iceland cod catches for 350 years and found a periodicity in catch dynamics of approximately 60 years. The periodicity apparently does not depend on the intensity of fishery and it is argued that it is caused by regular climate changes. Fluctuations of the cod catches in western and eastern Atlantic for the last 80 years have occurred almost simultaneously, which is likely to be caused by the same climatic mechanism (Garrod and Shumacher 1994).

Although most of the papers presented at the *Cod and Climate* include important information, they described the phenomenon of "climate–fishery correlation" rather than explained it. It is important, however, to analyze possible causal mechanisms linking catches and climate, and develop an approach to predict climate-dependent changes in fish production.

---

1 A number of commercial species mentioned in this paper using their common names (widely accepted in the world scientific community) have alternative names in the FAO statistics, as follows:

Common name used in the paper	Name in FAO nomenclature
Japanese sardine	Japanese pilchard
Peruvian sardine	South American pilchard
Californian sardine	California pilchard
European sardine	European pilchard
S.African sardine	Southern African pilchard
Peruvian anchovy	Anchoveta

A dependence of Japanese sardine catches on climate changes (expressed as surface air and water temperature on the hemispheric scale) was reported by Kawasaki (1992a). The same is true for Californian sardine (Lluch-Belda *et al*. 1992). Beamish and Bouillon (1993) showed that the long-term fluctuations of the Pacific salmon catches are in agreement with the dynamics of the regional Aleutian Low Pressure Index (ALPI). The latter is known to be one of the main climate-forming factors for the North Pacific.

Analysis of the ALPI dynamics over the last 93 years made it possible to forecast a probable decreasing trend in salmon populations in the early 21st century. Klyashtorin and Smirnov (1995) found a close correlation between the catch dynamics of Pacific salmon, Japanese, and Californian sardines, on the one hand, and the dynamics of hemispheric temperature anomaly for the last 75 years, on the other. Based on the climatic and production trends, the authors suggested that salmon populations were likely to decrease in the first decade of the next century (Klyashtorin 1997).

Bakun (1990, 1996) demonstrated a close correlation between the long-term fluctuations of the upwelling index in the most productive zones of the world ocean and catch dynamics of abundant, small pelagic fishes. The author believes that the global climate changes are accompanied with significant changes in the atmospheric circulation, direction and velocity of largest oceanic streams, and upwelling intensity. This, in turn, affects the rate of nutrient transport into the euphotic upper ocean layer and causes considerable changes to the oceanic primary production and fish harvest.

With this background, FAO (1994, 1996, 1997a, b) has initiated a range of detailed research programmes to analyze the state and perspectives of the world fishery and stimulate the development of new approaches to long-term forecasting of the fish stock dynamics.

Lluch-Cota and others (FAO 1997b) analyzed the dependence of sardine, anchovy and other pelagic species on selected regional climate indices worldwide and in the Pacific. The authors revealed close correlations between the dynamics of regional climate and production indices, but did not attempt to estimate future changes in fish production.

Beamish *et al*. (1999) considered correlations between the dynamics of Pacific salmon catch and a range of global and regional climatic indices in the Pacific for the most recent 100 years. They showed that the catch fluctuations depend on the long-term natural (climatic) changes rather than only on the impacts of commercial fisheries. The authors discussed the applicability of various climatic indices to characterise commercial catches in the future, but did not suggest a clear approach to climate-based forecasting of salmon stocks.

Klyashtorin and Sidorenkov (1996) showed that the stock and catch dynamics of the 15 main commercial fish species in the Pacific is in good agreement with the dynamics of the global temperature anomaly (dT), Atmospheric Circulation Index (ACI), and global geophysical index Length Of Day (LOD), which characterizes the earth rotation velocity.

The concept of synchronous cyclic fluctuations of the climate and fish production was used to predict the long-term stock and catch dynamics of Pacific salmon into the late 1990s and early 2000s (Klyashtorin 1997). The accuracy of the prediction is confirmed by recent statistical data on commercial catches of Pacific salmon and sardines.

Similarly, Klyashtorin (1998) demonstrated a close correlation between the peculiarities of the hemispheric atmospheric circulation and catches of 12 commercially important fish species, which constitute 35 to 50% of the total marine catch. Regular alternation of roughly 30-year "climatic epochs" (this study is described in more detail below) was shown to correspond to the outbursts of some fish species. The author believed that the analysis of regular fluctuations of popular climatic (dT, ACI) and geophysical (LOD) indices makes it possible to forecast the population dynamics of main commercial species in the Atlantic and Pacific for 10–15 years ahead.

In spite of some progress in our understanding of the climate change and fluctuations of commercial fish stock, long-term forecasting calls for further development of methods. To improve the present general concept of the climate–production dependence, it is necessary to substitute the simplistic correlative model with a better established, digital prognostic model intended for reliable forecasting of commercial catch of each of 12 main commercial species.

The evolution of our understanding of the "climate-stock" dependence may be presented as follows:

- 1960–1980s. First reports on the phenomenon of synchronous outbursts of sardine and anchovy in different regions of the world ocean.
- 1980/90s. Development of the concept of sardine and anchovy stock as dependent on the dynamics of several global and regional climatic indices.
- The late 1990s. New data indicate a close correlation between the climate changes and stock dynamics of ten main commercial species (including but not limited to sardine and anchovy). The first ideas on regular 50-70 year climate change and regular 25-30 year alternation of ACI epochs («zonal» and «meridional»). First approximation to the long-term forecasting of commercial stock dynamics was undertaken.
- Year 2000. An approximation to the climate-based prognostic model of commercial stock for 10–12 commercial fish species. Estimation of probable trends in fish production over vast regions (North Atlantic, North and South Pacific).

The main purpose of this work is to develop a predictive model based on the observed and logically consistent correlations between climate and fish production and forecast the dynamics of main commercial fish stocks for periods of 5–15 years ahead of the observed fisheries catch changes. To do that, it is necessary to forecast the future climate changes, which can be achieved using retrospective analysis of the long-term time series of some principal climatic indices.

2. DYNAMICS OF CLIMATIC AND GEOPHYSICAL INDICES

Regular and reliable climate observations with measurement and calculation of principal climatic indices were started only about 150 years ago, when organized and consistent global ocean and atmosphere observation systems were initiated.

The averaged surface air temperature anomaly (dT) is widely recognised to be the most important index characterising the global climate changes including "global warming" (Bell *et al*. 1998; Anisimov and Polyakov 1999).

Another single index of climate change is the Atmospheric Circulation Index (ACI) that characterizes the periods of relative dominance of either "zonal" or "meridional" transport of the air masses on the hemispheric scale. ACI, also known as the Vangengeim-Girs Index, has been calculated from data on basic atmospheric activities in the Atlantic-Euroasian region for more than 100 years (Girs 1974).

George Vangengeim, the founder of ACI, is a well-known Russian climatologist. The Vangengeim-Girs classification is the basis of the modern Russian climatological school of thought. According to this system, all observable variation in atmospheric circulation is classified into three basic types by direction of the air mass transfer: Meridional (C); Western (W), and Eastern (E). Each of the above-mentioned forms is calculated from the daily atmospheric pressure charts over northern Atlantic-Eurasian region. General direction of the transfer of cyclonic and anticylonic air masses is known to depend on the distribution of atmospheric pressure over the Atlantic-Eurasian region (the atmosphere topography).

The recurrence of each circulation form (W, E, or C) during the year is expressed in days. Total annual duration of the three circulation forms sums therefore to 365 (or 366 in a leap year). The index is defined by the number of days with the dominant form of atmospheric circulation. It is more conveniently expressed as an anomaly (actual data minus the long-term average). The sum of anomalies can be displayed in a chart of the so-called integral curve of the atmospheric circulation. The annual sum of the occurrence of all circulation anomalies is equal to zero: (C) +(W) + (E) = 0.

The periods dominated by any single form of atmospheric circulation have alternated with a roughly 30-year period for the last 100 years. These periods were named "Circulation epochs". These may be pooled into two principal groups: meridional (C) and combined "latitudinal" epochs (W+E): (W + E) = - (C)

Meridional (C) circulation dominated in 1890-1920 and 1950-1980. The combined, "zonal" (W+E) circulation epochs dominated in 1920-1950 and 1980-1990. Current "latitudinal"(WE) epoch of 1970-1990s is not completed yet, but it is coming into its final stage, and so the "meridional" epoch (C-circulation) is now in its initial stage. (It will be useful for the reader to note here the relation that shows that the "transition" from C to W-E is continuous, and the equation balances to 100%, in the form of a simple graphic without any other variables included).

It was found that "zonal" epochs correspond to the periods of global warming and the meridional ones correspond to the periods of global cooling. (Lamb 1972; Lambeck 1980). The generalised time series on the atmospheric circulation forms for 1891-1999 were kindly placed at our disposal by the Federal Arctic and Antarctic Research Institute (AARI) in St. Petersburg (Russia). This is also consistent with the theories and observations described by Leroux (1998).

The third important index is Length of Day (LOD) – a geophysical index that characterizes variation in the earth rotational velocity. Full time series of LOD cover more than 350 years, with the most reliable data obtained in the last 150 years (Stephenson and Morrison 1995). The long-term LOD

dynamics is in close correlation with the dynamics of the main commercial fish stocks (Klyashtorin and Sidorenkov 1996).

LOD Index is calculated as a difference of two values: actual (astronomical) length of day and the standard one. The continual registration of LOD and publication of the corresponding data is carried out by the International Time Bureau in Paris. The correlation coefficients were calculated using non-smoothed data ranges. Smoothed values, obtained using a Gaussian filter, were only used to improve the curve plots in the figures. Statgraphics (1988) software was used to detrend the time series.

Let us compare the dynamics global geophysical (LOD) and climatic indices for the last 150 years. For a more convenient visual comparison of the dT, ACI and the earth rotation velocity dynamics, the negative (-LOD) instead of the directly calculated LOD values was used. The dynamics of -LOD, dT and ACI for the last 140 years can be viewed as multi-decadal fluctuations against the background of age-long trends (Figure 2.1).

Global dT is known to have an ascending linear trend 1861-1999 with the increment of 0.059^{o} per 10 years (Sonechkin 1998).

Our planet as a whole conserves its angular momentum except for the known effects of external torque associated with the lunar-solar tide, which induces a gradual decelerating of the earth rotation velocity at a rate corresponding to the increase in the astronomic length of day (LOD) by about 1.4 millisecond per century (Munk and McDonald 1960). That is, -LOD has had a descending linear trend with the increment about 0.14 ms per decade (Figure 2.1). Different age-long linear trends of LOD and dT make it difficult to compare the dynamics of multi-decadal fluctuations of these indices. Figure 2.2a presents both -LOD and dT ranges, with the linear trends removed by fitting of linear regression and using a "detrending" procedure (Statgraphics 1988).

When detrended, the graphs of -LOD and dT are very similar in shape, and it is clear that -LOD runs several years ahead of dT, especially in its maxima. Shifting the -LOD curve by 6 years to the right (Figure 2.2b) results in almost complete coincidence of the corresponding maxima of the early 1870s, late 1930s, and middle of 1990s (Klyashtorin et al.1998).

The similarity in the dynamics of detrended -LOD and dT and ACI indices is clear: Large fragments of the curves are much alike not only in general shape, but in detail as well. In general, the long-term dynamics of both dT and -LOD have roughly a 60 year periodicity. The global climate system was reported to oscillate with a period of 65-70 years since 1850 (Schlesinger and Ramankutty 1994). The same 60-70 year periodicity has also been characteristic for the long-term dynamics of some climatic and biological indices for the last 150 years (Klyashtorin 1998).

Similarity between the -LOD and dT dynamics makes it possible to assume the existence of some common factors inducing and controlling the observable synchrony in geophysical (LOD) and climatic (dT) indices variation. The atmospheric circulation as a whole is strongly driven by the Equator-Pole Temperature Meridional Gradient. Greater warming in the polar region weakens this gradient in the lower troposphere, which leads to a general weakening of surface winds (Lambeck 1980).

The long-term dynamics of the atmospheric pressure fields over the Northern hemisphere during the last 90 years are characterised by the alternation of approximate 30-year periods ("circulation epochs") with relative dominance of either zonal or meridional atmospheric circulation (Dzerdzeevski 1969; Girs 1971; Lamb 1972; Lambeck 1980).

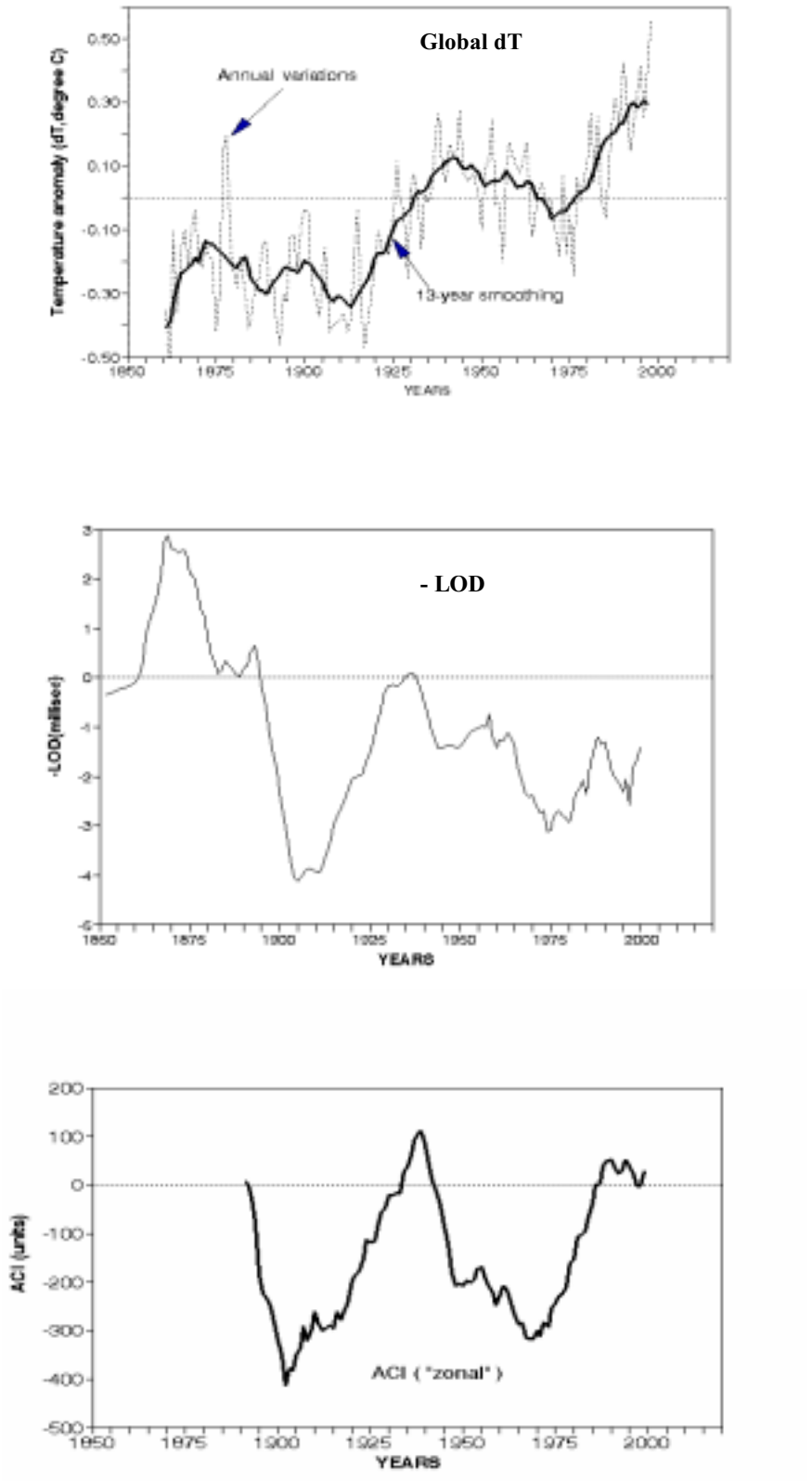

Figure 2.1 The dynamics of the global air-surface temperature anomaly (dT), 1861-1998, the negative Length of Day (-LOD), 1850-1998 and the "zonal" Atmospheric Circulation Index (zonal ACI), 1891-1999.

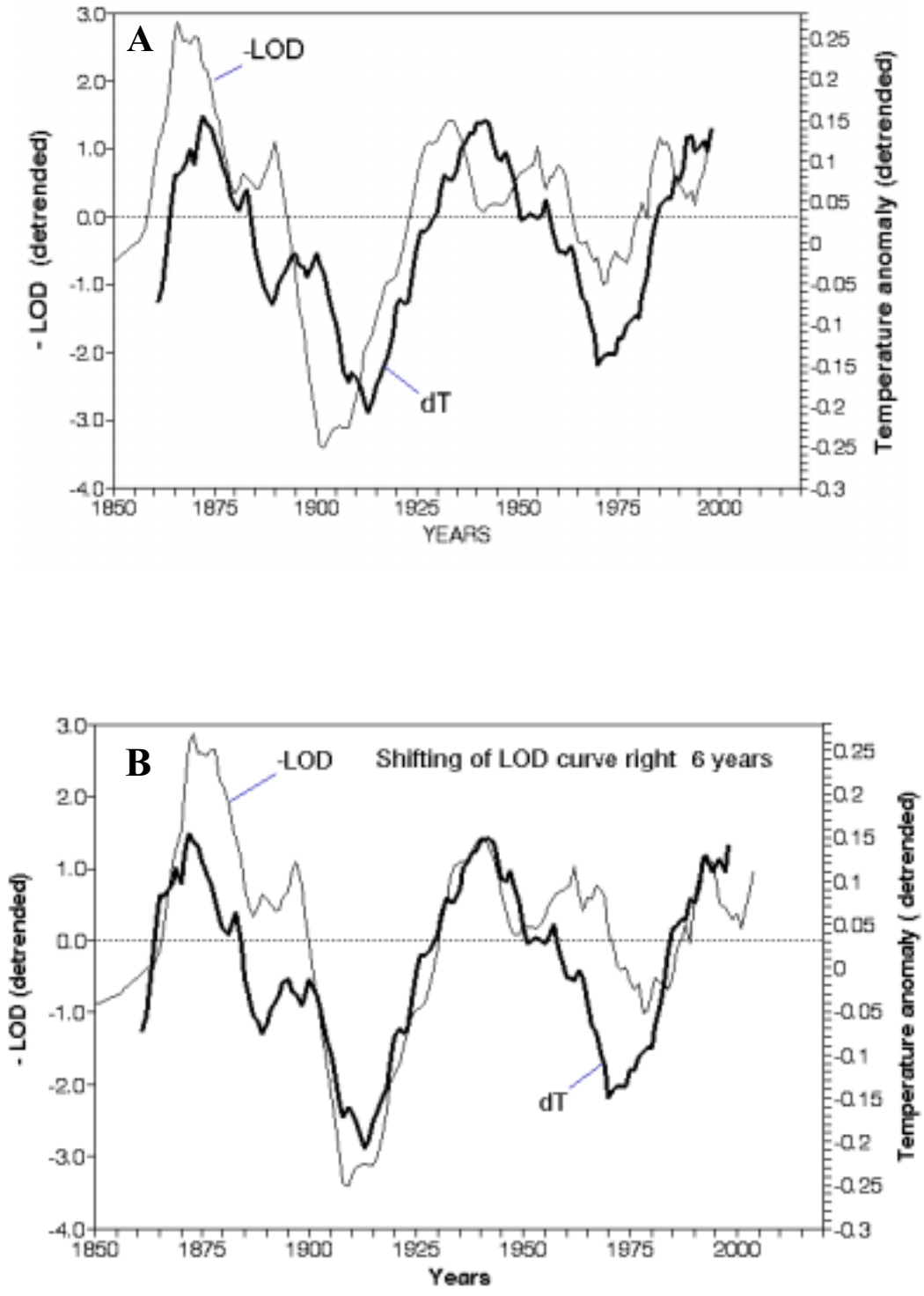

Figure 2.2 Dynamics of the detrended global temperature anomaly (dT) and detrended negative Length of Day (-LOD) (see text for details).The ACI ("zonal" form) has practically no pronounced general trend. Comparison of dT and ACI (Figure 2.3A) shows their close similarity in shape, but ACI runs several years ahead of dT. Shifting the ACI curve by 4 years to the right (Fig 2.3B) results in almost complete coincidence of the curve maximums of the early 1870s, late 1930s, and middle 1990s.

The first type, zonal circulation, is characterised by increasing intensity of the zonal circulation at all latitudes and pole-ward shift of the wind intensity maximums. The circulation is accompanied somewhat by a decrease in the overall range of surface-air temperature between the equator and poles and by an overall increase in the mean global surface-air temperatures. Ocean-surface temperatures tend to increase in high latitudes. The second type, meridional circulation, is characterised by weakening in zonal circulation, shift of the main atmospheric streams toward lower latitudes, and overall decrease in global temperature (Lamb 1972). Both easterly and westerly winds increase during the zonal type of circulation and both decrease in the periods of the meridional type of the circulation (Lambeck 1980).

Atmosphere is the most variable component of the global geophysical system exchanging relatively large proportions of its angular momentum with the solid earth below compared with other components (Salstein *et al*. 1993). A number of publications suggest that seasonal, inter-seasonal and inter-annual variations of the earth's rotation velocity are directly proportional to the relative angular momentum at the atmosphere, which primarily depends on the velocity of zonal winds (Langley *et al*. 1981; Rosen and Salstein 1983; Robertson 1991). On longer time scales, changes in LOD are correlated with the El Niño Southern Oscillation (ENSO) phenomenon, and strong wind anomalies associated with ENSO events (Salstein and Rosen 1986; Dickey *et al*. 1992a,b)

A formal derivation of the dynamic relation between the atmosphere and solid earth make it possible to calculate the changes in the earth's rotational velocity from the large-scale distribution of the atmospheric pressure and dynamics of the wind fields (Barnes *et al*. 1983). These data are available from several of the world's weather services (Salstein *et al*. 1993).

Thus, on a wide range of time scales from several days to years, there is an agreement between the dynamics of the angular momentum in the atmosphere and solid earth, which come into view as small but important changes in the rotation of the planet.

It is conceivable that the multi-decadal fluctuations of the earth's rotation velocity results from the redistribution of the angular moment between the atmosphere and solid earth due to the alternation of multi-decadal epochs of "zonal" and meridional atmospheric circulation.

It was shown (Lamb 1972; Lambeck and Cazenave 1976), however, that the observable changes in speed and direction of the air mass transfer may explain seasonal and annual, but not multi-decadal, LOD variations. Only 10% of the long-term LOD variation can be explained by the observable changes in atmospheric circulation. The calculations suggest that the average speed of zonal winds would have to be an order of magnitude larger than they are to explain the remaining 90% of the LOD changes. It seems improbable that some other unevaluated meteorological factors could provide additional explanation. Therefore, the hypothesis that the climatic changes are a consequence of the LOD changes should be rejected (Lambeck 1980).

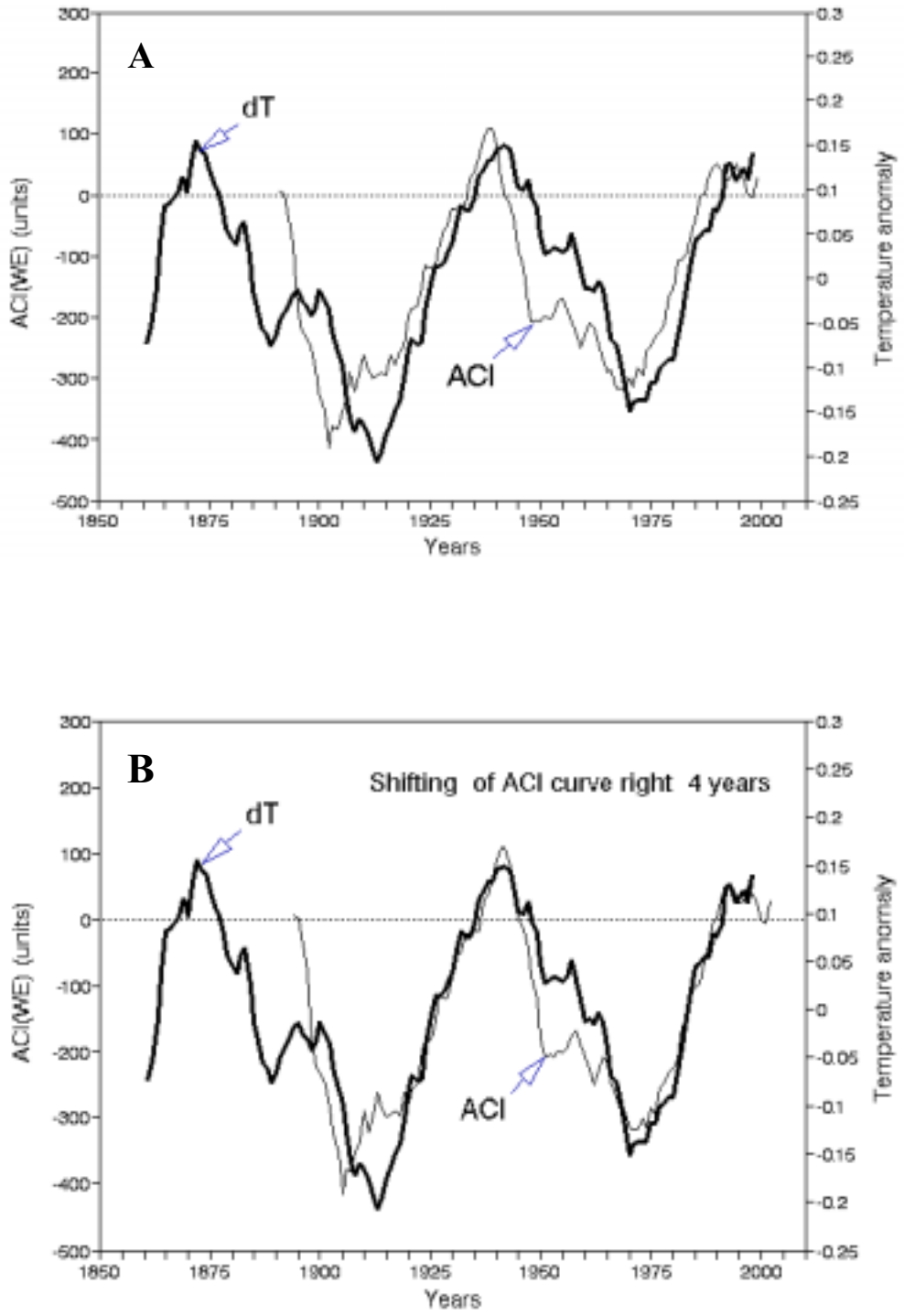

Fig 2.3 Dynamics of the detrended global temperature anomaly (dT) and the Zonal Atmospheric Circulation Index (zonal ACI) (see text for details).

2.1 SUMMARY

A phenomenon of close correlation between the main climatic index dT and geophysical index (-LOD) still remains an intricate puzzle of geophysics. Another challenging puzzle is the observable 6-year lag between the detrended run of dT and -LOD. Taking into account this lag, the LOD observations can be used as a predictor of the future climatic trends. Even without a mechanism for a causal relationship between the detrended climatic (dT) and geophysical (LOD) indices, the phenomenon of their close similarity for the last 140 years makes LOD a convenient tool to predict the global temperature anomaly (dT) for at least 6 years ahead.

Lambeck and Cazenave (1976) pointed out a high probability of an increasing global temperature trend in the 1970s and 1980s. Their prediction was correct.

Spectral density analysis of the LOD time series for 1850-1998 revealed clear, regular fluctuations with an approximate 60-year period length (see below). The multidecadal maxima of LOD took place in the early 1870s and mid-1930s, and the next maximum is likely to fall early in 2000. Based on this multidecadal periodicity of LOD, and the fact that LOD runs ahead of dT by 6 years, a gradually descending dT may be expected around 2005.

Although the interdependences between dT, ACI and -LOD may be complex, the empirical geophysical index (LOD) may still serve as a general predictor of future climate changes. This gives an opportunity to forecast climate change and, therefore, stock and catches of commercial species, which are related to climate.

3. DYNAMICS OF GLOBAL CLIMATIC INDICES AND MAIN COMMERCIAL CATCHES

An important question is whether the main commercial stock production is affected by common factors, which also control the synchronous fluctuations of the principal climatic, geophysical and biological indices.

The total world marine catch averages 73 million tons per year, which consists of about 550 species. However, as few as 12 species (about 2 percent of total number of commercial species) provide up to 40-50% of the world marine catch. These are: Japanese, Californian Peruvian and European sardine, Pacific salmon, Alaska pollock, Chilean jack mackerel, Peruvian anchovy, Atlantic cod, Atlantic and Pacific herring, South African sardine, and Peruvian anchovy. Seventy to ninety percent of the total commercial catches in Russia, Norway, Iceland, Japan, Peru, and Chile depend on these commercial species (hereafter referred to as the "major commercial species"). The remaining 538 species constitute the second half of total marine catch.

In the late 1980s, the annual commercial catch in the Pacific was close to 54 million tons. The total catch of the 5 main Pacific commercial species (Japanese and Peruvian sardine, Alaska pollock, Chilean jack mackerel, and Peruvian anchovy) made up 52% of this total (28 million tons). In the late 1960s, the total marine catch in the Atlantic was estimated to be 22 million tons, of which three of the five main Atlantic commercial species (Atlantic cod, Atlantic herring and South African sardine) made up 44% (9.6 million tons).

It was found that the 12 major commercial species could be divided into two principal groups, based on the peculiarities of their long-term dynamics (Fig. 3.1 and 3.2). The first group consisted of Japanese, Californian and Peruvian sardine, Pacific salmon, Alaskan pollock, Chilean jack mackerel, Peruvian anchovy and European sardine. The maximum catch of these species occurred in the late 1930s and early 1990s, with the minimum catch in the 1960s. The second group comprises Atlantic cod, Atlantic and Pacific herring, South African sardine, and Peruvian anchovy. The maximum catch for this group was in the 1960s, and the minima occurred in the 1930s and 1990s. Therefore, the catch dynamics of the two groups are opposite in phase.

Several characteristics are used to indicate the climate changes. The global temperature anomaly (dT) is a widely known climatic index, but as described above, it is quite variable and its trend can only be traced reliably after considerable (> 10 year) smoothing. Unlike dT, ACI is less variable and so is a more convenient index.

The catches of these groups undergo synchronous, long-term fluctuations, which are likely to be caused by changes in some common natural factors, such as global climate change. Therefore, an important issue is the degree of correlation between the stock dynamics of highly abundant commercial species and ACI.

The catches of the first group are closely correlated with the zonal ACI curve (Figure 3.3; correlation coefficients vary within the range of 0.7-0.9). The catches of the second group of species are closely correlated with the meridional ACI form (Figure 3.4; correlation coefficients are in the range 0.62-0.74). The correlation coefficient for Peruvian anchovy is about 0.4, but even in this case the run of the two curves is generally the same. The dependence of Peruvian anchovy catch on climate characteristics is very specific and considered below (see Chapter 10).

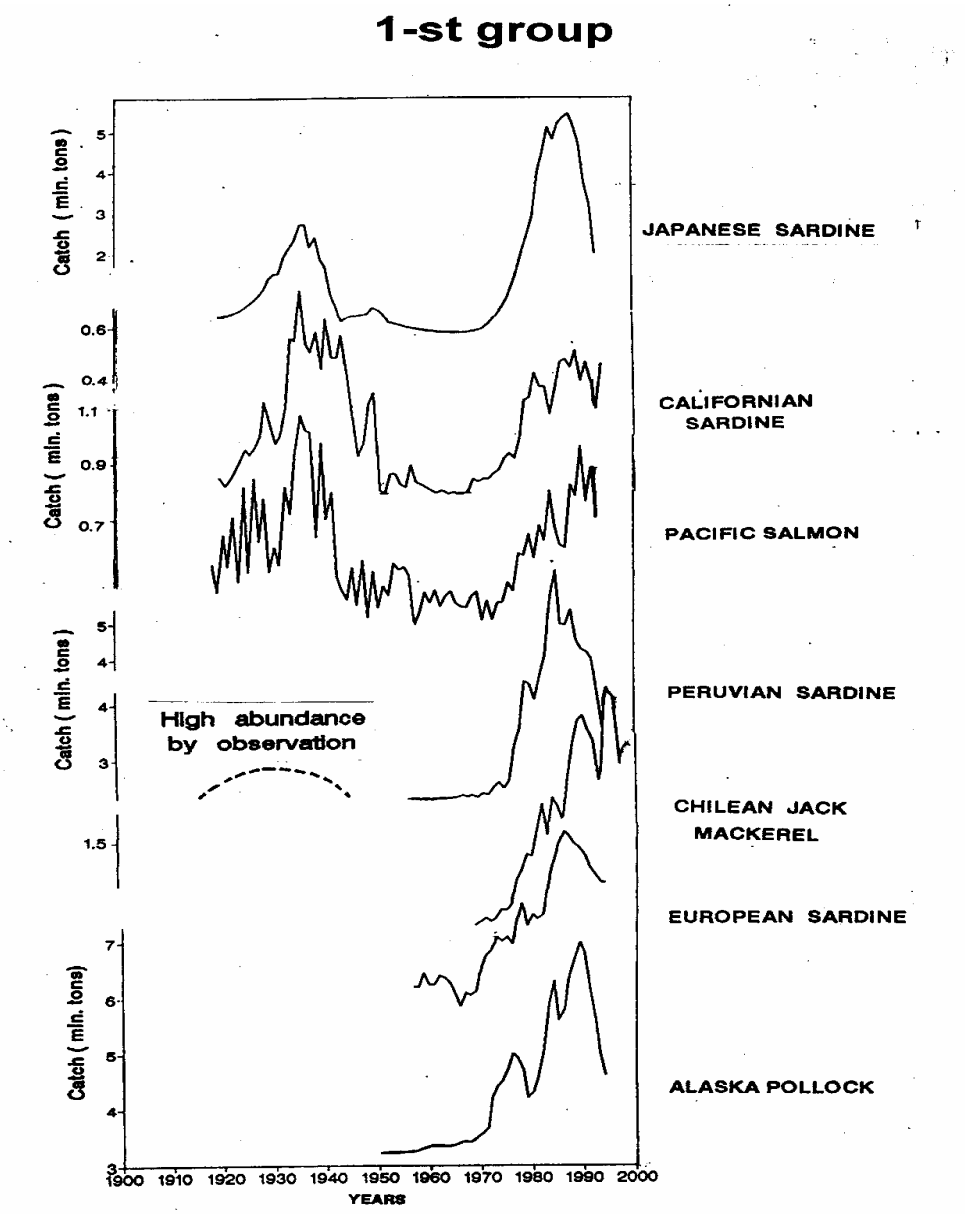

Figure 3.1 Synchronous catch fluctuations of "zonal-dependent" main commercial species (see text for details).

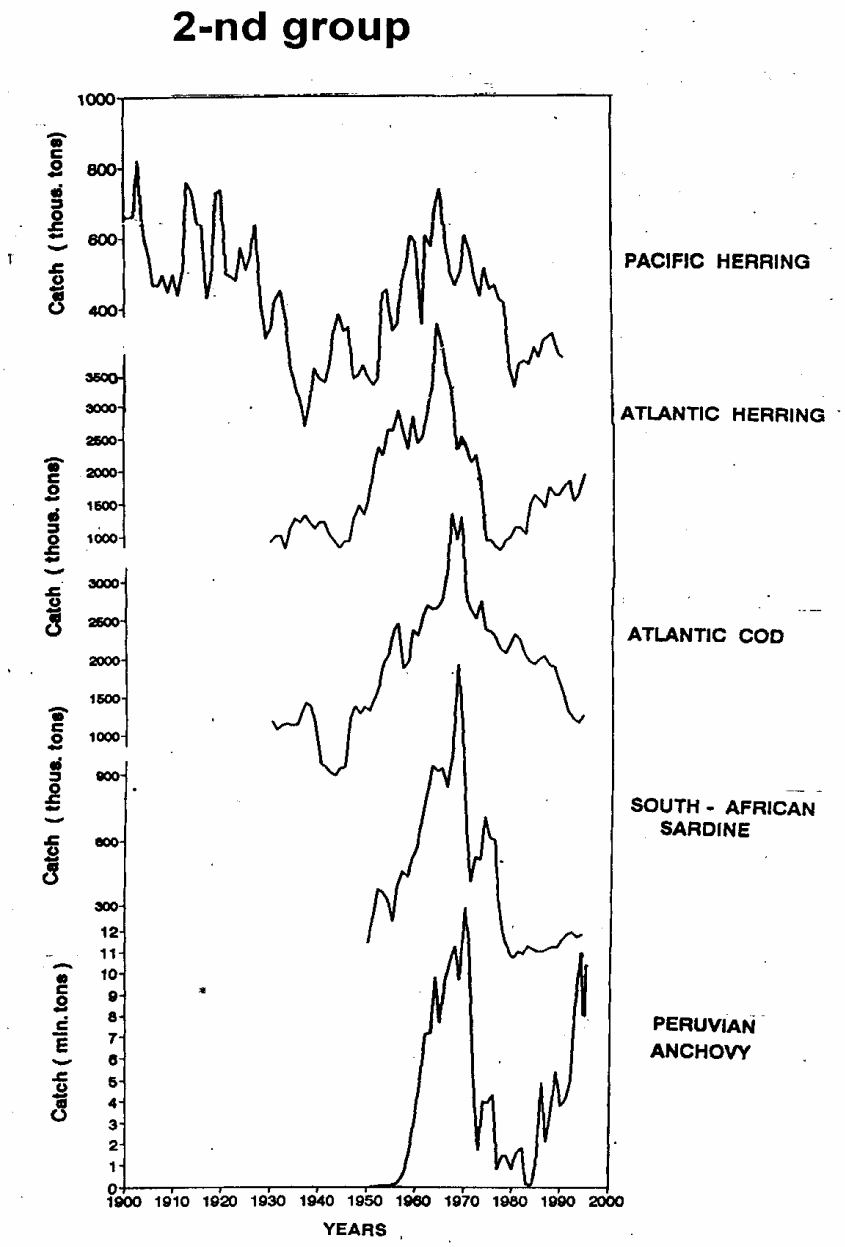

Figure 3.2 Synchronous catch fluctuations of "meridional-dependent" main commercial species (see text for details).

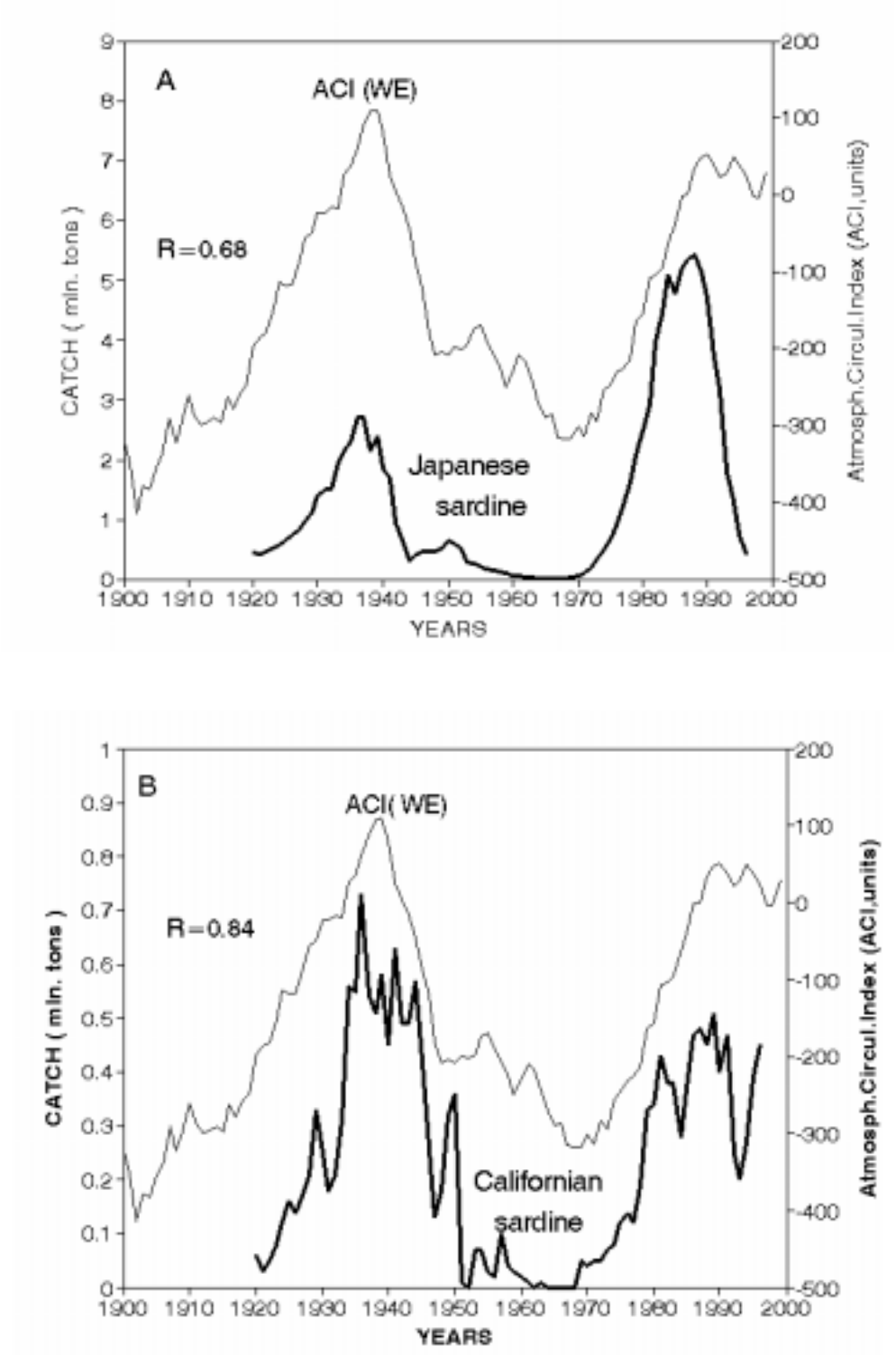

Figure 3.3 Correlation between dynamics of "zonal" ACI and catch of the major commercial "zonal–dependent" species.

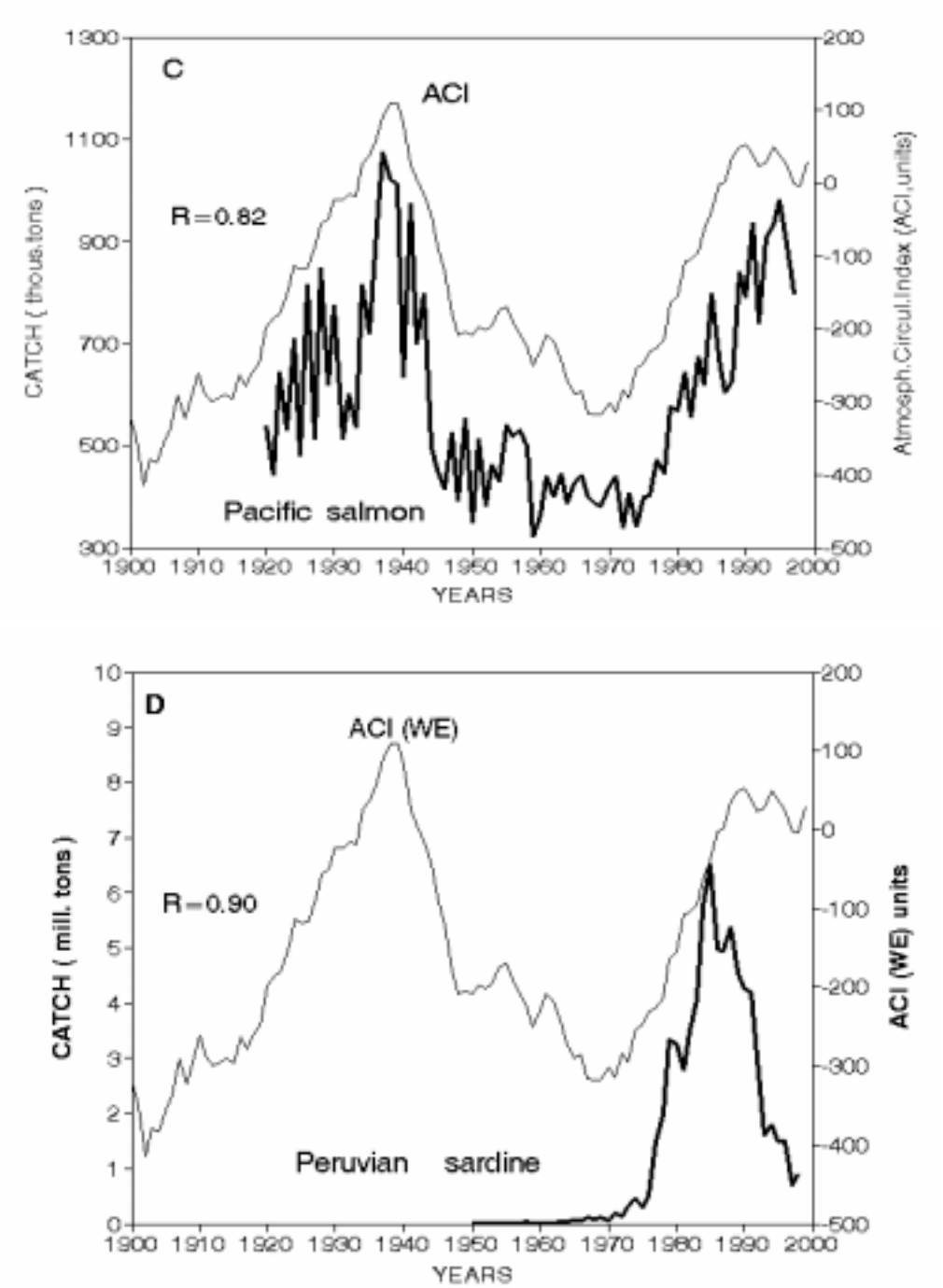

Figure 3.3 (continued). Correlation between the dynamics of "zonal" ACI and catch of the major commercial "zonal–dependent" species.

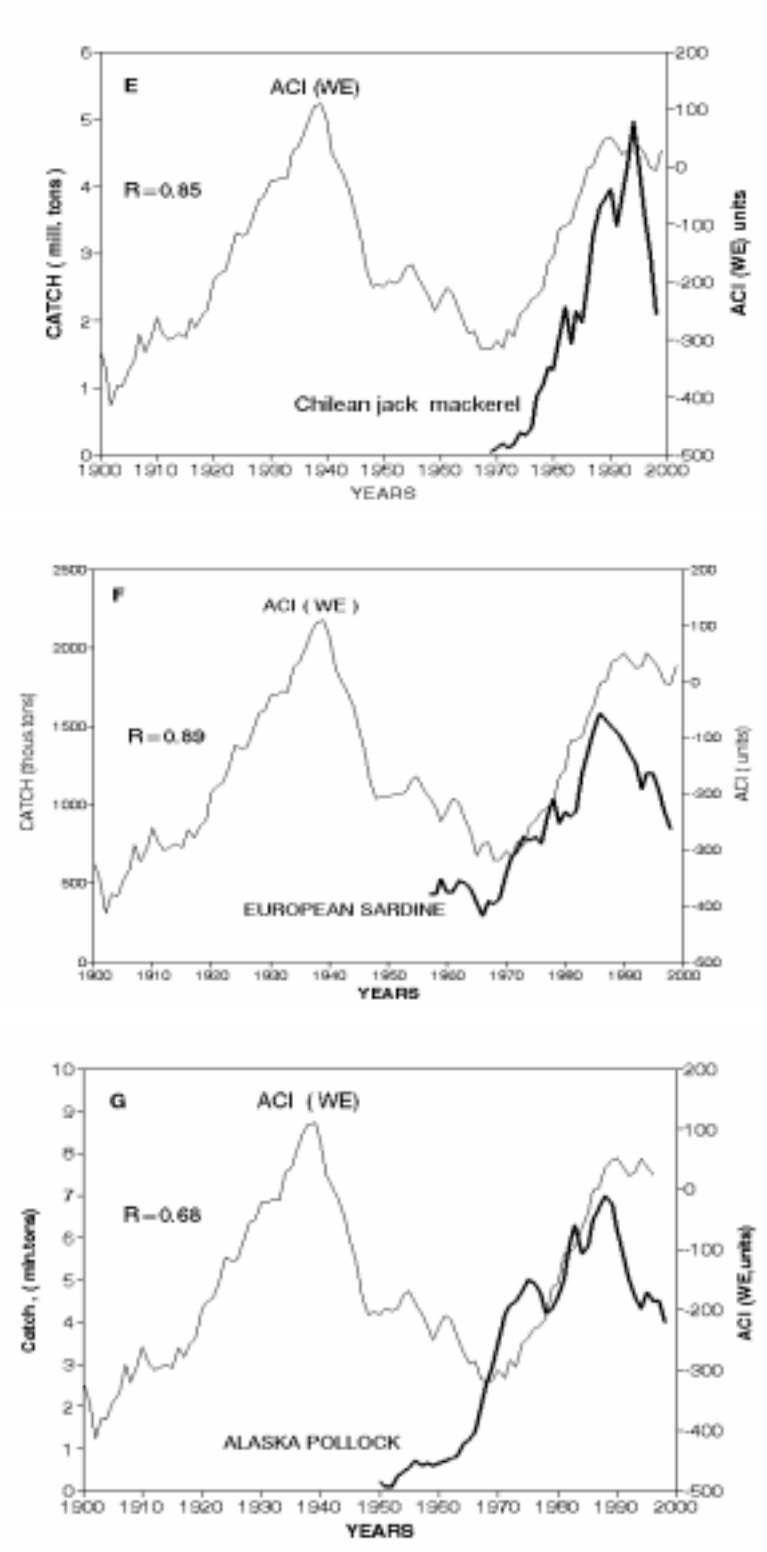

Figure 3.3 (continued). Correlation between dynamics of "zonal" ACI and catch of major commercial "zonal–dependent" species.

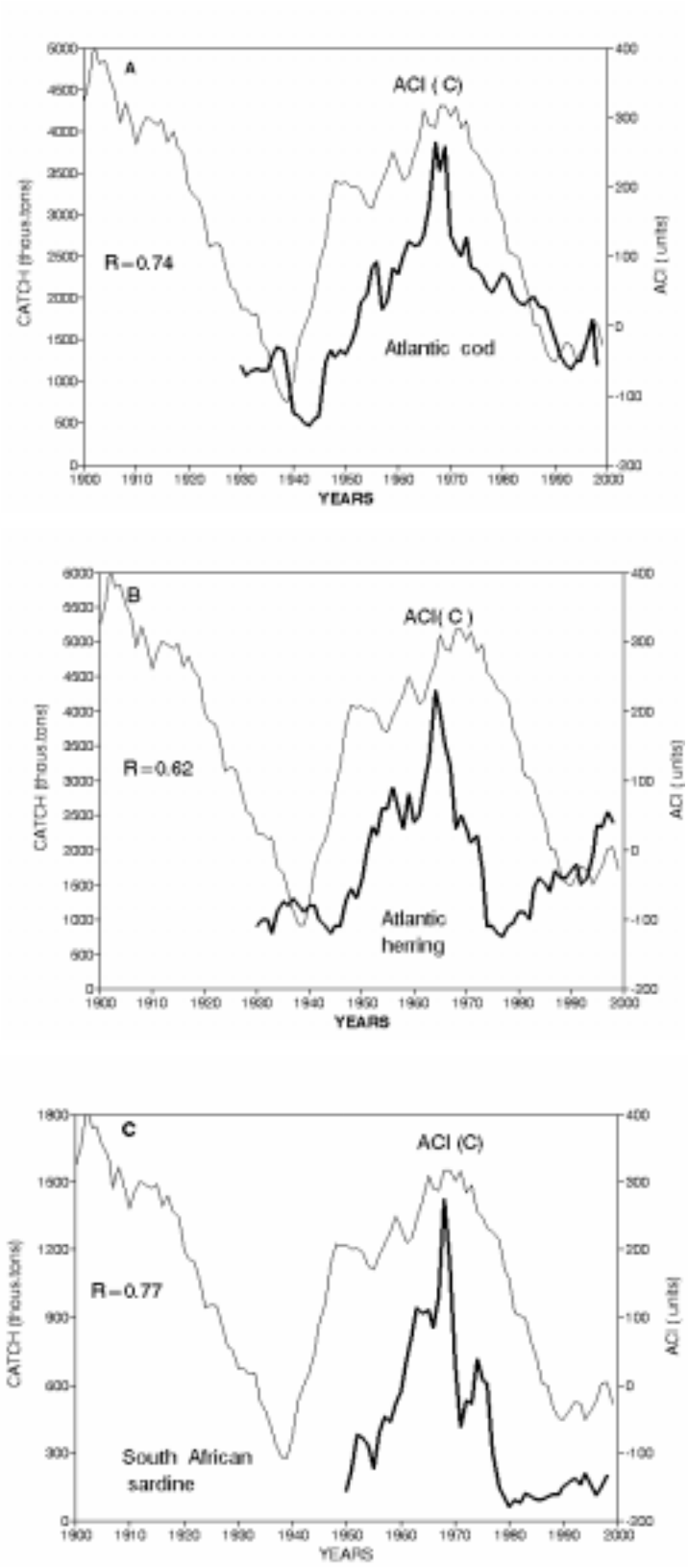

Figure 3.4 Correlation between dynamics of "meridional" ACI and catch of the major commercial " zonal-dependent" species.

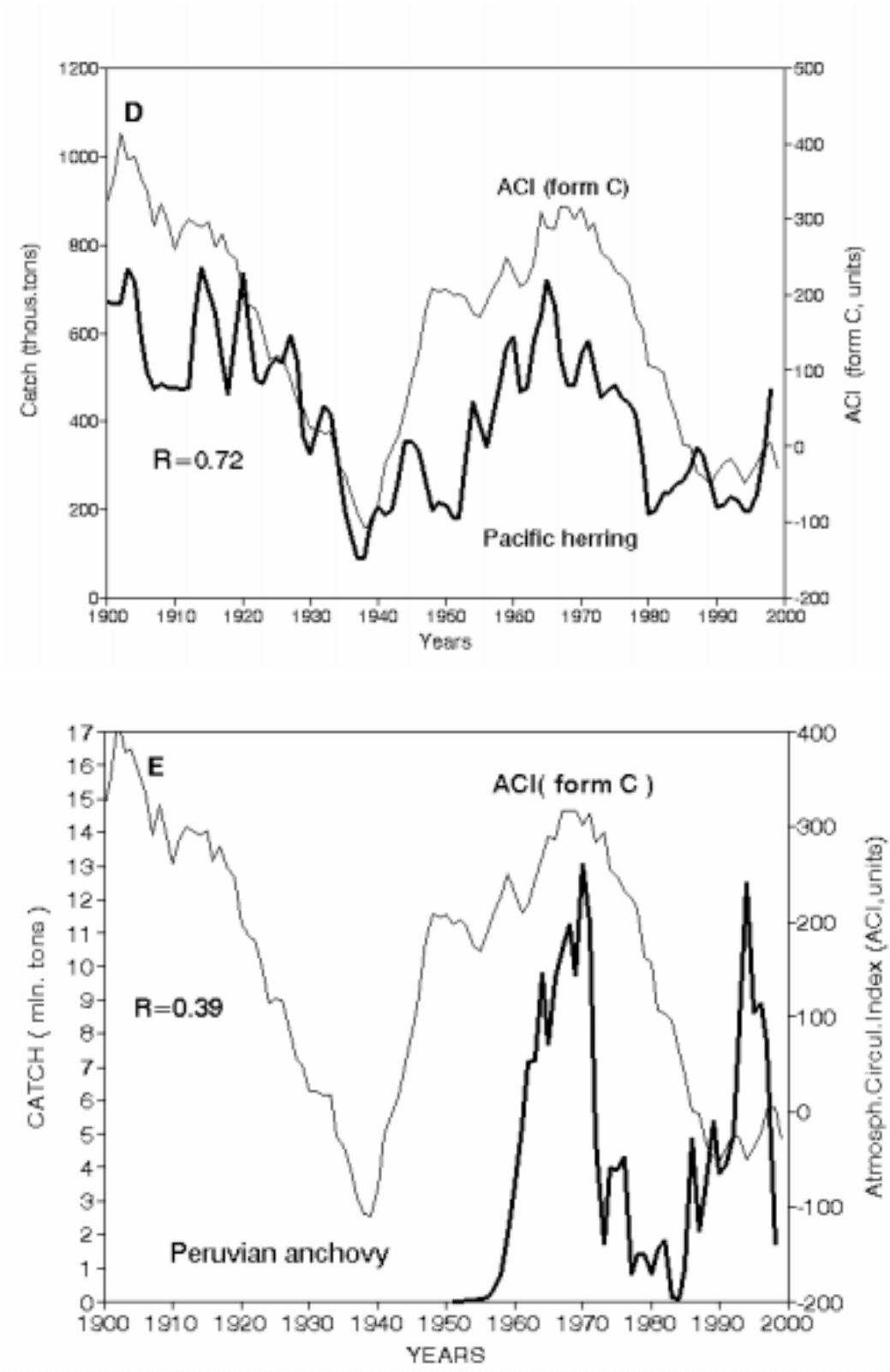

Figure 3.4 (continued) Correlation between the dynamics of "meridional" ACI and the catch of the major commercial "meridional-dependent" species.

The production of main commercial fish species in both the Atlantic and Pacific undergoes long-term climate oscillations (Figure 3.5A). The corresponding curves reflect two principal processes: (i) large-scale regular fluctuations in the fish production, and (ii) gradual increases in fishing grounds and fishing capacity. The capacity of the world fishing fleets has increased almost linearly by 12 million tons over 1973-1993. However, the relative commercial catch per 100 ton capacity has stayed practically stable for the same period (FAO 1994; Moiseev 1995). When the long-term trend is removed, the regular fluctuations of the major commercial fish production in both Atlantic and Pacific oceans become clearer (Figure 3.5B).

The Atmospheric Circulation Index (ACI), though measured in the Atlantic-Eurasian sector of the Western Hemisphere, almost coincides in dynamics with both dT and LOD, and therefore can be considered as a global index. It has no overall trend and can be directly compared with fishery indices, such as catch dynamics.

The ACI dynamics (Figure 3.6A) exhibits regular, roughly 30-year, alternation of the "circulation epochs" characterised by predominance of either «zonal» or «meridional» components. These epochs correspond to the periods of either global warming or global cooling. In fact, only the upper parts (peaks) of C (“meridional”) and WE (“zonal”) curves are of practical significance (Figure 3.6B)

The alternation of “cool” (meridional) and "warm" (zonal) circulation epochs correspond also to the long-term changes in the catch of main commercial species over the Atlantic and Pacific. The maximum production of seven of the twelve major commercial species fall on the "warm" period, whereas the production of the remaining 5 species is in good agreement with the "cool" periods (Klyashtorin 1998).

The relationship between the circulation epochs and maximums of the major commercial fish production in both the Atlantic and Pacific oceans is shown in Figure 3.7. The long-term fish production follows the regular alternation between the "meridional" and "zonal" circulation epochs. Regular alternation of the epochs for the last 110 years suggests that the present epoch of "zonal" circulation is coming into its final phase and the new "meridional" epoch is due.

What changes are expected to occur in commercial fish production in the oncoming circulation epochs? The most important fishery regions are the North Atlantic and North Pacific. A close agreement between the dynamics of climatic indices and commercial catches in the North Pacific is shown in Figure 3.8. The long-term fluctuations of the major pelagic fish species in the North Pacific can be described as the sequential passing of two climate-governed "waves" with the maxima falling on 1940-50s and 1970-90s.

The last (current) “wave” is coming into its final phase similar to that of 40-50s. This means that the population of main commercial species in North Pacific (Japanese Sardine, Alaska pollock and Pacific salmon) is expected to decline in the near future.

Unlike the North Pacific, the maximum of commercial fish production in the North Atlantic falls on the "meridional" ACI epoch of 1950-70s. The oncoming "meridional" circulation epoch in the North Atlantic is similar to that of 50-70s when production of herring, and cod and other gadoids reached up to 9 million tons. Therefore, with the coming of the meridional circulation epoch, we may expect an increase in these species population (herring, and cod and other gadoids) in the North Atlantic over the next decade.

More recent data confirm this viewpoint. The population of Atlantic (and Pacific) herring has already started to rise. Since the cod population has always followed herring in the past, the same dynamics may be expected in the future decade as well.

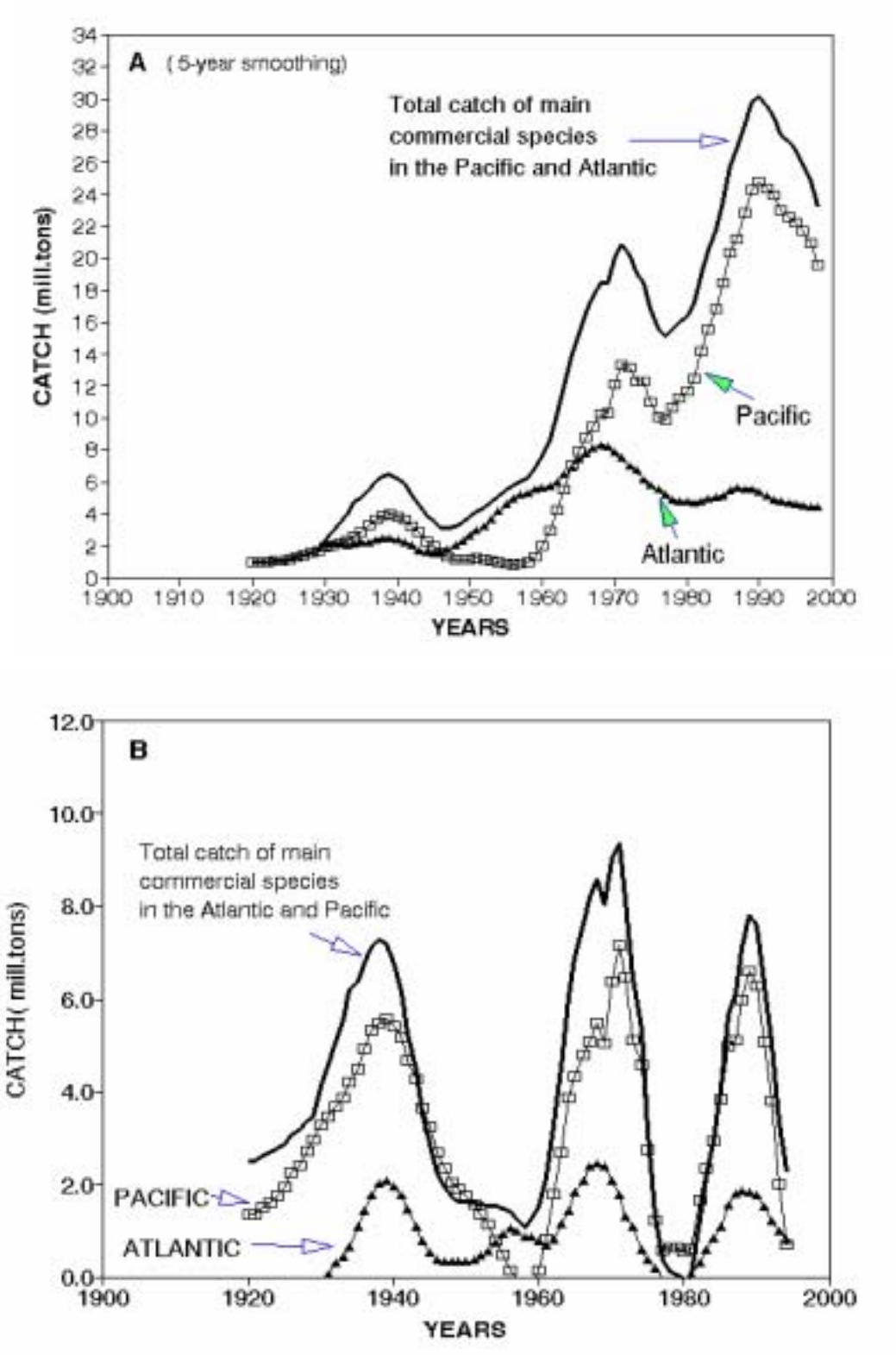

Figure 3.5 Long-term catch dynamics of main commercial species in the Atlantic and Pacific: A – before trend removal; B - detrended (see the text for details).

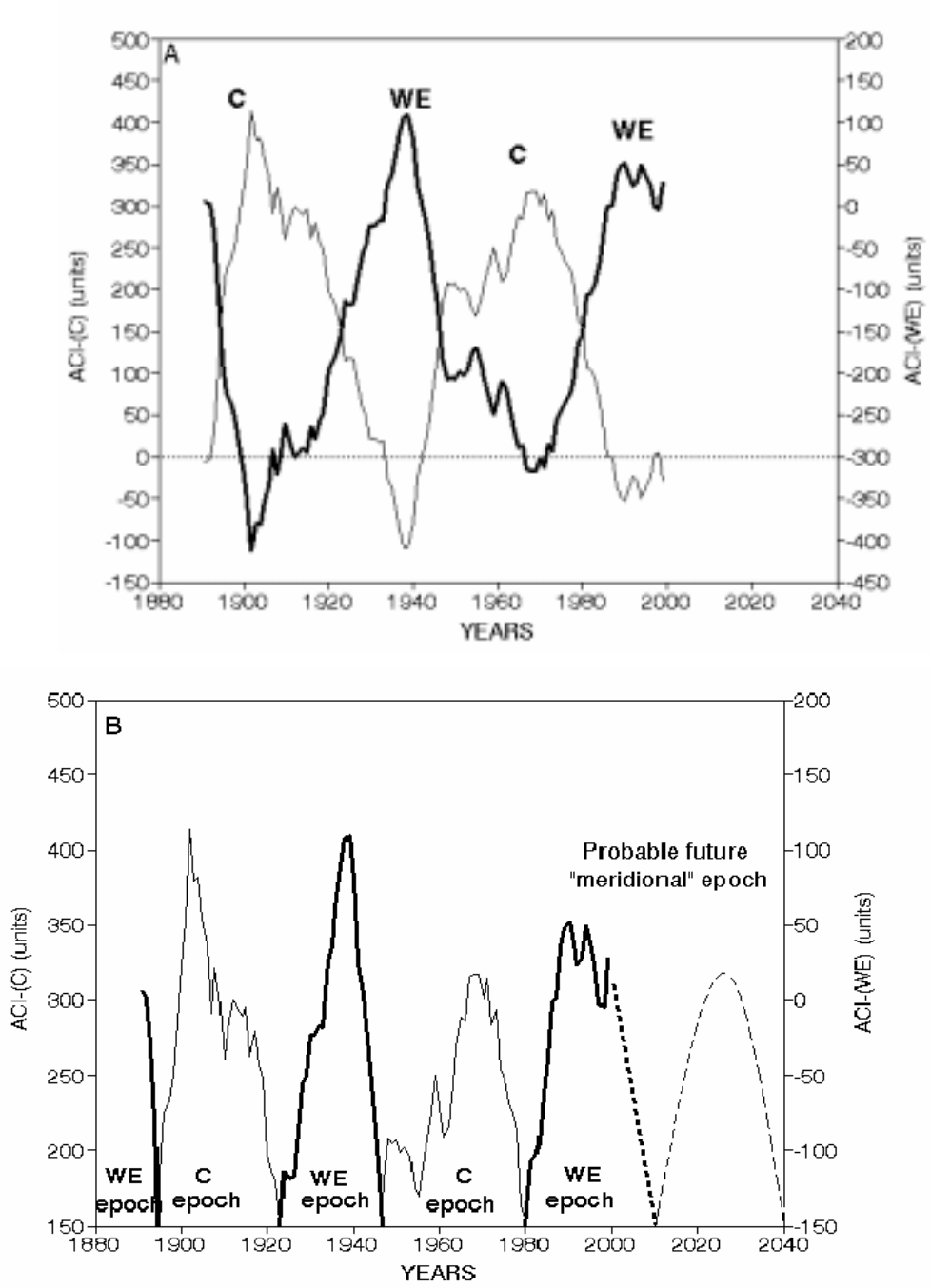

Figure 3.6 Dynamics of “meridional” (C) and “zonal” (WE) forms of the Atmospheric Circulation Index (A), and alternation of “meridional” and “ zonal” circulation epochs (B) (see the text for details).

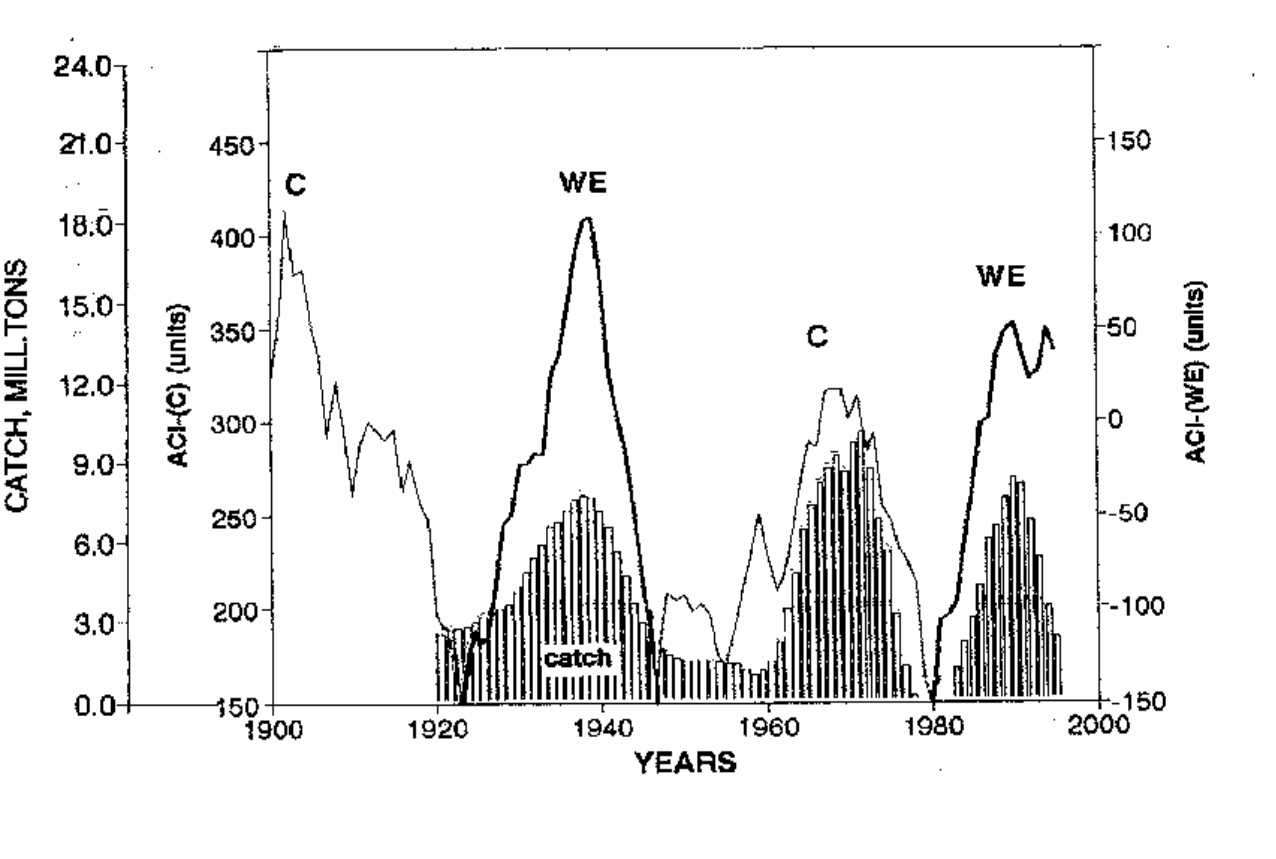

Figure 3.7 Catch oscillation of total major commercial species in the Pacific and Atlantic as compared with alternating meridional and zonal circulation epochs.

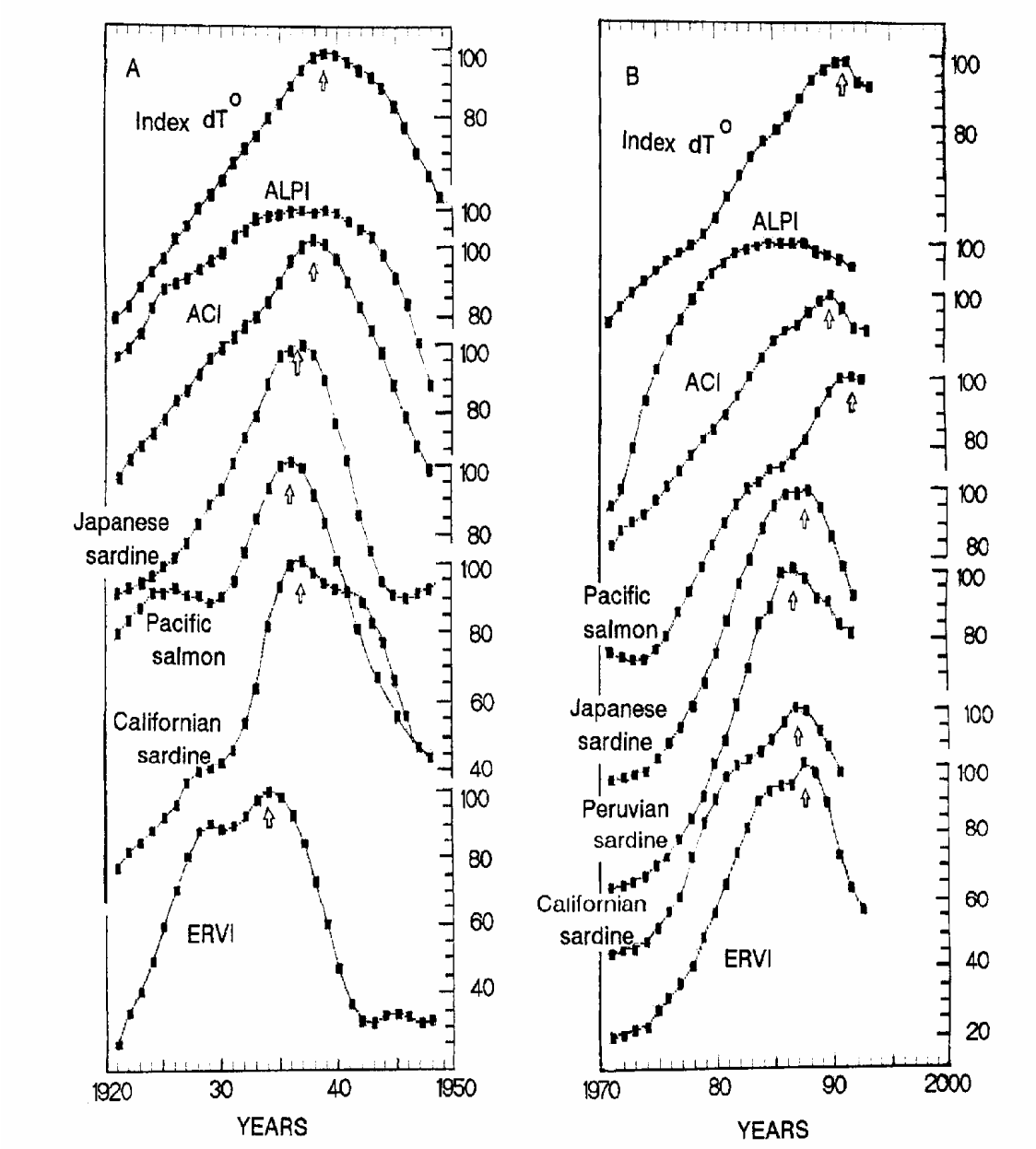

Figure 3.8 The general scheme of patterns in climatic indices and commercial catches in the Pacific for the periods of the 1920-1950 (A) and 1970-1995 (B). All curves are presented relative to a specific maximum taken as 100 percent and marked by arrows (from Klyashtorin 1998). dT:Global air surface temperature anomaly. ACI: Atmospheric Circulation Index. ALPI:Aleutan Low Pressure Index. ERVI: Earth Rotation Velocity Index (- LOD). See text for the details.

3.1 SUMMARY

ACI may be considered as a reliable climatic index related to long-term regular changes in the major commercial fish stocks.

The new "meridional" epoch of the atmospheric circulation is beginning to shift from the present "latitudinal" epoch. In the next decade, the production of the major commercial species is expected to decrease in the North Pacific and increase in the North Atlantic.

The data suggest a good agreement between the catch dynamics of the major commercial species and the patterns in various climatic indices. Climate indices may therefore be a useful tool with which to develop preliminary forecasts. To develop more reliable predictions, it is necessary to have longer time series, which go beyond available fishery statistics. This requires data on climate and fish populations covering hundreds and even thousands of years, which will be described in Chapter 4.

4. DYNAMICS OF REGIONAL CLIMATIC INDICES AND MAIN COMMERCIAL CATCHES

In addition to the global climatic indices described in previous chapters, there are several regional climatic indices, which cover time series of more than 100 years. These indices may also be considered as predictors of long-term changes in fish production.

Aleutian Low Pressure Index (ALPI) is used as indicator of major climate processes in the North Pacific region. ALPI is calculated as the area (million square kilometers) of the North Pacific Ocean covered by the Aleutian Low Pressure system (less than 100.5 kPa). ALPI characterizes the intensity of the Aleutian Low Pressure Center in the region, where ALPI refers to the area of low atmospheric pressure (Beamish *et al.* 1999).

The North Pacific Index (NPI) is measured as the average atmospheric pressure at sea level over the North Pacific. NPI is almost the inverse of ALPI and characterizes the same processes – i.e. changes in the atmospheric pressure in the North Pacific (Trenberth and Hurrell 1995)

Pacific Decadal Oscillation (PDO) characterizes long-term fluctuations of the average North Pacific sea surface temperature (Manthua *et al.* 1997).

Southern Oscillation Index (SOI) measures the difference in the atmospheric pressure between Darwin (Australia) and Tahiti (along the equator). SOI is related to the El Niño Southern Oscillation index (ENSO). El Niño events occur when the sea level atmospheric pressure in Darwin is abnormally high (Manthua *et al*. 1997).

In relation to the dynamics of regional climatic indices, there are two basic questions that need to be addressed. (1) How closely are long-term changes in regional indices correlated with changes in global indices? (2) Do the dynamics of regional indices correspond to changes in the stocks, and therefore catches, of the main commercial species? Figure 4.1 compares the dynamics of global and regional climatic indices with commercial catches of major fish species. It is readily seen that the dynamics of regional North Pacific climatic indices (ALPI, NPI, PDO) and the global geophysical index (- LOD) are very similar both in phase and magnitude (Klyashtorin 1999).

The Southern Oscillation Index (SOI) also corresponds closely in phase (but not in magnitude) to the dynamics of regional North Pacific climatic indices and (-LOD).

All four regional climatic indices (ALPI, NPI, PDO, and SOI) and LOD have two main (1930s and 1980s) and one intermediate (1960s) maxima. At the same time, global indices dT and ACI have only two maxima of 1930s and 1990s, with an interim period of about 60 years.

Interestingly, the dynamics of the PDO index (the sea surface temperature) has a weak intermediate maximum during the 1960s, but otherwise the general run of PDO is similar to the dT and ACI dynamics.

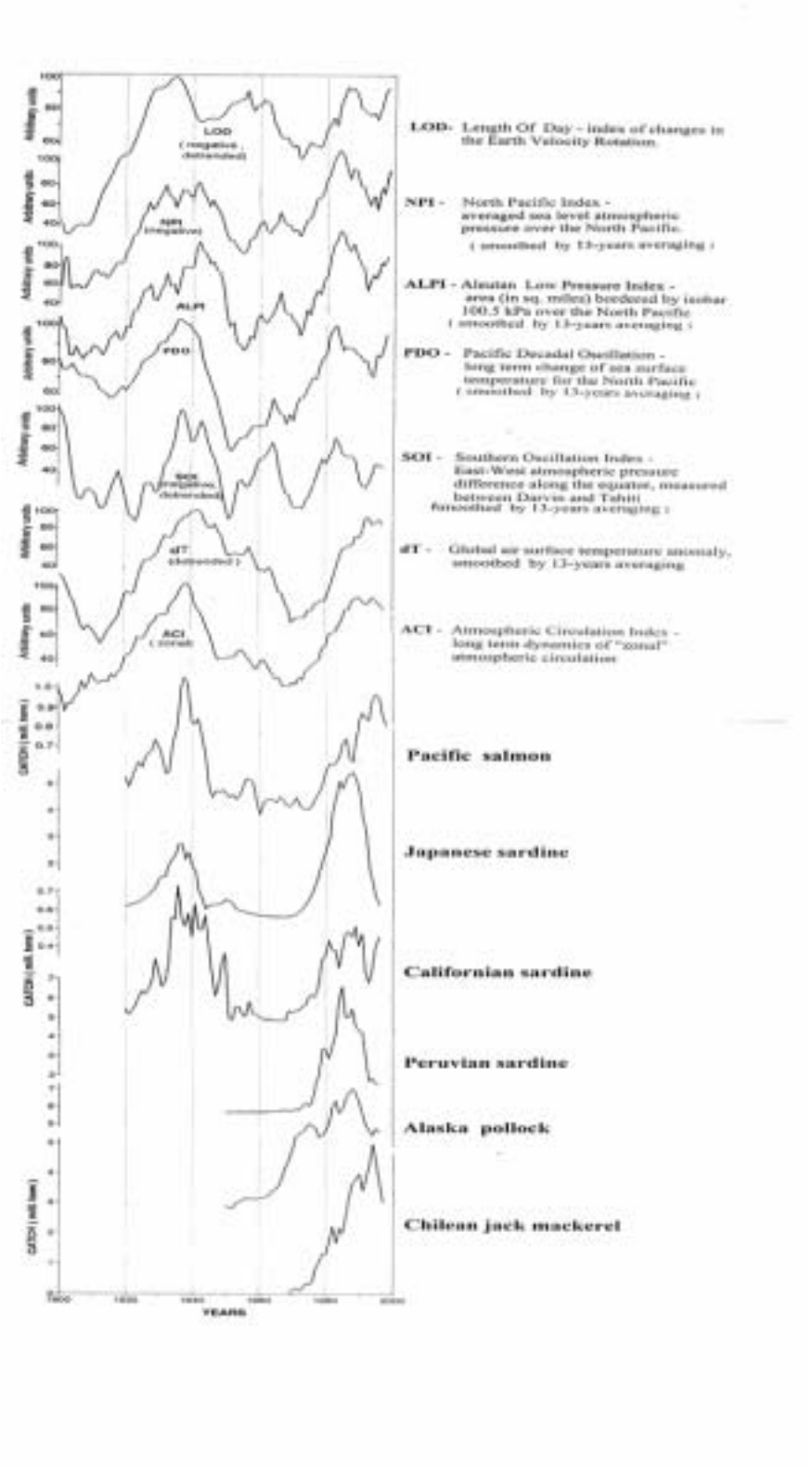

Figure 4.1 Dynamics of the global and regional climatic indices, and catch of the major commercial species in the Pacific region.

4.1 SUMMARY

It might be expected that regional climatic indices should better agree with the fish production dynamics in the corresponding regional ecosystems compared to global indices. However, Figure 4.1 suggests that the catch dynamics of the main Pacific commercial species (Pacific salmon, Japanese, Californian, and Peruvian sardine, Alaska pollock and Chilean jack mackerel) are in closer correlation with the global climatic indices dT and ACI, compared to the corresponding regional indices.

The true significance of regional indices is likely to be shown in more detailed studies on climate–production dependence. For example, pink salmon catch over the last 80 years is better correlated with ALPI, compared to global climatic indices (Klyashtorin 1997).

5. LONG-TERM AND SHORT-TERM TIME SERIES OF GLOBAL CLIMATIC INDICES AND FISH STOCK

To begin with, it is necessary to clarify the term "climate" in the context of this study. Climate can simply be defined as weather conditions statistically generalized over a time period large enough to smooth annual and decadal fluctuations (Battan 1983, Monin 2000). According to common practice and recommendations of the Climatological Congress of 1933, climatic events should be described using 10 and 30-year averaging periods for areas of many thousands square miles. The term "climate" is not used to describe meteorological events of several days to several months scale, but refers to the expected, or "average" weather, which we have seen, based on 30-year periods over the last century or so.

The time series of the climate indices at our disposal can be divided into two main groups: (1) Long-term time series of hundreds and thousands of years and (2) short-term time series covering the period of instrumental observations (100–150 years).

5.1 LONG-TERM CLIMATIC TIME SERIES

Surface air temperature for the last 1420 years reconstructed using ice cores sampled from a Greenland glacier ("Ice core temperature").

Polar glaciers contain paleo-climatic information in the form of the isotopic composition of the oxygen as described by the delta-function: the parts per thousand (‰) deviation of the heavy oxygen isotope (^{18}O) concentration in the ice from that of Standard Mean Ocean Water. Continuous delta-profiles of the oxygen isotope down the polar ice cores are interpreted in terms of climatic variation. The most suitable location to perform global paleo-temperature reconstruction using this method is the central region of the Greenland ice sheet, where the conditions for snow and ice accumulation are believed to have remained stable over the last 1500 years. «Nowhere else in the world is it possible to find a better combination of a reasonable high accumulation rate, simple ice flow pattern (which facilitates the calculation of the time scale), high ice thickness (which offers a detailed record, even at a great depths) and meteorologically significant location (close to the main track of North Atlantic cyclones).» (Dansgaard *et al.* 1975). Analysis of the ^{18}O content in the ice core at more than 500m in depth (with an annual section of 0.29 m) made it possible to reconstruct the mean annual air surface temperature for the last 1423 years, from 552 to 1975 (Fig 5.1A)[2].

Summer surface air temperature for the last 1400 (500-1900) years reconstructed from the tree rings of Scots pine.

The tree growth in the polar region takes place only in the warm (late spring–summer) season, which makes the tree ring widths clear enough to perform reliable, long-term measurements (Briffa *et al.* 1990). The temperature data reconstructed from the tree rings are different from those obtained using the ice cores. The average-annual dT calculated from the ice cores display the annual fluctuations depending primarily on the winter temperature regime, whereas the temperature dynamics estimated

[2]Dr. W. Dansgaard (Geophysical Isotope Laboratory, University of Copenhagen, Denmark) kindly provided these data, which belong to the Institute of Geography, Russian Academy of Sciences. I am very grateful to Dr. V.A. Nikolaev from this institute for his permission to use the data.

using the tree rings characterize the summer temperature regime (Fig. 5.1B). Thus, both time series reflect the long-term climate changes, but each series has its own particulars.

Sardine and anchovy populations reconstructed from the data on fish scales in varved sediment cores.

Varved sediments of southern California provide a historical record of pelagic fish populations. Anaerobic conditions in layered sediments preserve fish scales and produce a yearly record of pelagic fish population structure. The variation of sardine and anchovy abundance in the Californian upwelling were obtained from layer-by-layer analysis of the sediment cores, and be can be determined from the resolution of a 10-year sampling window (Baumgartner *et al.* 1992). The author presented direct data on the variation in fish abundance for almost 1700 years. The data suggest that the sardine and anchovy outbursts have occurred regularly for 1700 years with a period about 60 years. The fluctuations of sardine and anchovy stock (and catches) in the last century, when subject to considerable fishing pressure, are not different by period nor magnitude from the corresponding fluctuations during the past 1700 years when the fishery effect was obviously negligible.

Figure 5.1c and Figure 5.1d present the reconstructed time series of sardine and anchovy populations biomass reproduced from the originals by Baumgartner *et al*. (1992). The time series of temperature reconstructed by the Greenland Ice cores ("Ice core temperature") and by Tree ring analyses present the annual values, whereas the fish population indices are averaged over ten year periods.

5.2 SPECTRAL ANALYSIS OF THE LONG-TERM TIME SERIES

Spectral analysis was used to distinguish the most regular dominant oscillations in all these time series. The low-frequency part of the time series is omitted in the picture for clearer comparison. Figure 5.2 shows similar spectral characteristics between those of the "Ice core temperature" and sardine abundance for the last 1500 years: principal maxima of the spectral density in both time series are of 54-57 and 223-273 years. The first fluctuation period (54-57 years) is similar to both "Ice core temperature" and sardine biomass and is of greatest importance for fishery forecasting.

The spectrum of anchovy fluctuations is significantly different from the spectrum of "Ice core temperature", but close to the spectrum distribution of "Tree ring temperature". Dominant fluctuation periods in this case are about 100, 70 and 55 years. The maximum of 30 years is also well pronounced.

The sardine outbursts occur in phase with the increase in global temperature and "zonal" epoch of atmospheric circulation (see above), whereas the anchovy maxima fall on the periods of global temperature decrease and "meridional" epoch of atmospheric circulation. This dependence is likely to determine the observable differences in the spectra of these two species.

A generalized spectrum (Fourier-aggregated signal) of four of the time series is presented in Figure 5.2. The figure includes only the oscillations common for the four time series (individual details are omitted). The most pronounced peak is around 58 years, but oscillations of 44, and 30 years are significant as well.

For comparison, Figure 5.3. presents the full spectrum of annual (non-smoothed) values of "Ice core temperature" for the last 1420 years. It is clear that the period of 54 years is the only dominant multidecadal frequency, with similarly pronounced oscillations only at a much higher frequency (13 and 19 years).

The low-frequency oscillations with a period of 160 years are also well manifested. This type of periodicity is not of direct significance for our purposes, though it may be a useful tool to understand better the present age-long increase in the global temperature anomaly (dT) commonly referred to as “global warming”.

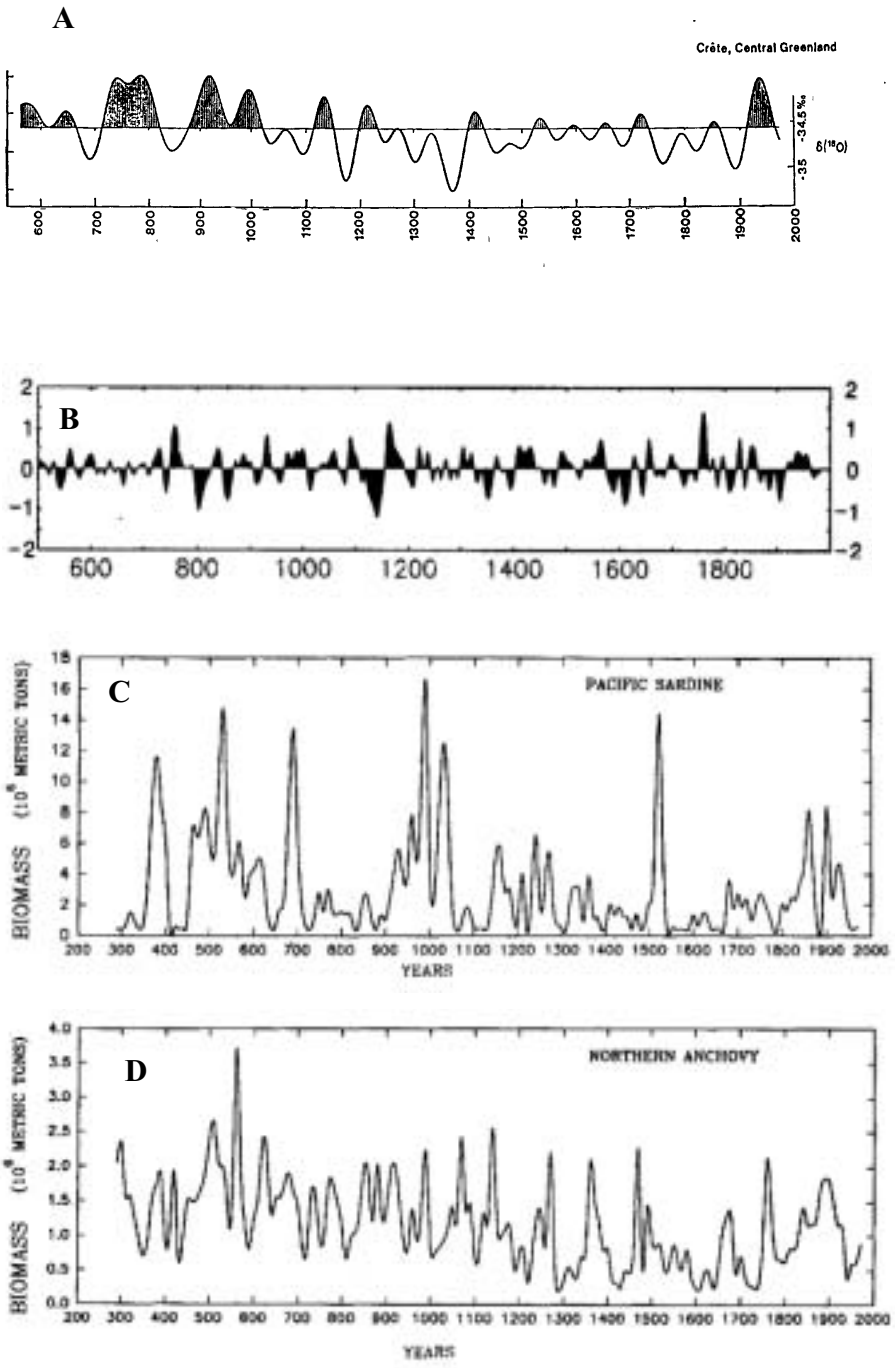

Figure 5.1. Reconstruction of: A - air-surface temperature by Greenland Ice Cores O^{18} for the last 1420 years (Dansgaard *et al.* 1975); B - summer temperature by Scots Pine Tree Rings for the last 1400 years (Briffa *et al.* 1990); C and D – sardine and anchovy biomass estimated from Californian varved bottom sediments for the last 1700 years (Baumgartner *et al.* 1992). Time series of sardine and anchovy abundance are averaged by 10-year sections. Cyclic fluctuations of climate and commercial fish stocks are believed to have a period of at least several decades.

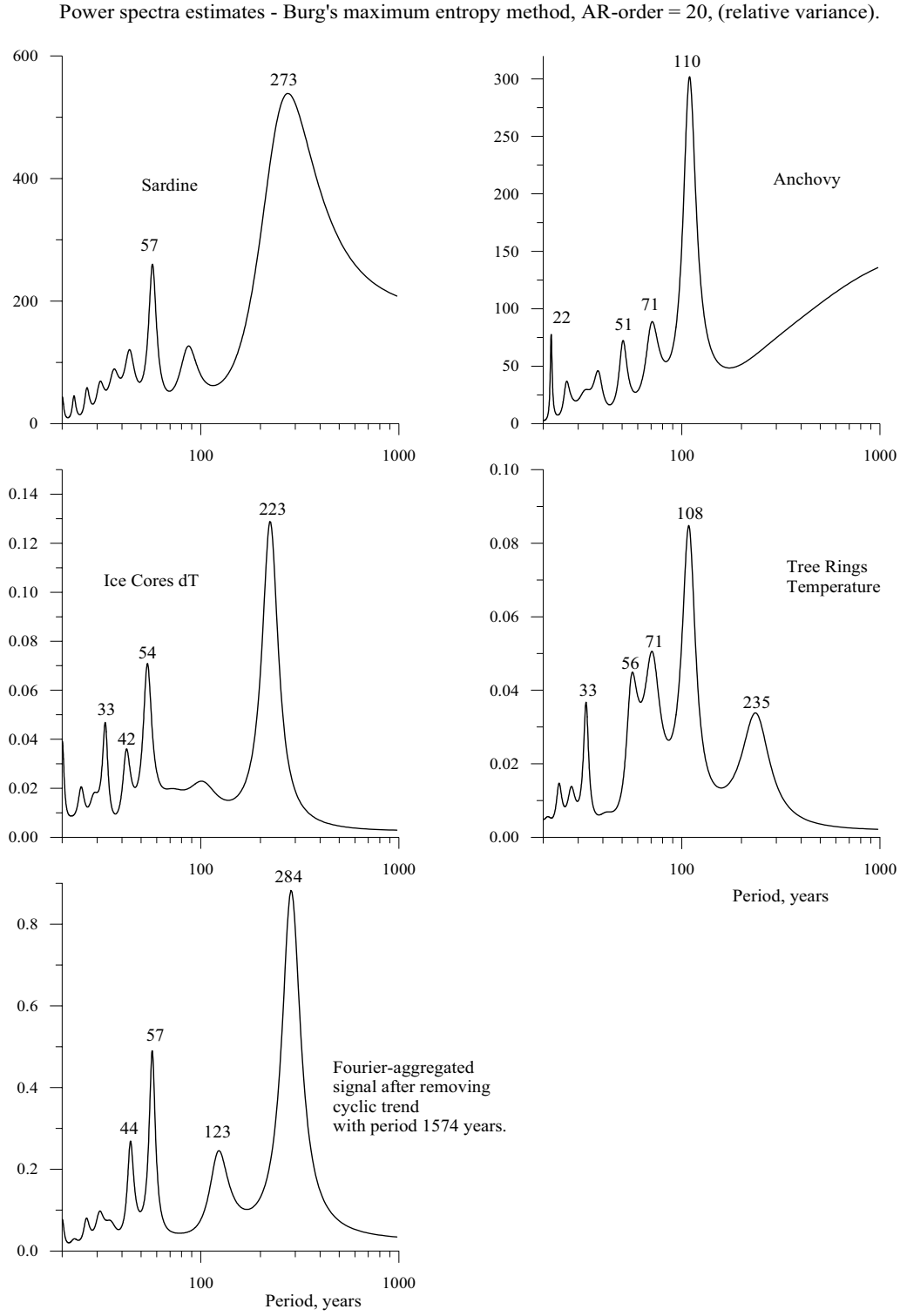

Figure 5.2 The spectra of the reconstructed time series of temperature based on samples from ice cores, tree rings, and sardine and anchovy biomass estimates for the last 1500 years. (All data were smoothed by a 10 year moving average).

5.3 SPECTRAL ANALYSIS OF THE TIME SERIES OF THE "INSTRUMENT MEASUREMENT PERIOD"

As was shown in Chapter 3**,** average annual values of global temperature anomaly (dT)**,** that have been measured since1861 are characterised by high interannual variability. Use of dT as a climate index is

possible only after 10–13 year moving average smoothing of the time series, which considerably limits its utility as a predictive index. Moreover, the dT dynamics exhibit a significant age-long trend, which restricts its comparison with the dynamics of commercial fish stocks.

Length of Day index (LOD) is less variable, since it is measured using precise astronomical methods and data on its actual dynamics can be obtained anytime. However, LOD is a geophysical index that is not only directly dependent upon global climate changes. Its dynamics have a range of causes, and is complicated by the age-long trend, which limits its direct application as a reliable predictor.

The Atmospheric Circulation Index (ACI), as shown in Chapter 3, although measured over the Atlantic-Eurasian sector of the Western Hemisphere, almost coincides in dynamics with both observed dT and LOD. It can therefore be considered as a global scale index. It has no age-long trend and may be directly compared with fishery parameters, such as catch dynamics.

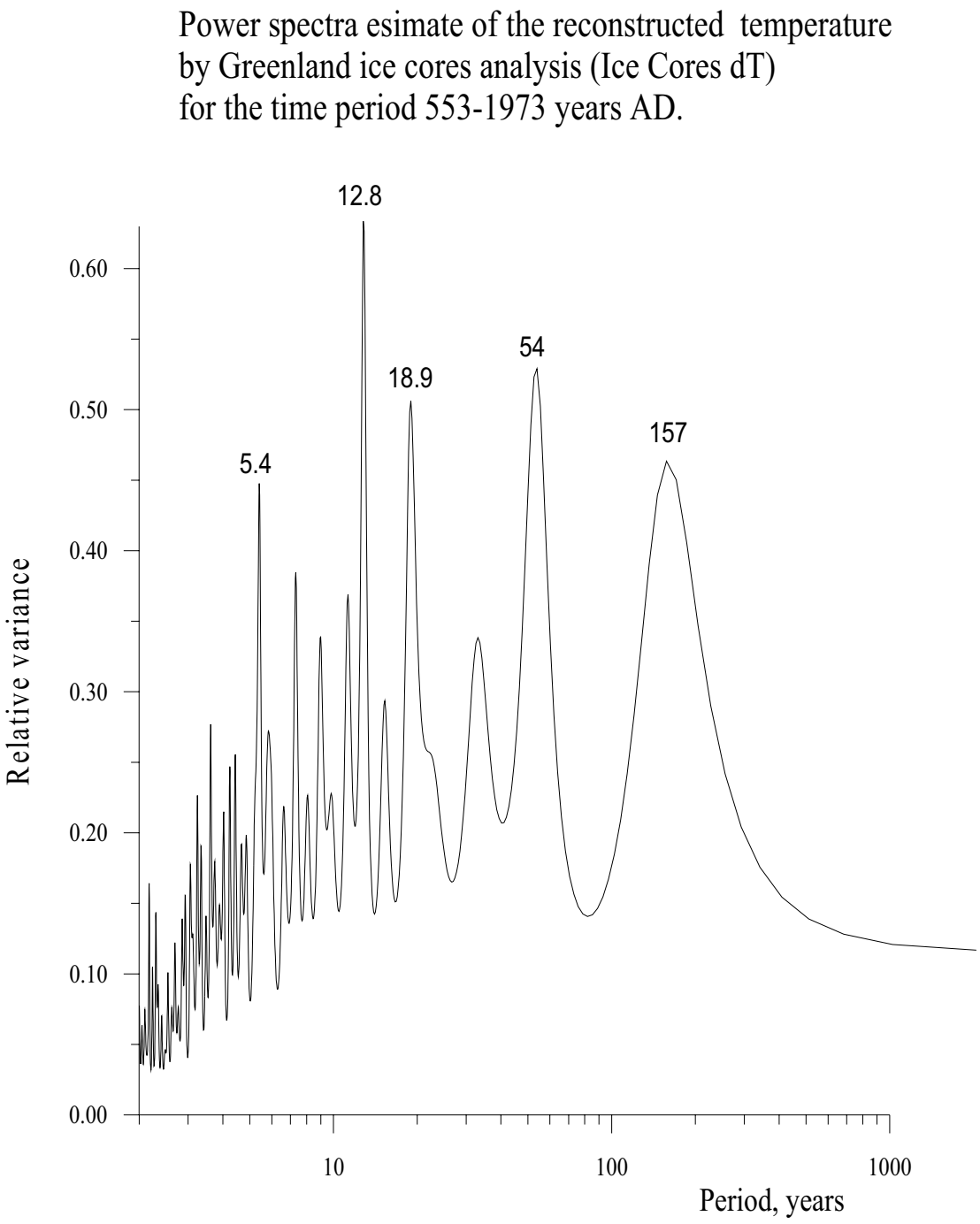

Figure 5.3 The full spectrum of unsmoothed reconstructed temperatures from ice core samples for the last 1420 years.

Spectral analysis of the time series of dT, ACI and LOD are presented in Fig 5.4. It is clear that the spectra of dT, ACI and LOD are rather similar. Primary maxima of dT and ACI are 50-55 years, and the period of the LOD cycle is 64 years. Other maxima are less pronounced, although there are clear peaks of ACI and LOD values (19 and 23 years, respectively) in the high frequency (left) range of the spectrum. The latter indicates that there is a global climate cycle with a frequency of about 20 years. Its effect on biota should be taken into account.

Table 5.1 Primary and secondary spectral maxima of measured and reconstructed time series.

Climate indices	Time period (years)	Primary Maximum	Secondary Maxima	
Global temperature anomaly (dT)	(1861 - 1998)	55	18	5
ACI	(1891- 1999)	50	19	8
LOD	(1850- 1998)	64	23	9
"Ice core temperature"	(552 - 1973)	54	42	33
Anchovy	(500 - 1970)	110	71	51
Tree rings dT	(500 - 1970)	108	71	56

Table 5.1 compares the spectral characteristics of long-term (1500 year) and short-term (150 years and less) time series. The table suggests that primary spectral maxima of dT, ACI, LOD, "Ice core temperature" and Sardine peaks are similar (the average maximum is about 56 years). On the other hand, the fluctuations of "Tree ring temperature" have a periodicity closer to the anchovy outbursts. The maximum in this case occurs at about 110 years, which is close to double the periodicity of the other time series (dT, ACI, LOD, "Ice core temperature", and sardine). Additional studies are necessary to clarify these phenomena. The spectra of long-term anchovy stock dynamics have pronounced maxima with the periods of 51 and 71 years.

5.4 COMPARING THE DYNAMICS OF MEASURED (DT) AND RECONSTRUCTED ("ICE CORE TEMPERATURE") TIME SERIES

It is important to know whether the long-term temperature oscillations reconstructed by ^{18}O content in the ice cores corresponds to the dynamics during the shorter recent period for which direct temperature measurements are available. Figure 5.5 presents the spectral signal of "measured dT" in comparison with the reconstructed "Ice core temperature". The dynamics of reconstructed temperatures based on Greenland ice cores is practically the same as that estimated from direct measurements of global dT. Therefore, both time series are coherent during the last 112 years (1861–1973), which confirms the reliability of the reconstructed time series.

5.5 SUMMARY

The most pronounced spectral maximum of the long-term fluctuations for all "long-term" time series (excluding anchovy) varies within the interval of 54–58 years. The corresponding climate cycles (both measured and reconstructed) vary within the range of 50–65 years (in average, 56 years). Other, less significant cycles (13- and 20-year fluctuations of summer temperature) may also be of interest, but no reliable correlation between these cycles and commercial catch fluctuations has been found.

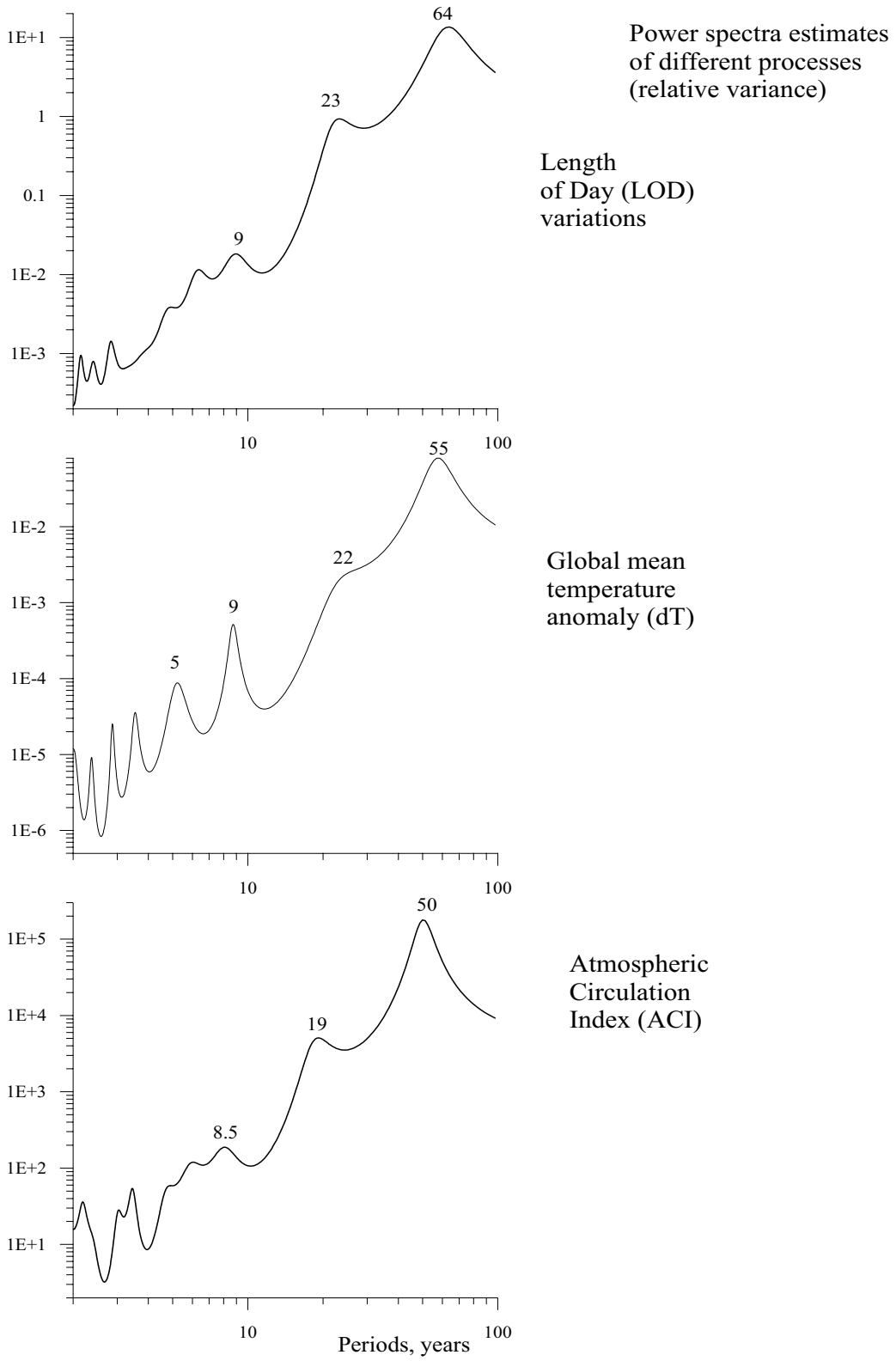

Figure 5.4 .The spectra of the instrumental time series LOD, dT and ACI (see text for details).

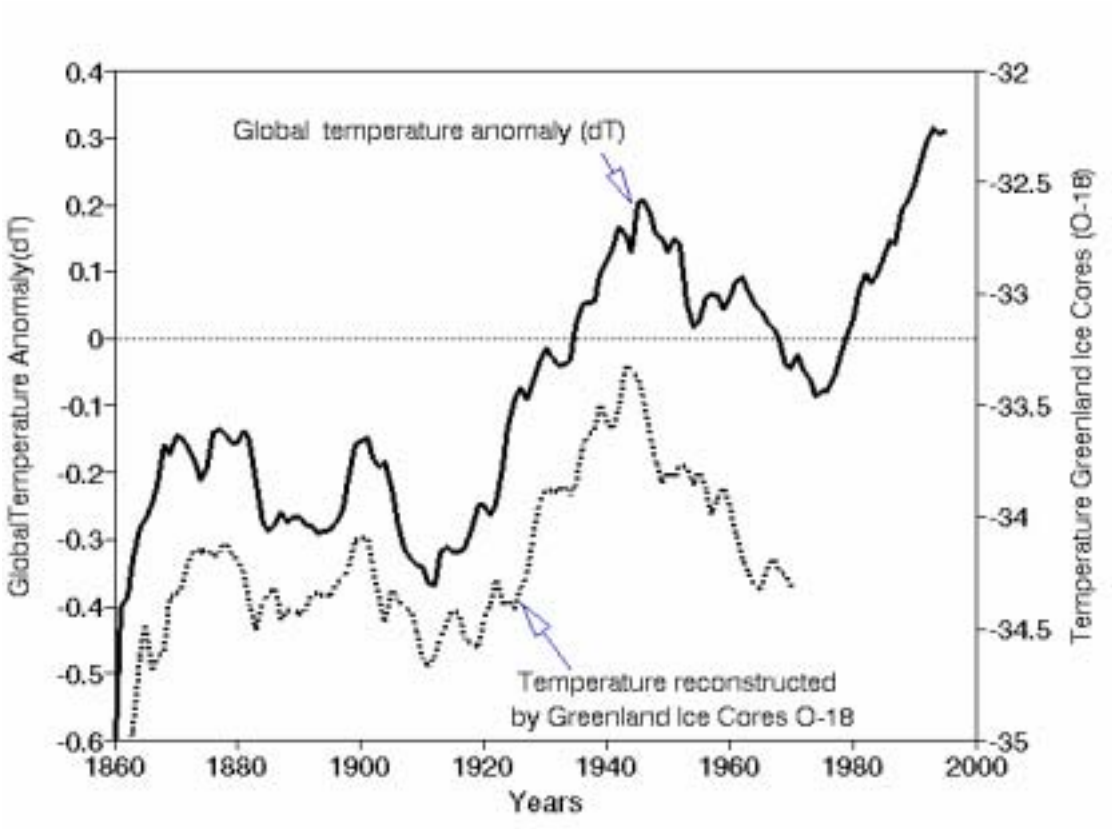

Figure 5.5.Comparing the dynamics of measured global temperature anomaly (dT) and temperature reconstructed by Greenland Ice Cores ^{18}O.

6. ANALYSING STATISTICAL TIME SERIES OF MAIN COMMERCIAL SPECIES

The catch alone is acknowledged to be a crude measure of abundance, but the changes in catches of main commercial species have been so marked, that there can be little doubt that they reflect real change in population size (Lluch-Belda *et al.* 1989). In Chapters 3, 4 and 5, it was shown that the catch dynamics of the most abundant commercial species is in close correlation with regular changes of climatic indices dT and ACI. Thus, the long-term time series of these indices may be used as a long-term index of population size of the major commercial species.

Specific features of the catch dynamics of these species may be discovered by spectral analysis of the long-time series of the catch statistics. The following series were analyzsed (data for period 1950-1998 taken from FAO 2000):

Pacific Ocean

- Pacific salmon (1920-1998)
- Pacific herring (1900-1998)(W. North Pacific, Large Marine Ecosystem No 46)
- Japanese sardine (1920-1998),
- Californian sardine (1920-1998)
- Peruvian sardine (1950-1998)
- Alaska pollock (1950-1998)
- Chilean jack mackerel (1969-1998)
- Peruvian anchovy (1950-1998)

Atlantic Ocean

- Atlantic cod (1930-1998)
- Atlantic herring (1930-1998)
- European sardine (1957-1998)
- South -African sardine (1950-1998)

The most interesting results were obtained from analyzing the longest time series: Pacific salmon, Japanese sardine, Californian sardine and Pacific herring. These and other spectra are presented in Figure 6.1 and Table 6.1.

The spectral characteristics of Pacific salmon, North-West Pacific herring, and Japanese sardine dynamics appear close to those of climatic series (all spectra exhibit maxima at 50–53 years). Spectral characteristics of the Alaska pollock and Atlantic cod time series (62 and 53 years, respectively) are close to the spectra of Pacific herring and Japanese sardine dynamics.

In contrast, the spectrum of Japanese sardine catch seems to be "abnormal" (basic periodicity is of 34 years), although this species is thought to be a good example of the climate–production dependence (Kawasaki 1992a, 1994; see Figure 3.3). Nevertheless, the sardine outbursts fall in the 1930s and 1980s, whereas the general dynamics of this species corresponds to roughly 50-year periodicity that are characteristic for climate fluctuations as well. However, statistical treatment of the corresponding time series does not reveal this regularity, but instead indicates a clear maximum at 34 years. A reason for this could be an artefact of the mathematical model. The applied mathematical method was

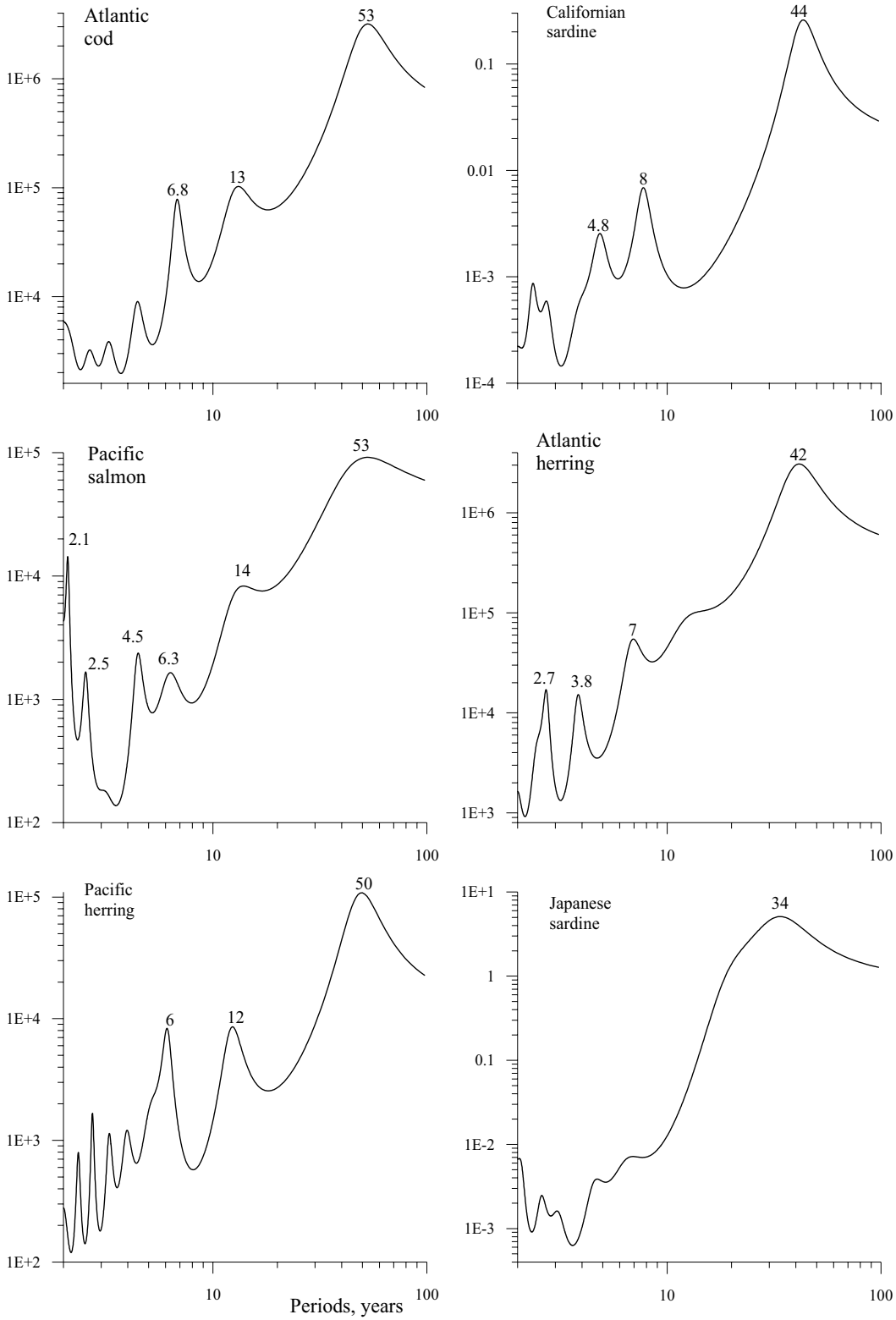

Figure 6.1 Power spectra estimates of the fish catch time series (abscissa- periods, years; ordinate-relative variance) (see text for details).

Table 6.1 Basic spectral parameters of the catch time series for the main commercial species.

Species	Main Maximum	Secondary Maxima	Comments
Pacific salmon	53	14 and 6.3	
Pacific herring	50	12 and 6	North-West Pacific
Japanese sardine	34		See comments in the text
Californian sardine	44	8 and 5	
Alaska pollock	62		
Chilean Jack	43		
Peruvian anchovy	29		See Chapter 10
Peruvian sardine	29		See comments in the text
Atlantic cod	53	13 and 7	
Atlantic herring	42	7 and 4	
European sardine	47		
S. African sardine	42		

developed to analyse sinusoidal or close to sinusoidal cyclic processes. In our case, however, the time series does not satisfy this condition, but consists of two sequential, non-sinusoidal outbursts. Strictly speaking, the considered time series is not a "continuous" process, but a sequence of two separate events with a quiescent period between. The same reason (non-sinusoidal shape of the catch dynamics) could also explain the low spectral frequency of Californian sardine (44 years).

The catch dynamics of other species: Peruvian, European and South African sardine, Atlantic herring and Chilean jack mackerel, are characterised by a single maximum, and correct estimation of their fluctuation frequency is more dependent upon the shape of their respective catch-dynamics curves, as well as their quite different life history patterns (Sharp, Csirke, and Garcia 1983).

For these very short series, we used a time series model with a single harmonic cyclic trend. This method could be called fitting an AR(2)-model with single cyclic trend with unknown period (see Chapter 8). Because of the short length of the series, it was not possible to define the period value from the power spectra estimates.

Catch dynamics depend on economic and market factors as well as stock fluctuations. If commercial fisheries always removed the same proportion of the fish production, the catch dynamics may better reflect the climate–production dependence (e.g. Pacific salmon). For example, at initial stages of an outburst, commercial fisheries seem to lag behind the fish population growth (because of information lag), whereas the corresponding shrinkage of a commercial fishery may start well before the minimum in fish stock size is reached because of decreasing profitability. This may result in "narrower" catch dynamics compared to actual stock dynamics, and underestimate the fluctuation periods derived from the spectral analysis. Such "understatement artefacts" may affect the spectra of Peruvian sardine and anchovy time series (29 years). At the same time, catch maxima of the major commercial species departs slightly from the maxima of climatic indices (for example "zonal" or "meridional" ACI epochs). These species-dependent specifics of each commercial fishery may cause the observable differences between the spectra of the climate indices and catch dynamics.

6.1 CONFORMITY OF THE CLIMATE DYNAMICS TO COMMERCIAL STOCK FLUCTUATIONS

Regular fluctuations in the stocks and catches of abundant fish species are mentioned in a number of recent publications. Beamish and Bouillon (1993), Klyashtorin and Smirnov (1995) and Klyashtorin (1997, 1998) have called attention to the approximate 60-year periodicity in the fluctuations of Pacific salmon. Reconstructed time series of sardine population for the last 1500 years (Baumgartner *et al.* 1992) also suggested around 60-year between sardine outbursts. Jonsson (1994) indicated the same periodicity in the time series of Atlantic cod catch for 300 years. In more last years, many researchers

have reported on regular 50–70 year fluctuations of global climate parameters (Minobe 1997, 1999). A close correlation between the catch dynamics of the major commercial species and approximately 60-year climate fluctuations was also recently shown by Klyashtorin (1998).

Japanese chronicles contain information on the Japanese sardine outbursts for the last 400 years. Changes in availability and abundance of sardine stocks caused the development as well as collapse of various coastal fishing villages (Kawasaki 1994). Outbursts of Japanese sardine have occurred simultaneously with increasing temperature trends, up to, but not beyond the temperature dynamics maxima with the average period of about 60 years (Figure 6.2). The temperature dynamics for the period of direct measurement during the last 150 years is in good agreement with the temperature reconstructed from the Greenland ice cores.

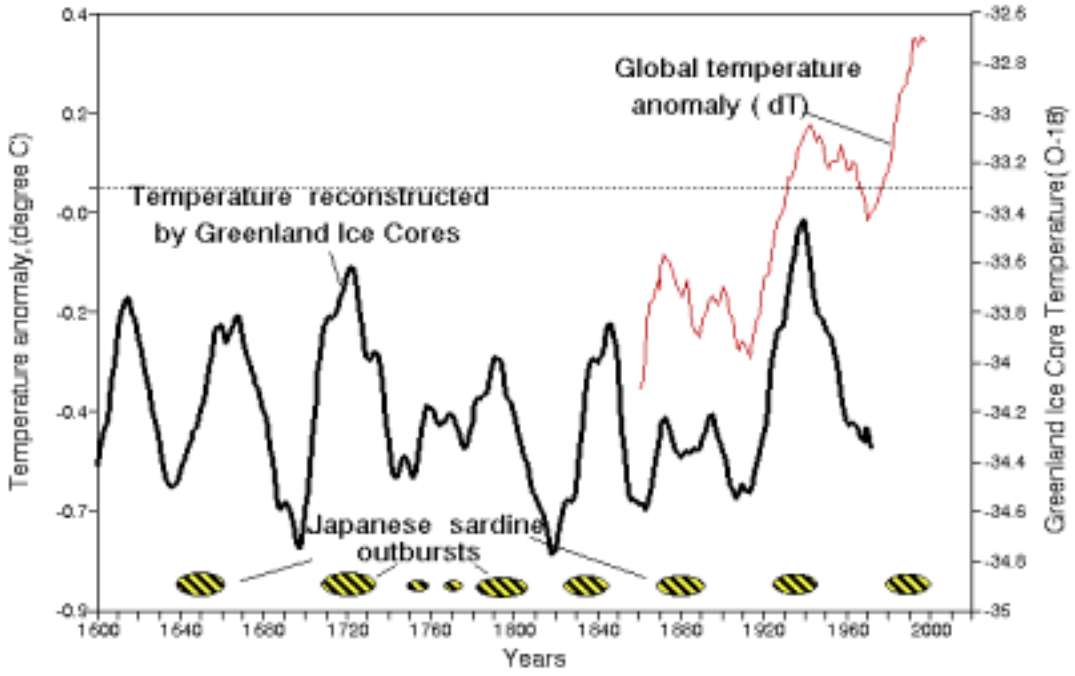

Figure 6.2 Cyclic temperature fluctuations and Japanese sardine outbursts for last 400 years by Japanese historic chronicles 1640-1880 and for 1920-1998 from fisheries statistics.

7. ESTIMATING RELIABLE TIME SCALES TO MODEL CLIMATE AND STOCK CHANGES

Considering the correlations between climate and stock fluctuations, the dynamics of global climatic indices and commercial catches of abundant fish species certainly undergo synchronous regular fluctuations. To develop a predictive model, it is necessary to identify mathematical descriptions that satisfy two basic conditions: (i) a successful model should fit the past dynamics of the indices well, and (ii) it should establish future changes in the fish stocks for up to 30–40 years ahead. An important feature of the suggested model is its ability to forecast cyclic climatic trends, and therefore the corresponding future trends in commercial fish stocks.

An important practical question to be answered before modelling fish stock dynamics on the basis of climate–population dependence is: which periods (cycle lengths) are of most predictive significance? As shown above, the spectral analysis of the dynamics of global climatic (dT, ACI) and geophysical (LOD) indices point to the spectrum maxima at 50, 55 and 64 years. The reconstructed temperature time series of the "Ice core dT" from isotopic analyses suggests an average spectral maximum at 54 years, whereas the time series of commercial fish stocks has an average spectral frequency corresponding to 46 years. There are several reasons to believe that this frequency may underestimate stock size changes (see Chapter 6). The most reliable time series of commercial catches (Pacific salmon and Pacific herring) have spectral maxima at 50 and 53 years, respectively.

The average climate period estimated from the time series is close to 55 years, and this period is used as a basis to forecast the fluctuations of major commercial fish stocks and catches. Recent estimates of global climatic indices show cycles in the range of 50 to 70 years (Schlesinger and Ramankutty 1994; Minobe 1997, 1999). Thus, the data do not permit us to determine an exact period for either climate or fish population fluctuations. It is only possible to estimate that the average period varies within the ranges of 50–56 years (average of 53 years) and 60–65 years (average of 62 years). Therefore, taking into consideration all available time series, we cannot be limited to a fixed value, and shall operate with the probable spectral range of 55 to 65 years, with a base value of 55 years.

The time series of the surface air temperature for the last 1500 years, reconstructed from the Greenland ice cores (Ice core dT), is an important data source for independent estimation of climate cycles and trends. The close similarity between both the reconstructed temperature dynamics and measured dT time series is shown in Figures 5.5, 9.2 and 9.3. Box-Jenkins time series analysis (Box and Jenkins 1970) makes it possible to model the basic harmonics of the climate changes, which have taken place in the last 1000 years. Changes in global temperature are presented in Figure 7.1 as a "topographic map". Colour intensity is directly proportional to the manifestation (recurrence) of the climatic changes in the period on the X-axis. It is easy to see that the climate periodicity of 120-140 years was most pronounced from 500s to 1300s AD. A 70–75 year period was characteristic from the 900s to 1700s, whereas a 55–56 year period dominated from around 1500 to the 1970s. Most probably, this periodicity will remain into the next century. As to oscillations of higher frequency, the 20-year and (much less clear) 30-year maxima have been the most significant over the last millennium. Recent publications on climate dynamics report regular 20-year fluctuations of global climatic indices in addition to the well-known 50–70-year periodicity (Minobe 1997, 1999).

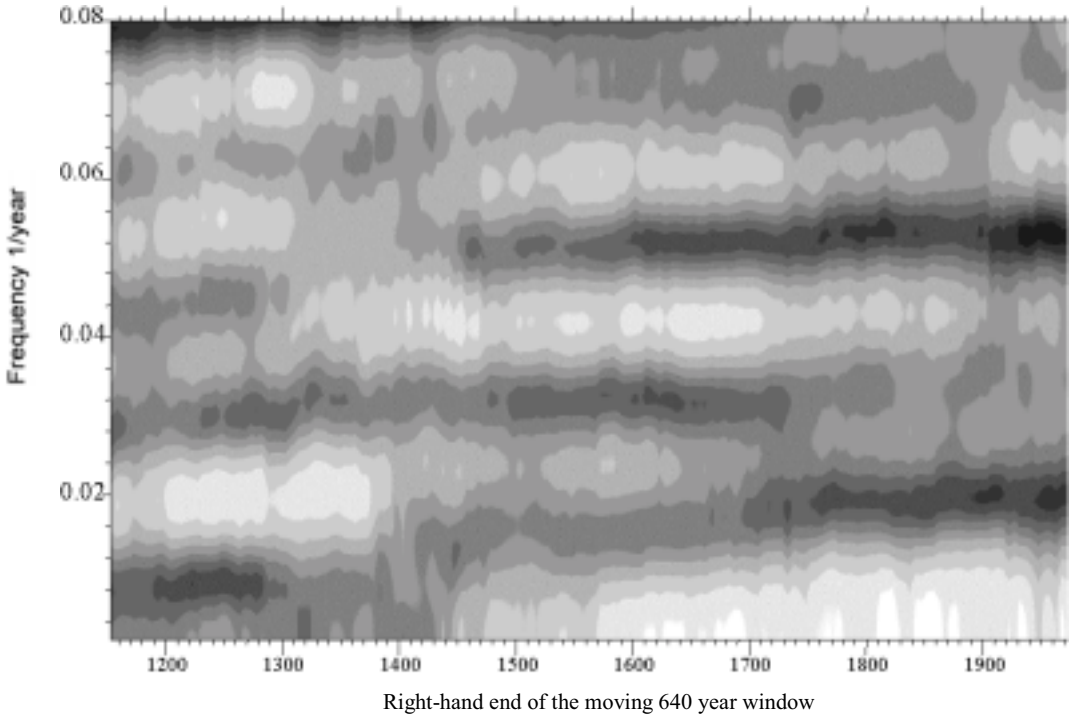

Figure 7.1 Temporal dynamics of the power spectra of the temperatures reconstructed from the Greenland ice cores (Ice Core dT) for the time period 553-1973 years AD. Shading intensity is directly proportional to the manifestation (recurrence) of the climatic changes in the period marked at the X-axis.

An advantage of Box-Jenkins models is that they enable one to trace the long-term development of the harmonics and estimate their dynamics and future trends. We analysed the data for a possible dependence of the climate indices on the variation of climate periods within the latter range. Figure 7.2 presents the generated time series of three basic harmonics of 55, 60, and 65 years. The disagreement between the three curves for the first 30 (and even 60) years is quite small in terms of our prognostic purpose and the variability of our initial data. We understand that such "forecasting" of fish stocks for 60–120 years ahead is a theoretical analysis rather than a practical or formal prognosis. However, the exercise provides a good illustration of the possibility of reliable forecasting climate changes and fish production on a smaller time scale (30-40 years).

7.1 SUMMARY

Regular climate changes have taken place over the last millennium with a period of 55–65 years. Forecasting of the major commercial fish stocks for the future 30–40 years is insensitive to the choice of periodicity within this range. Therefore, the exact period of climate changes (55, 60, or 65 years) is not critical for the purpose of catch forecasting or managing fisheries.

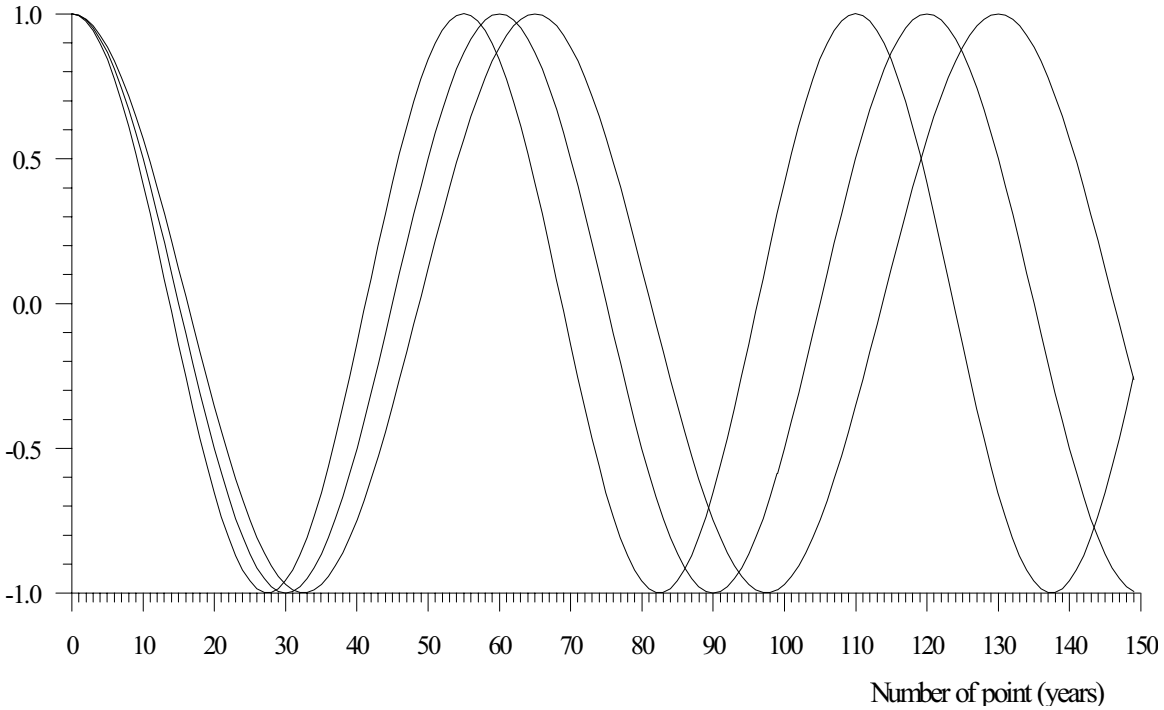

Figure 7.2 Example of the three harmonics with periods of 55, 60, and 65, with the same amplitude A=1 and the same phase angle (see the text for details)

8. STOCHASTIC MODELS FOR PREDICTION OF THE CATCH DYNAMICS

The modelled time series are represented by catch variations of the 12 main commercial species. The sampling interval of the time series is 1 year, and all series finish in 1996 and cover the following periods:

- 1900 (1 series - Pacific herring, 97 observations),
- 1920 (3 series - Californian and Japanese sardine, and salmon, 77 observations),
- 1930 (2 series - Atlantic cod and herring, 67 samples),
- 1950 (4 series - Peruvian anchovy and sardine, Alaska pollock, South African sardine, 47 observations),
- 1957 (1 series - European sardine, 40 observations),
- 1969 (1 series - Chilean jack mackerel, 29 observations)

All considered time series undergo well-manifested cyclic variation. The time series can be represented as the following sum:

$$\mathbf{x(t) = \xi(t) + F(t)\ ,} \qquad \mathbf{x(t),\ t=t_0,\ \ldots,\ t_0+N-1,} \tag{1}$$

where **x(t)** is the catch volume in the year **t, t_0** is the starting year of the series, **F(t)** is deterministic function (trend), and **ξ(t)** is a stationary component (including random noise) of the time series. The stationary component has no trends in mean or variation. The deterministic part of the model (**F(t)**) is taken as a multiple cyclic trend with **m** periods $\mathbf{T_i}$, **i=1, …, m** (Anderson 1971; Kashyap and Rao 1976):

$$\mathbf{F(t) = \sum_{i=1}^{m} (B_i \sin(\theta_i(t)) + D_i \cos(\theta_i(t)) + G}\ , \text{ where } \theta_i(t)=2\pi(t-t_0)/T_i, \tag{2}$$

where $\mathbf{B_i}$, $\mathbf{D_i}$ are unknown amplitudes, and **G** is an unknown static shift constant. Equation (2) can also be expressed as:

$$\mathbf{F(t) = \sum_{i=1}^{m} A_i \cos(\theta_i(t) - \varphi_i) + G}\ , \text{ where } \mathbf{A_i^2 = B_i^2 + D_i^2}\ , \ \tan(\varphi_i)=B_i/D_i \tag{3}$$

The stochastic part, **ξ(t)**, may be represented as an autoregressive Box-Jenkins model (Box and Jenkins 1970; Anderson 1971; Kashyap and Rao 1976) of the given order **p** (or AR(**p**)-model):

$$\mathbf{\xi(t) = -\sum_{k=1}^{p} a_k x(t-k) + \varepsilon(t)} \tag{4}$$

where **p** is the number of autoregressive parameters, $\mathbf{a_k}$, and **ε(t)** is a residual signal, which is considered to be Gaussian[3] white noise with zero mean and unknown variance $\mathbf{s^2}$. Combining formulae (1) and (4), the general model is presented as follows:

[3] The Gaussian probability distribution, also known as the Normal distribution, is often appropriate when errors show constant variation.

$$x(t) = -\sum_{k=1}^{p} a_k x(t-k) + \sum_{i=1}^{m} (B_i \sin(\theta_i(t)) + D_i \cos(\theta_i(t)) + G + \varepsilon(t) \quad (5)$$

Thus, unknown parameters of model (5) to be estimated from the data, are: **p** autoregressive parameters a_k; **2m** harmonic amplitudes B_i and D_i; a static shift constant **G**; and variance s^2 of the residual signal $\varepsilon(t)$. These parameters are estimated using the maximum likelihood method (Kashyap and Rao 1976), which in case of Gaussian noise $\varepsilon(t)$ coincides with the least squares method. Let us define **Y(t)** as the following (**p+2m+1**)-dimensional column vector:

$$Y(t) = (-x(t-1), \ldots, -x(t-p), \sin(\theta_1(t)), \cos(\theta_1(t)), \ldots, \sin(\theta_m(t)), \cos(\theta_m(t)), 1)^T \quad (6)$$

where the index "**T**" indicates a transposed (i.e. column) vector, and the parameters' column vector **c** of the same dimensionality is:

$$c = (a_1, \ldots, a_p, B_1, D_1, \ldots, B_m, D_m, G)^T \quad (7)$$

Then the model (5) in matrix form could be described as follows:

$$x(t) = c^T \cdot Y(t) + \varepsilon(t) \quad (8)$$

where c^T = row vector of parameters.

The following gives a detailed account of the method used to fit the parameters. It is not necessary to understand the fitting method to understand the results of the model. But it is useful to follow the principles used here for robust regression to understand how the particular results are derived. The parameters, **c,** can be estimated by minimising the sum:

$$\sum_{t=t_0+p}^{t_0+N-1} \varepsilon^2(t) = \sum_{t=t_0+p}^{t_0+N-1} (x(t) - c^T \cdot Y(t))^2 \rightarrow \min_c \quad (9)$$

A solution of (9) can be obtained as the solution to the Normal equations (i.e. standard least-squares regression):

$$c = A_0^{-1} \cdot R_0, \text{ where matrix } A_0 = \sum_{t=t_0+p}^{t_0+N-1} Y(t) \cdot Y^T(t), \text{ vector } R_0 = \sum_{t=t_0+p}^{t_0+N-1} x(t) Y(t) \quad (10)$$

and the unbiased maximum likelihood estimate of the variance of $\varepsilon(t)$ is:

$$s^2 = \sum_{t=t_0+p}^{t_0+N-1} \varepsilon^2(t) \Big/ (N-p) \quad (11)$$

Estimates defined by equations (10) and (11) are the least squares estimates and maximum likelihood where the errors are genuinely normally distributed. The least squares estimates can be very sensitive to outliers, so that only a few outliers can lead to parameter estimates, which are considerably different from the "true" values (Huber 1981). The outliers may occur in fishery data for various reasons, which cause a temporary violation of the assumptions of the model: increases in illegal activities or the influences of rare but powerful events (war, economic crisis, etc.). One way to make estimates more resistant to outliers is to apply maximum likelihood estimates, but with the assumption that the distribution of the residual signal $\varepsilon(t)$ is Gaussian for small values of ε and Laplacian for large values of ε. This kind of distribution has the following density (Huber 1981):

$$p(\varepsilon) = \frac{\beta}{s} \exp\left(-\frac{\varepsilon^2}{2s^2}\right) \text{ for } |\varepsilon| \le s \cdot a \quad (12a)$$

$$p(\varepsilon) = \frac{\beta}{s} \exp\left(-\frac{a}{s}\left(|\varepsilon| - \frac{as}{2}\right)\right) \text{ for } |\varepsilon| > s \cdot a \quad (12b)$$

where **a** is a robustness parameter, which usually takes values 1-3 (we use **a**=2), **s** is a scale parameter (analogous to standard deviation in Gaussian law), and β is normalising constant:

$$\beta = \beta(a) = 1/(2(\exp(-a^2/2)/a + \int_0^a \exp(-z^2/2)dz)) \qquad (12c)$$

Maximum log-likelihood method for the model (12) leads to the following problem (with accuracy to an additive constant, which depends on **a** only):

$$J(c,s) = \sum_{t=t_0+p}^{t_0+N-1} \log\left(p(\varepsilon(t))\right) = -(N-p)\cdot\log(s) - \frac{1}{2s^2}\sum_{|\varepsilon(t)|\le sa}\varepsilon^2(t) - \frac{a}{s}\sum_{|\varepsilon(t)|>sa}|\varepsilon(t)| \to \max_{c,\,s} \qquad (13)$$

Solution of equation (13) can be obtained using an iterative method, which is a combination of a generalised Newton-Raphson method for vector **c** and a simple iteration method for **s**:

$$\mathbf{c}^{(j+1)} = \mathbf{c}^{(j)} + \mathbf{A}^{-1}(\mathbf{c}^{(j)}, s^{(j)})\cdot\mathbf{R}(\mathbf{c}^{(j)}, s^{(j)}) \quad , \quad s^{(j+1)} = 1/\chi(\mathbf{c}^{(j)}, s^{(j)}) \qquad (14)$$

where **j=0, 1, …** is the iteration index. Matrix **A(c, s)** and vector **R(c, s)** are computed as follows:

$$\mathbf{A}(c,s) = \sum_{t=t_0+p}^{t_0+N-1} F''(\varepsilon(t),s)\cdot\mathbf{Y}(t)\cdot\mathbf{Y}^T(t) \quad , \quad \mathbf{R}(c,s) = \sum_{t=t_0+p}^{t_0+N-1} F'(\varepsilon(t),s)\cdot\mathbf{Y}(t) \qquad (15)$$

where

$$F'(\varepsilon,s) = \begin{cases} \varepsilon, & \text{if } |\varepsilon| \le as \\ sa\cdot\mathrm{sign}(\varepsilon), & \text{if } |\varepsilon| > as \end{cases}, \quad F''(\varepsilon,s) = \begin{cases} 1, & \text{if } |\varepsilon| \le as \\ 0, & \text{if } |\varepsilon| > as \end{cases} \qquad (16)$$

Function $\chi(c, s)$ is defined as:

$$\chi(c,s) = (\sqrt{\gamma^2 + 4\alpha} - \gamma)/(2\alpha) \qquad (17)$$

where

$$\alpha = \sum_{|\varepsilon|\le as}\varepsilon^2(t)\Big/(N-p), \quad \gamma = a\cdot\sum_{|\varepsilon|>as}|\varepsilon(t)|\Big/(N-p), \quad \varepsilon = \varepsilon(t,c) = x(t) - \mathbf{c}^T\cdot\mathbf{Y}(t) \qquad (18)$$

Derivation of equation (17) is the following. If we consider the dependence of value (13) on parameter **s**, it could be noticed that the major part of this dependence is due to multipliers $1/(2s^2)$ and a/s. If δs is a small variation of **s**, then variation of the sums:

$$\sum_{|\varepsilon(t)|\le sa}\varepsilon^2(t) \text{ and } \sum_{|\varepsilon(t)|>sa}|\varepsilon(t)| \qquad (19)$$

multiplied by $1/(2s^2)$ and a/s, are much smaller than the variation of $1/(2s^2)$ and a/s alone. Hence, for a small compute variation of **J(c, s)** with respect to δs, values (19) can be considered approximately constant, so:

$$\delta J(c,s) \approx -\left(\frac{(N-p)}{s} - \frac{\alpha}{s^2} - \frac{\gamma}{s}\right)\delta s \qquad (20)$$

Applying the condition for the maximum point, $\delta J(c, s)=0$, results in one non-trivial solution for **s** in the form of a quadratic equation: $\alpha r^2 + \gamma r - 1 = 0$, where $r=1/s$. This has a unique positive root:

$$r = \chi = (\sqrt{\gamma^2 + 4\alpha} - \gamma)/(2\alpha) = 1/s$$

However, the values of α and γ are dependent on **s,** so the last equation should be used in an iterative procedure to refine the value of **s** (the 2nd equation in (14)). It should be noted that if the value of the robustness parameter **a** is large, then $\gamma=0$ and, according to (20), $s=\sqrt{\alpha}$, which is the same as (11). The iterative procedure starts from an initial approximation, which is given by the least squares' method (10) and (11). It was found that values converged reasonably rapidly within 5-10 iterations.

The order of the autoregression, **p,** and number **m** of harmonics in cyclic trend and their periods $\mathbf{T_i}$ need to be set before estimating the parameters of the model (5). The autoregression order (**p**) was assumed to be equal to 2 for all cases as the minimum value for describing a wide range of types of stochastic oscillations (Box and Jenkins 1970). As for choice of values of **m** and periods $\mathbf{T_i}$, two possible approaches were used.

8.1 THE FIRST APPROACH – NUMBER OF HARMONICS AND THEIR PERIODS ARE DEFINED FROM FISHERY TIME SERIES THEMSELVES

Let us define the time series of more than 64 samples as "long" and others as "short" time series data sets.

For "long" time series, the number of harmonics **m** and their periods $\mathbf{T_i}$ are defined from power spectra estimates of the appropriate series. The value of **m** varies from 1 to 6 and is usually equal to 3-4. Values of periods $\mathbf{T_i}$ were taken as periods corresponded to the essential peak values of power spectra estimates. Although the time series are labelled as "long", their lengths (from 67 up to 97 samples) has rather few observations for applying common procedures of spectra estimates based on the Fourier transform. For such a short series, parametric methods are more advantageous in terms of frequency resolution (Marple 1987). We use the autoregression approximation for the series, which is the procedure estimating parameters of the following model:

$$x(t) + \sum_{j=1}^{q} \alpha_j x(t-j) = \eta(t) \qquad (21)$$

where α_j, $j=1, \ldots, q$ are autoregressive parameters, $\eta(t)$ is the residual signal, which is assumed to be Gaussian white noise with zero mean and variance σ^2. Equation (21) applies the designations for parameters of the AR(**q**)-model different from those for the AR(**p**)-model in equations (4) and (5), to stress that although these models are the same, they are used for distinctly different purposes. The AR-members in formulae (4) and (5) are introduced to describe essential features of stochastic oscillations of the signal close to the deterministic cyclic trend. That is why we assumed a small order **p**=2. The AR(**q**)-model (21) is estimated to describe the spectral structure of the signal and for this purpose needs many more parameters (i.e. larger **q**). The larger the value of **q**, the more sensitive is the power spectra estimate. At the same time, increase in **q** results in the corresponding increase in the statistical fluctuations of the estimate. Thus, the choice of **q** is a compromise between sensitivity and stability. Usually, for short series **q=N/5-N/3**, where **N** is the length of time series. We used **q**=20. As soon as parameters of the model (21) are estimated, the power spectra estimate could be computed using the following equation:

$$S_{xx}(\omega) = \frac{\sigma^2}{2\pi \left| 1 + \sum_{j=1}^{q} \alpha_j \exp(-i\omega j) \right|^2} \qquad (22)$$

where ω is a cyclic frequency: $\omega=2\pi/T$, **T** = period, measured in units of sampling time interval (1 year in our case), **i** = imaginary unit. AR-methods of power spectra estimates differ from each other by procedures of estimating parameters of the model (21). We use Burg's method of maximum entropy as the most reliable and providing the best frequency resolution for short time series (Marple 1987).

For the "short" series, we used the model (5) with **p**=2 and single harmonic cyclic trend: **m**=1. Because of lack of samples in the series, we could not define the period value $\mathbf{T_1}$ from power spectra estimates. That is why it was defined by minimization of $\mathbf{s^2}$ after estimating the autoregression parameters $\mathbf{a_1}$ and $\mathbf{a_2}$, amplitudes $\mathbf{B_1}$, $\mathbf{D_1}$ and static shift constant **G** for different trial values of the period: $\mathbf{s^2(T_1) \rightarrow min}$. The last task of one-dimensional minimization is solved by a Golden Section method. This method will be defined as fitting an AR(2)-model with single cyclic trend with unknown period.

After the model had been fitted, it was used to forecast the interval 1997-2056 (the near 60-year cycle). The procedure is described below. For some species, the forecasted time series took negative values during some future time intervals. In such cases, we interpret these as a negligible forecasted catch and substituted all negative values with zero.

8.2 THE SECOND APPROACH – AR(2)-MODEL WITH A SINGLE CYCLIC TREND WITH THE PERIOD LENGTH TAKEN FROM THE CLIMATIC TIME SERIES

Earlier we used those periods in the equation (1), which follow naturally from the power spectra of the fishery time series, or those periods for which the cyclic trend is the best approximation to the data. However, such values of periods may be too sensitive to patterns in the data, which are not useful for forecasting. A long-term prediction based on the short-term behaviour of a signal is risky. The catch depends not only on natural processes in the ocean, but on economic politics of fishing-dependent countries, availability of fuel for fleets, power resources for fish processing, military and economic collisions in various regions of World ocean, etc. It is hardly possible to forecast all these (and other) factors for 10-20 years ahead. It is therefore prudent to confine the model to patterns, which can be established through independent means.

From all the above, it may be concluded that the period lengths derived from the fishery time series and then used in model (5), are estimated and therefore depend on realization and length of the sample. At the same time, there are time series for global climatic processes which, although believed to be somewhat affected by human activities or changes in local measurement environments, are much less "human-dependent" than fish stocks are.

These are:

- mean global temperature - **dT** time series, 138 annual samples for 1861-1998;
- atmospheric circulation index - **ACI** time series, 109 annual samples for 1891-1999;
- length of day (i. e. Earth rotation velocity) - **LOD** time series , 151 annual samples for 1850-2000.

In addition, the following long-term series were analyzed:

- Reconstructed air surface temperature for the period of 552-1975 AD by Greenland Ice Cores – 1420 annual samples.
- Reconstructed summer air surface temperature for the period of 500-1990 AD by Tree Rings of Scots pine –140 samples aggregated by a 10-year moving average.
- Reconstructed sardine and anchovy population by analysis of varved sediment cores located in Californian upwelling for the period of 500-1950 AD – 145 samples aggregated by 10–years averaging.

Climatic processes definitely affect the productivity of major commercial marine species, although in an undefined way. Thus, we applied model (5) to make forecasts, but the periods were derived not only from fishery time series, but also from using the most significant climate cycles. Applying such cyclic trends to model (5) results in more reliable values for the modelled (and forecasted) period lengths.

The values of the period lengths derived from the climatic and geophysical (LOD) time series are the following:

- for **dT** - 55, 9, 5 years (evaluation from power spectrum estimate), 64 years (evaluation from single cyclic trend fitting with unknown period);

- for **ACI** - 50, 19 years (evaluation from power spectrum estimate), 58. 5 years (evaluation from single cyclic trend fitting with unknown period);

- for **LOD** - 64, 23 years (evaluation from power spectrum estimate).

Thus, we examined the AR(2)-model with a single cyclic trend with the following modelled periods close to those derived form the above-mentioned climatic (geophysical) time series: 55, 60 and 65 years.

8.3 FORECASTING

To make the forecast, we applied a “bootstrap” method (Efron and Tibshirani 1986) to generate a probability distribution for the forecasts. The method consisted of generating a large number, **M** (we take **M**=1000), of independent stochastic artificial trajectories of the model (5), starting from the last sample of the series into the future time interval of the given length. These trajectories differ from each other only by independent realizations of the white noise component **ε(t)**. All other parameters (including variance $\mathbf{s}^2$) are fixed as the estimates. Each trajectory presents a scenario for a future time series following model (5) drawn from a probability distribution based on the variation in data. Thus we have a “bundle” of **M** samples of generated trajectories which fill some “strip” on the plane of (**t, x**). For each value of **t** in the future we can compute the average value among **M** values, corresponding to the different realisations and a variance (a width of the projected “strip”). These mean values constitute the forecasting curve, and the variance values reflect standard deviations bars for each future **t** value (for more explanation see Chapter 9)

Besides forecasting, we also applied the same bootstrap technique for “forecasting the past” or "hindcasting" (see figures of Chapter 9, dashed line). In this case, **M** bootstrap trajectories were generated starting from the third rather than first data point of the series because the AR(2) used the first two values to initiate the autoregression. This procedure can be regarded as a test of the model by visual comparison between the mean values (i.e. expected from the model) and observed time series. It should be noticed, however, that such mean trajectory depends on the first two samples taken as initial values. Other methods can also be used to test model (5), such as the usual statistical criteria to test whether the residual signal **ε(t)** is Gaussian white noise or more sophisticated tools such as the AIC (Akaike Informational Criterion) to decide upon which terms to include (Kashyap and Rao 1976).

9. CLIMATE AND CATCH MODELLING

Figure 9.1 shows the results of modelling the detrended global dT and zonal ACI based on a 55-year period of climate oscillations. The figures indicate that a harmonic with this period length is in good agreement with the past oscillations of both dT and ACI, and suggest that similar cyclic changes are likely to continue during the future 30–60 years.

Figure 9.2 shows the temperature dynamics reconstructed from the Greenland ice cores data for the last 400 years combined with the detrended dT dynamics, calculated from the time series of directly measured temperature for the last 150 years (Figure 9.3). It is clear that the dynamics of the measured temperatures for 1861–1975 coincide with the reconstructed Ice Core dT dynamics. With a 55-year period length, the projected model curve is in good agreement with the observed fluctuations of both reconstructed and measured dT.

These data illustrate a good general similarity between the curves of measured and reconstructed temperature time series for the last millennium. There are many reasons to suppose that the climate periodicity, which has lasted over many decades, will remain similar for the next 30 years.

The scheme presented in Figures 9.1–9.3 is applied to forecast commercial catches of two basic groups of fish species: (1) those correlated with the dynamics of the zonal ACI ("zonal-dependent" species) and (2) those correlated with the dynamics of meridional ACI ("meridional-dependent" species) (see Figure 3.6). “Zonal” and “meridional” circulation epochs coincide in phase with the long-term increase and decrease of global temperature, respectively (Lambeck 1980).

Figures 9.4 - 9.14 show the model-generated catches of 12 major commercial species (excluding Peruvian anchovy). The graphs were developed using three basic periods of the climate cycles: 55, 60, and 65 years. In general, all three graphs are in good correspondence with the past catch cycles. The catch trends of Atlantic and Pacific herring, and Atlantic cod fit best to the 55-year periodicity compared to the periods of 60 and 65 years.

The model-generated forecast of commercial catches (Tables 9.1 and 9.2) is based on the following assumptions:

1) Catch dynamics correspond to the smooth "model" curve shown in Figures 9.4 - 9.14.
2) Average catch in the maximum of the forecasted cycle corresponds to that in the maximum of the previous cycle. That is, if average catch of Atlantic cod in the mid 1960s was about 3 million tons, then the forecasted catch in the mid-2020s will also be about 3 million tons.

9.1 MODELLING OF THE CATCH DYNAMICS OF "MERIDIONAL-DEPENDENT" FISH SPECIES

Figures 9.4 - 9.7 show the model-generated catch dynamics of Atlantic herring and cod, Pacific herring and South African sardine. Excluding stock dynamics of Peruvian anchovy (considered separately in Chapter 10), the catch trends of four "meridional-dependent" species have already passed a depression in the 1980s, and, in line with the climatic trend, both population and catches of these species have been increasing since the mid 1990s. Judging by the past climate cycles, the catch maxima of these species is likely to fall on the middle of the next decade.

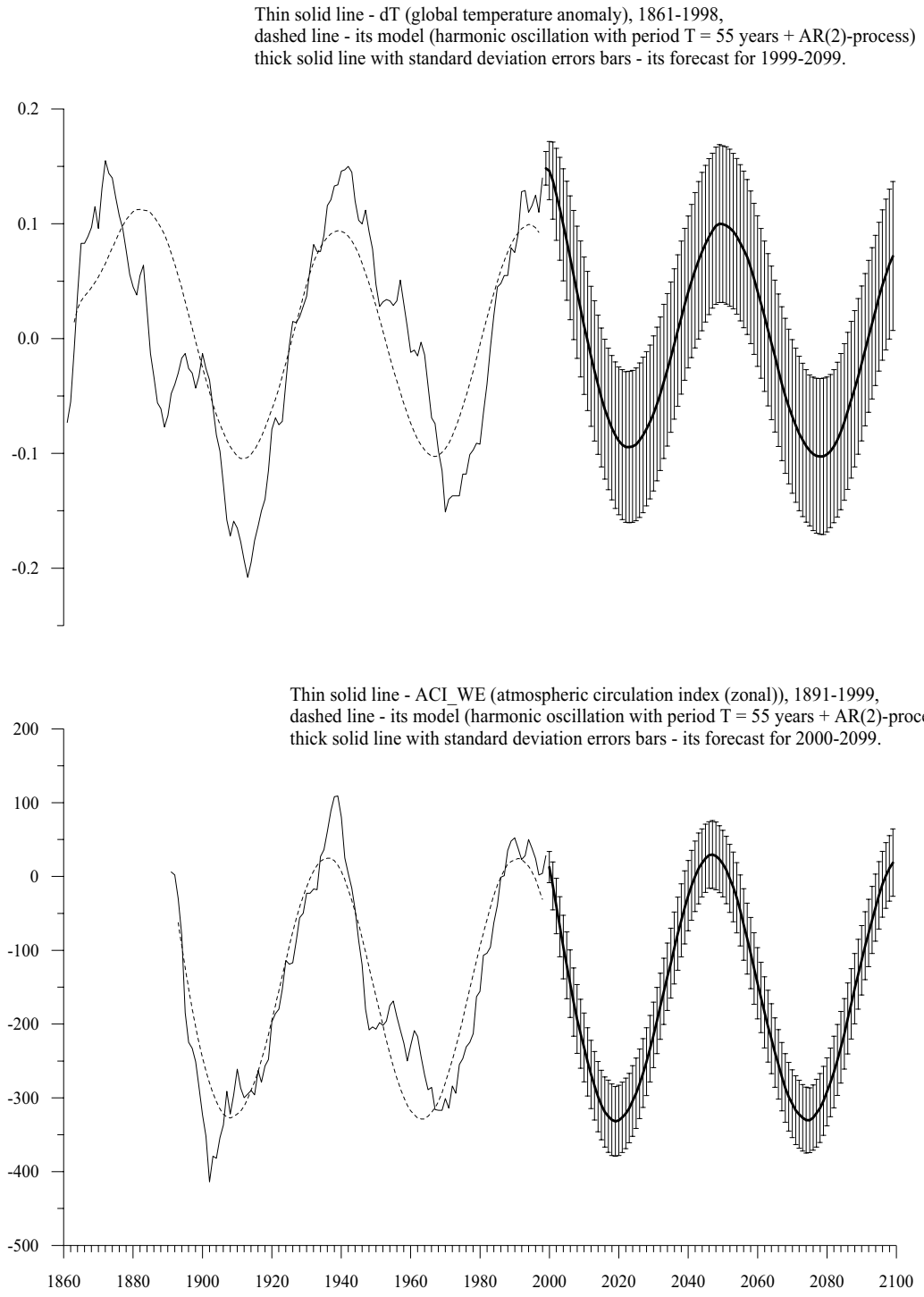

3)

Figure 9.1 The future fluctuations of detrended Global temperature anomaly (top) and "zonal" form of Atmospheric Circulation Index (bottom).

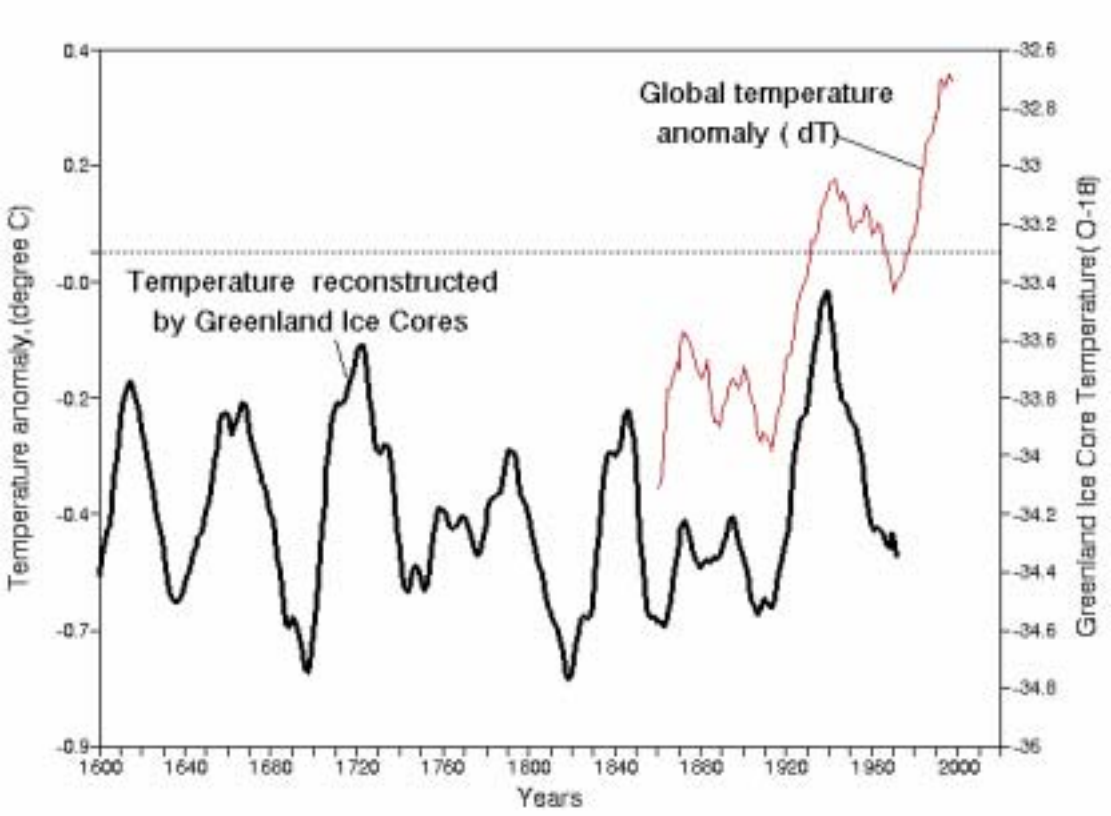

Figure 9.2. A comparison of global temperature anomalies (dT) with the temperature dynamics reconstructed from Greenland Ice Cores (Ice Core dT).

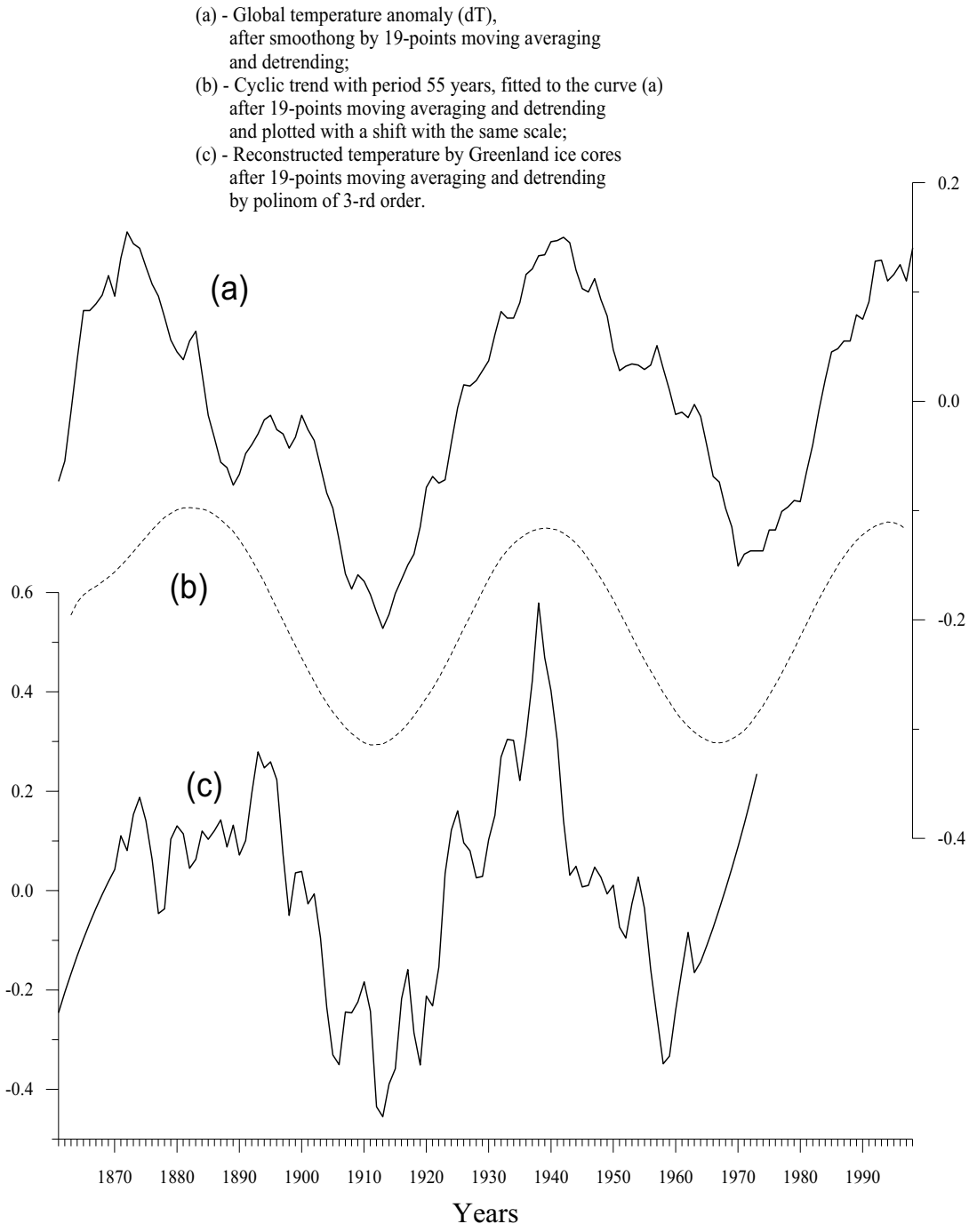

Figure 9.3 A comparison of the detrended global temperature anomaly (dT), the modelled 55-year period climate oscillation curve and the detrended reconstructed ice cores temperature (Ice Cores dT).

The peak of Atlantic cod is shifted by 5 - 7 years to the right (i.e. delayed) from the corresponding peak of Atlantic herring, which is characteristic also for the past dynamics of both species.

Thus, the catch cycles of the four "meridional-dependent" species look as follows: a minimum in the beginning and mid-1980s increasing to the mid-1990s, slowing down in the 2010s to a maximum in 2015–2025, and decreasing from 2025 to a new minimum in the mid-2030s. Catch forecasting for the next 30-years is of the greatest importance for our purposes, although the catch dynamics beyond the 2030s is also of interest (Table 9.1).

Table 9.1 Model-generated commercial catches (million tons) of meridional-dependent" species in 2005—2040

Years	Atlantic Herring	Atlantic cod	Pacific herring	South African Sardine
2005	2. 2	1. 5	0. 60	0. 30
2010	2. 5	2. 0	0. 65	0. 50
2015	3. 0	2. 5	0. 70	0. 70
2020	2. 5	3. 0	0. 70	1. 00
2025	2. 0	3. 5	0. 75	0. 60
2030	1. 5	2. 8	0. 65	0. 40
2035	1. 2	2. 3	0. 50	0. 35
2040	1. 0	1. 7	0. 35	0. 20

9.2 MODELLING OF THE CATCH DYNAMICS OF "ZONAL-DEPENDENT" FISH SPECIES

Figures 9.8 - 9.14 show the model-generated dynamics of catch fluctuations for Japanese, Californian, Peruvian, and European sardines, Pacific salmon, Alaska pollock, and Chilean jack mackerel. All seven species are in close correlation with "zonal" ACI, and now exhibit decreases in population and catches, though each are at different stages of the depression. For example, the catch dynamics suggests that Japanese, Peruvian, and European sardine, and Alaska pollock have passed the point of maximum stock and started to decrease in the mid to late1980s. The catch is forecast to reach its minimum by the mid 2010s, followed by the new increase to a maximum in the early 2040s. As to the other species of this group, the maximum catch of Pacific salmon lags behind the corresponding maximum of Japanese sardine by almost 10 years (in the mid-1990s), followed by gradual decrease (Klyashtorin 1997, 1998). Similar dynamics are characteristic of Californian sardine and Chilean jack mackerel. The model predicts a minimum population of these three species in the 2010s, to be followed by a gradual increase to the maximum in the mid-2040s. The model-generated dynamics of "zonal-dependent" species are presented in Table 9.2.

Thus, cyclic catch fluctuations of "zonal-dependent" species looks as follows: a maximum in the mid-1980s, then a decrease in the early 2000 to a minimum around 2015, followed by a gradual increase in the mid-2020s leading to a new maximum in the 2040s.

Table 9.2 Model-generated commercial catches (million tons) of "zonal- dependent" species in 2005–2040.

Years	Japanese sardine	Peruvian Sardine	European sardine	Alaska pollock	Californian sardine	Pacific Salmon	Chilean jack mackerel
2005	0. 10	0. 25	0. 50	2. 5	0. 25	0. 70	2. 0
2010	0. 05	0. 05	0. 40	2. 0	0. 10	0. 50	1. 5
2015	0. 05	0. 05	0. 30	2. 0	0. 05	0. 35	0. 5
2020	0. 30	0. 10	0. 30	2. 2	0. 02	0. 35	0. 5
2025	1. 00	0. 50	0. 40	2. 5	0. 05	0. 40	0. 7
2030	2. 50	1. 50	0. 80	3. 5	0. 10	0. 50	1. 0
2035	3. 50	2. 50	1. 00	4. 5	0. 25	0. 60	1. 5
2040	4. 50	3. 50	1. 20	6. 0	0. 35	0. 70	2. 5

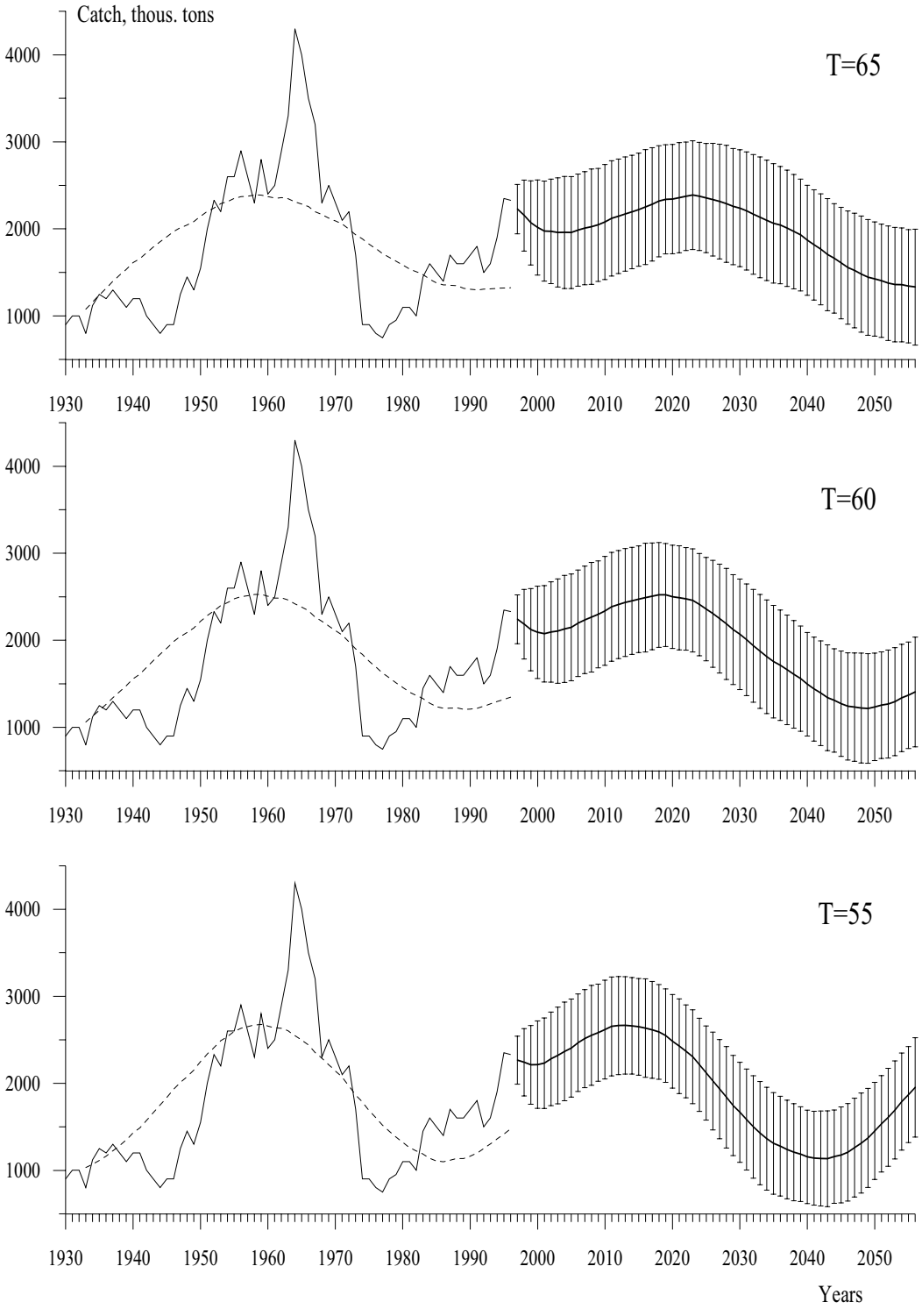

Figure 9.4 Thin solid line - Atlantic herring catch, 1930-1996, thick solid lines with standard deviations error bars - mean value for 1000 bootstrap realizations for 1997-2056 for different periods T (years) of cyclic trend, dashed line - mean value for 1000 bootstrap realizations for 1933-1996.

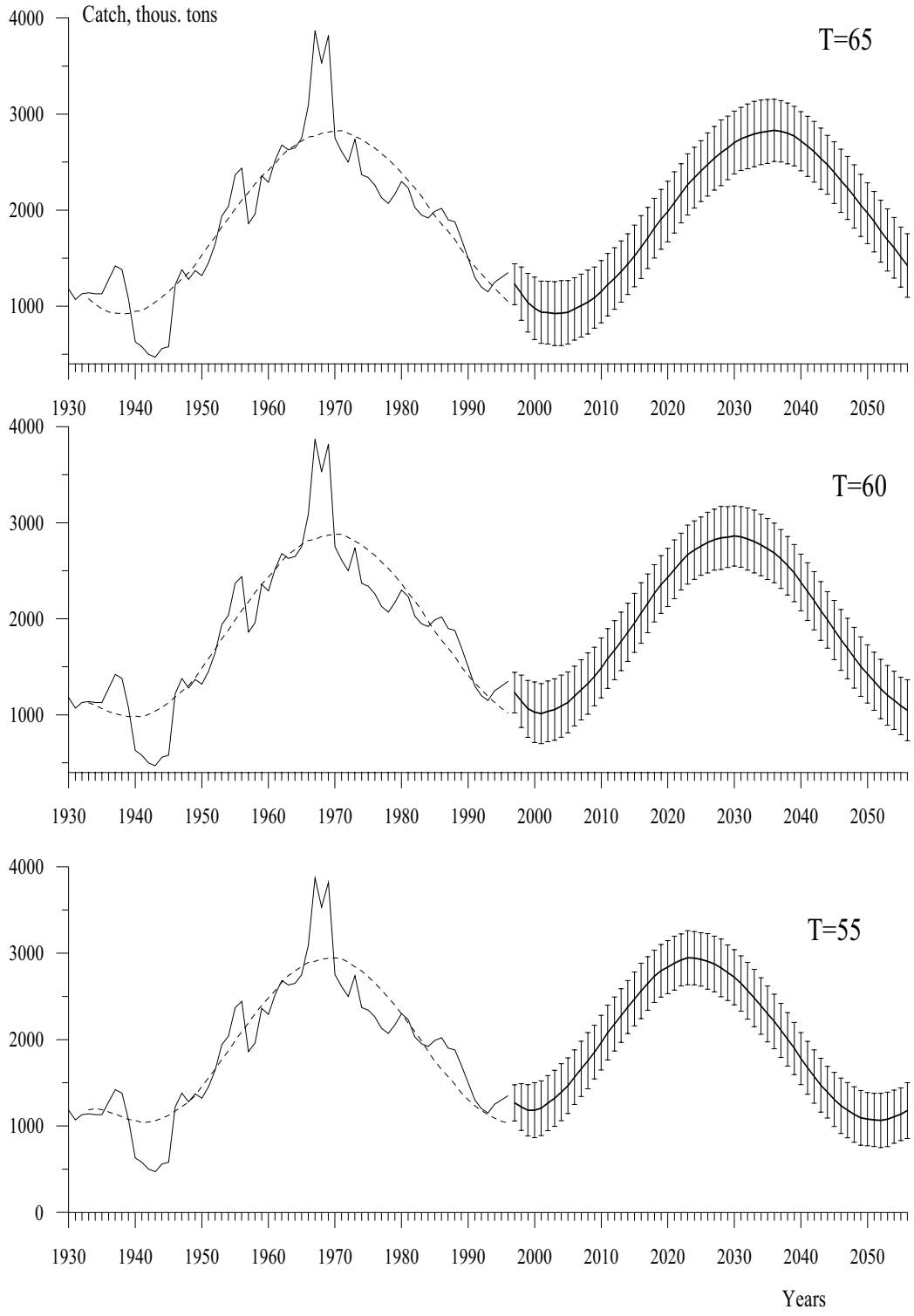

Figure 9.5 Thin solid line - Atlantic cod catch, 1930-1996, thick solid lines with standard deviations error bars - mean value for 1000 bootstrap realizations for 1997-2056 for different periods T (years) of cyclic trend, dashed line - mean value for 1000 bootstrap realizations for 1933-1996.

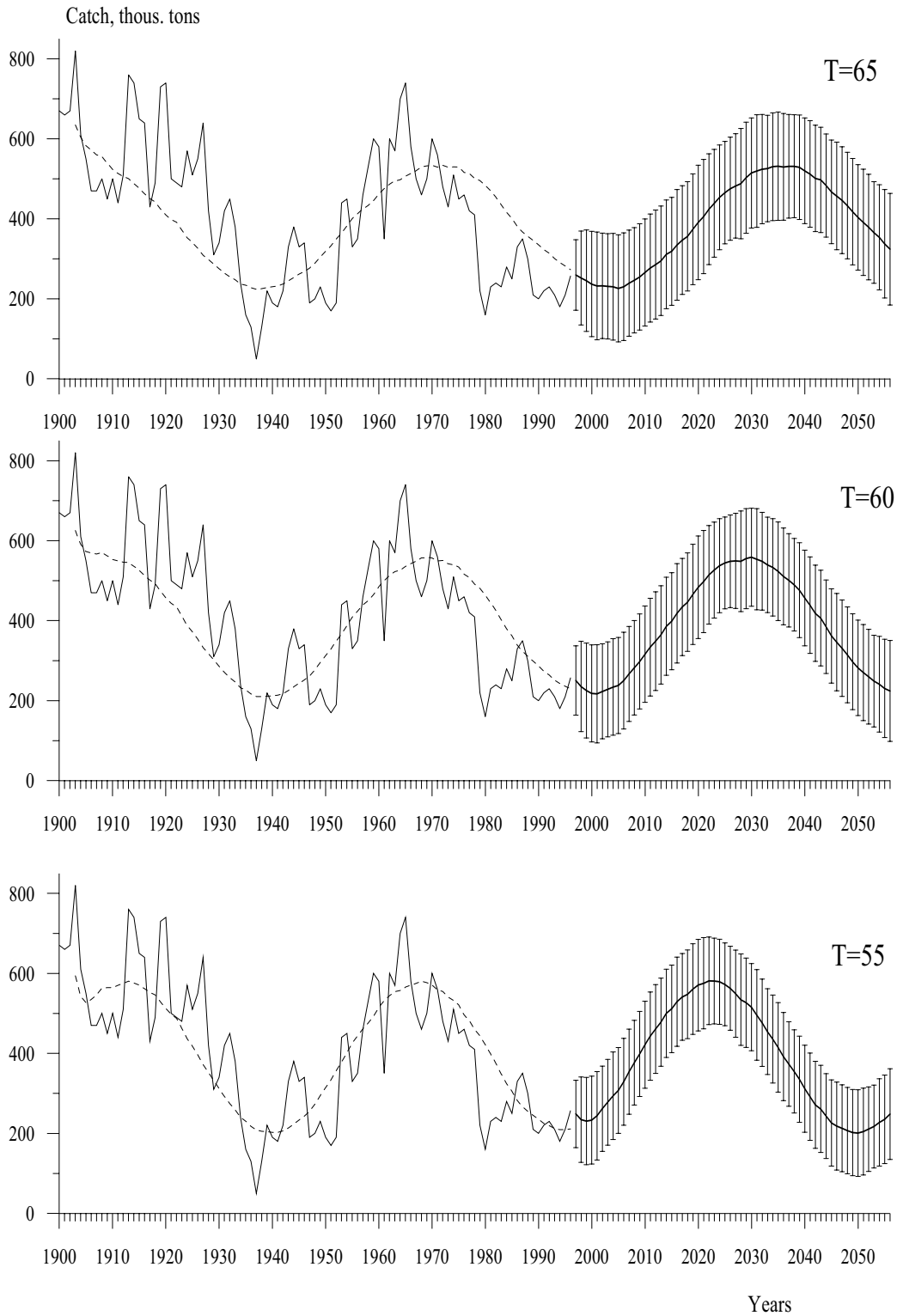

Figure 9.6 Thin solid line - Pacific herring catch, 1900-1996, thick solid lines with standard deviations error bars - mean value for 1000 bootstrap realizations for 1997-2056 for different periods T (years) of cyclic trend, dashed line - mean value for 1000 bootstrap realizations for 1903-1996.

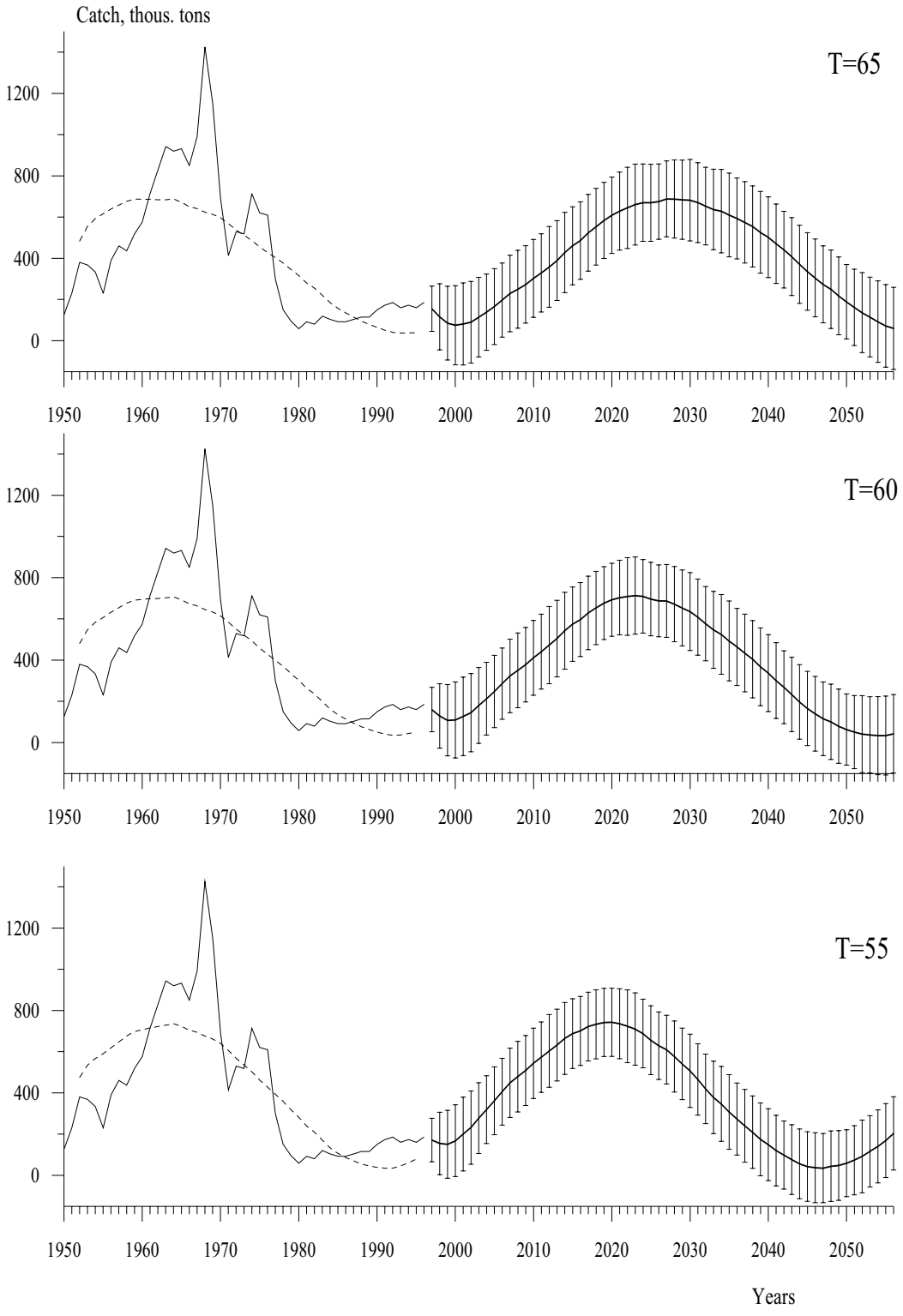

Figure 9.7 Thin solid line - South African sardine catch, 1950-1996, thick solid lines with standard deviations error bars - mean value for 1000 bootstrap realizations for 1997-2056 for different periods T (years) of cyclic trend, dashed line - mean value for 1000 bootstrap realizations for 1953-1996.

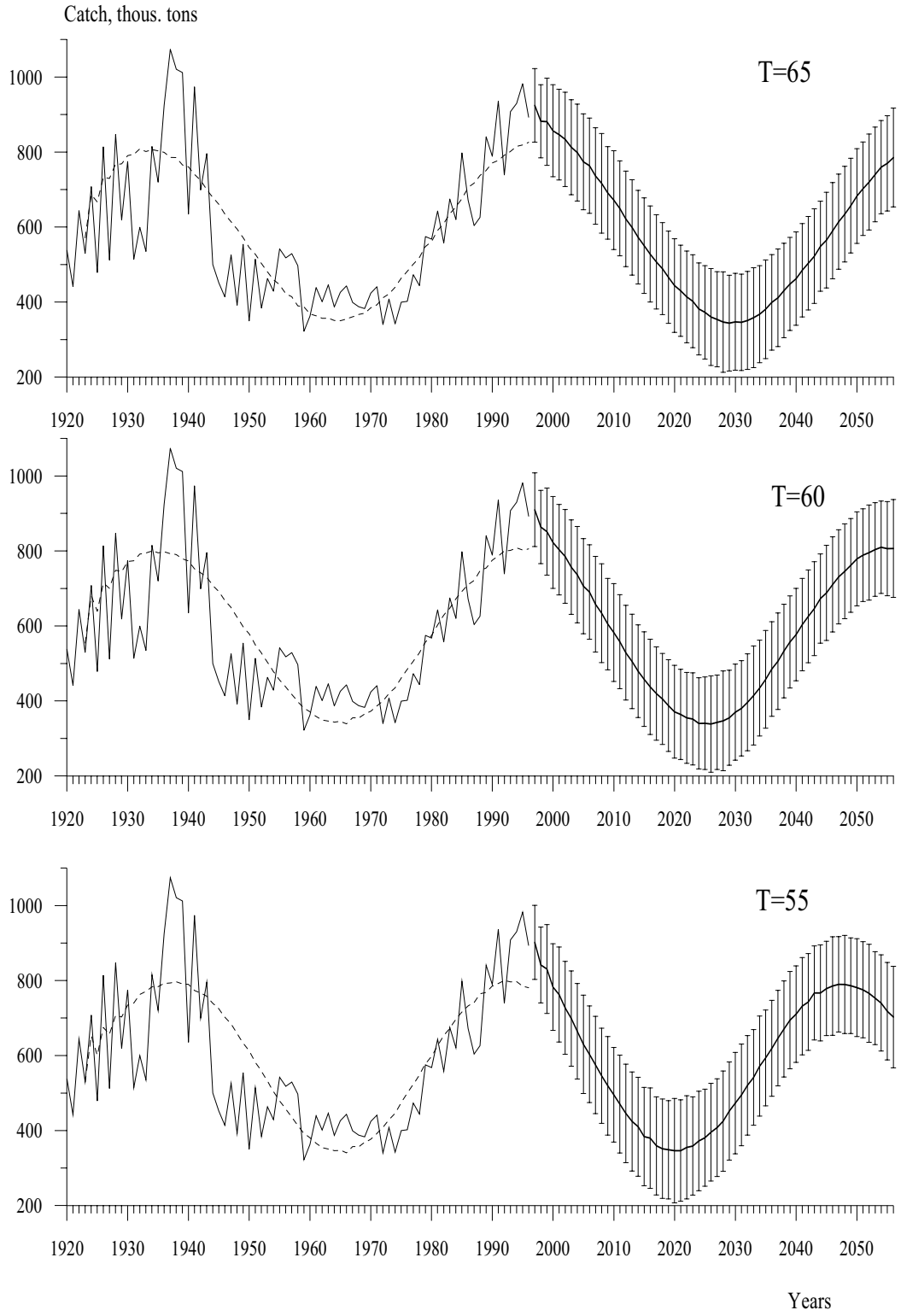

Figure 9.8 Thin solid line - Pacific salmon catch, 1920-1996, thick solid lines with standard deviations error bars - mean value for 1000 bootstrap realizations for 1997-2056 for different periods T (years) of cyclic trend, dashed line - mean value for 1000 bootstrap realizations for 1923-1996.

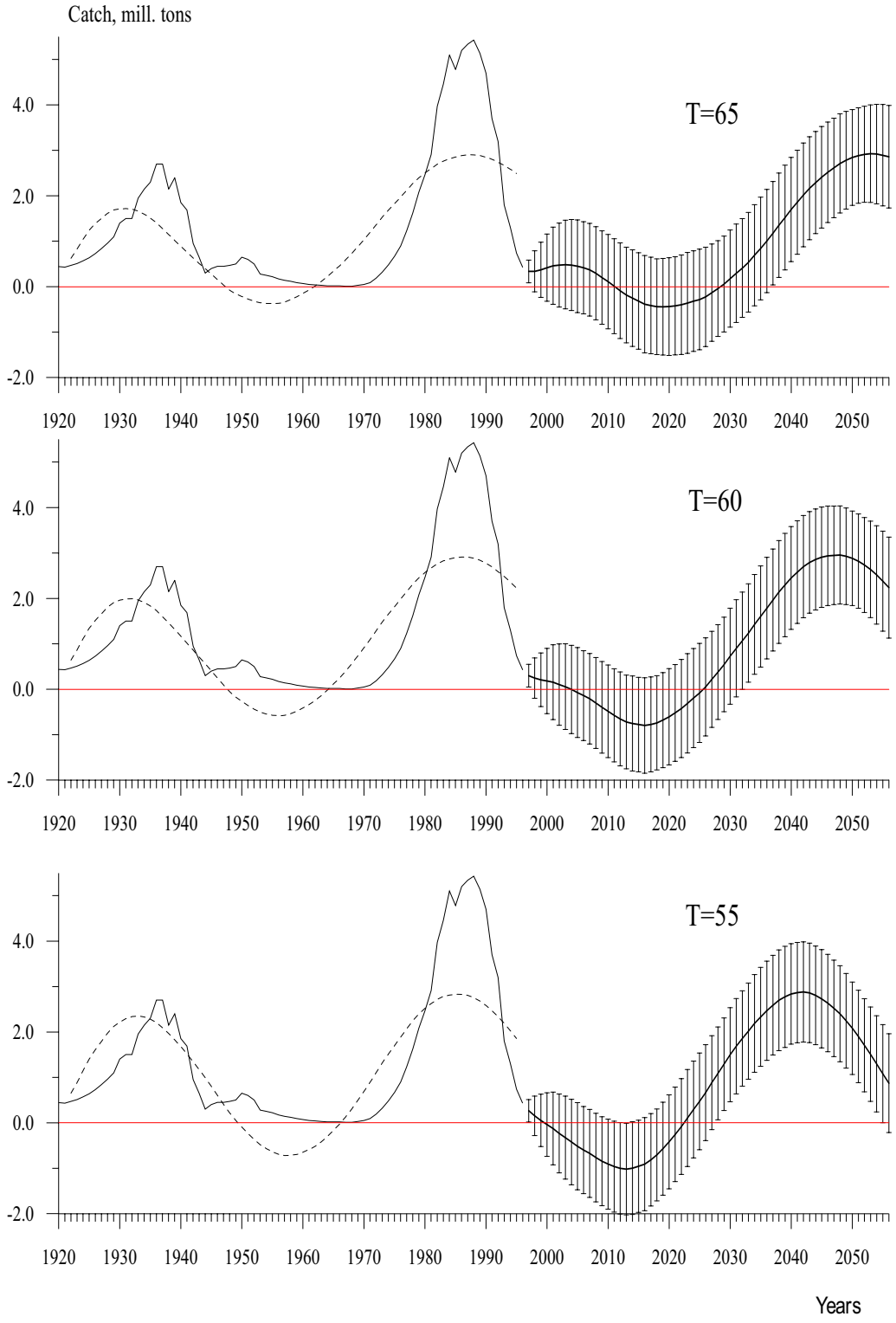

Figure 9.9 Thin solid line - Japanese sardine catch, 1920-1996, thick solid lines with standard deviations error bars - mean value for 1000 bootstrap realizations for 1997-2056 for different periods T (years) of cyclic trend, dashed line - mean value for 1000 bootstrap realizations for 1923-1996.

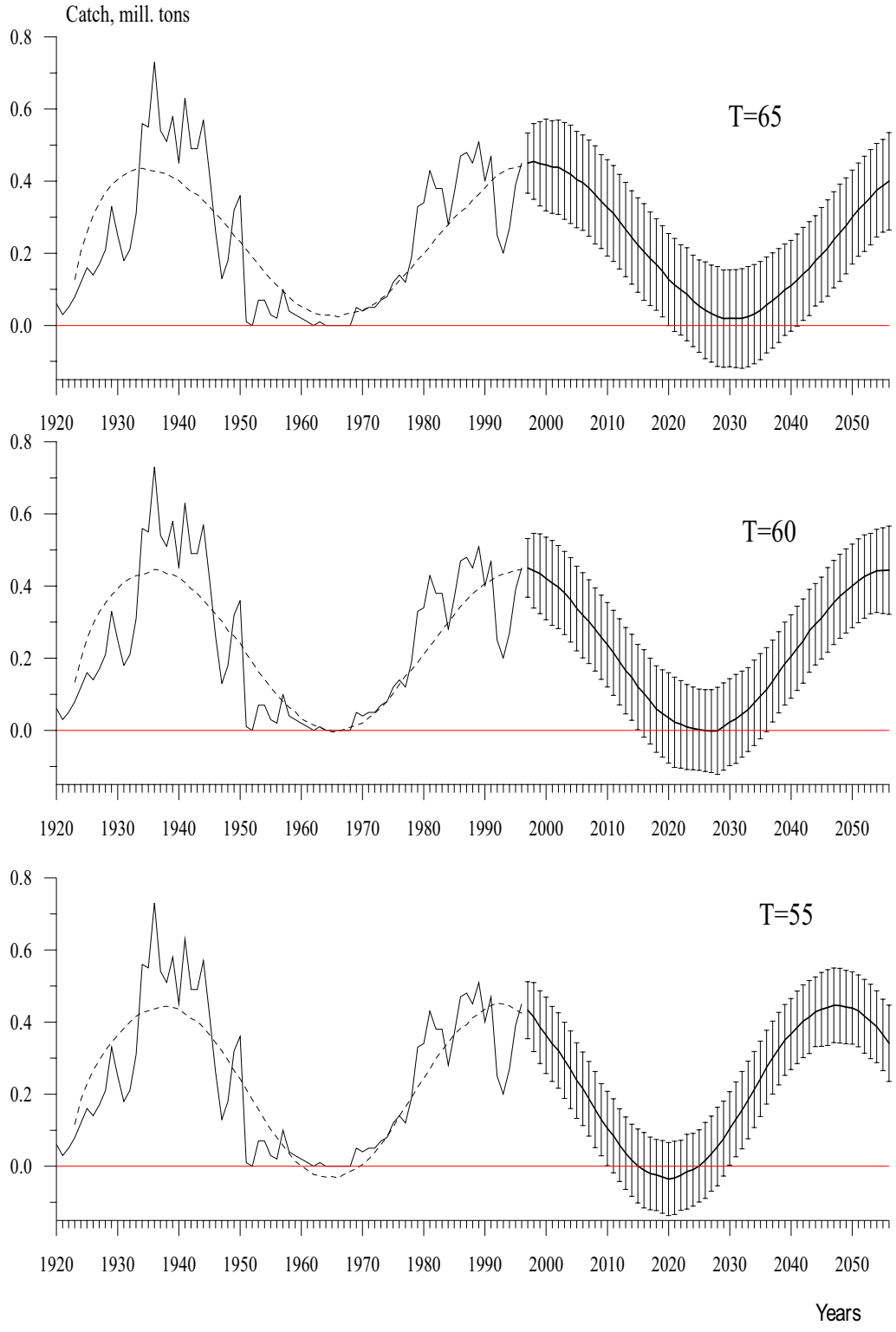

Figure 9.10 Thin solid line - Californian sardine catch, 1920-1996, thick solid lines with standard deviations error bars - mean value for 1000 bootstrap realizations for 1997-2056 for different periods T (years) of cyclic trend, dashed line - mean value for 1000 bootstrap realizations for 1923-1996.

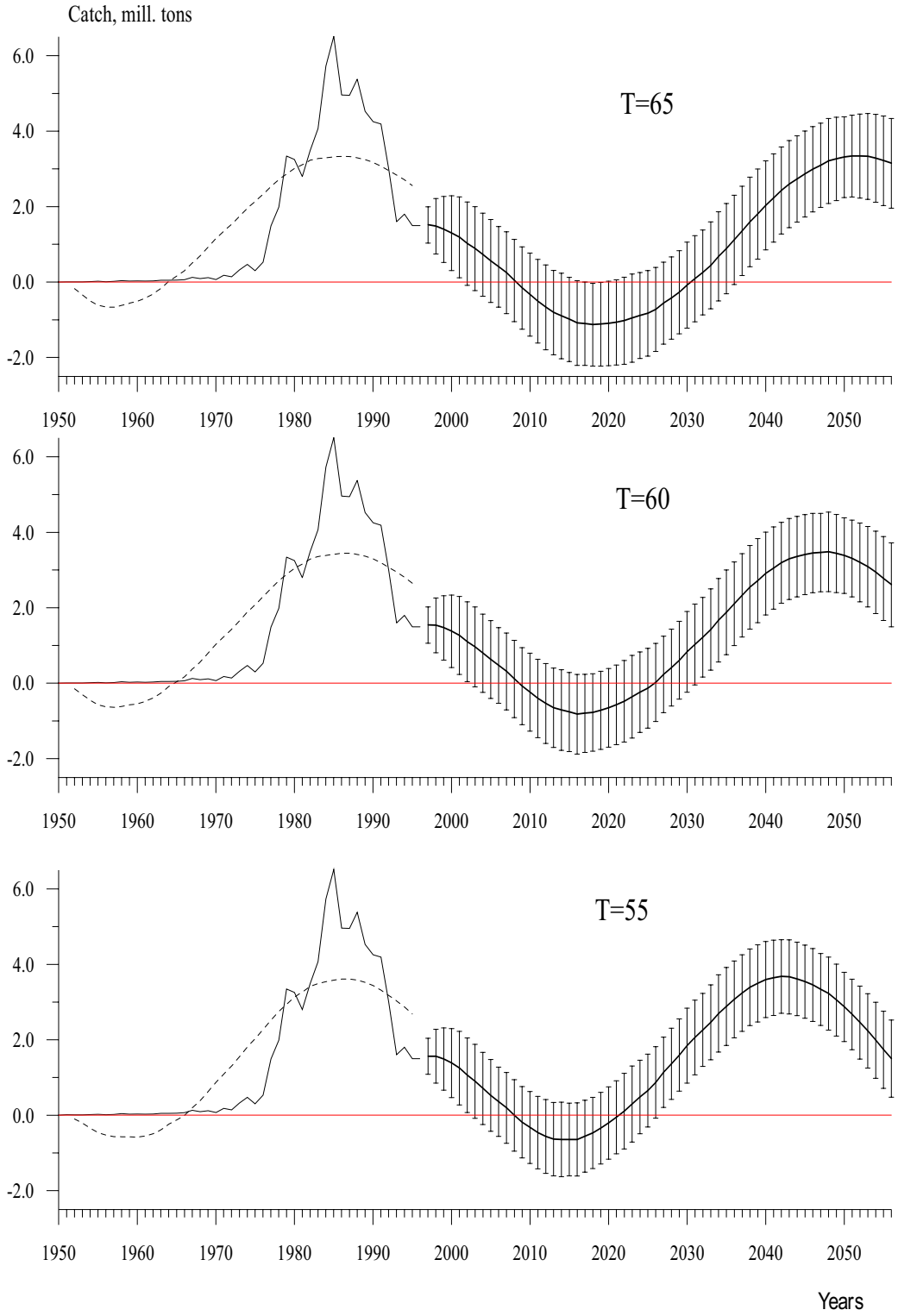

Figure 9.11 Thin solid line - Peruvian sardine catch, 1950-1996, thick solid lines with standard deviations error bars - mean value for 1000 bootstrap realizations for 1997-2056 for different periods T (years) of cyclic trend, dashed line - mean value for 1000 bootstrap realizations for 1953-1996.

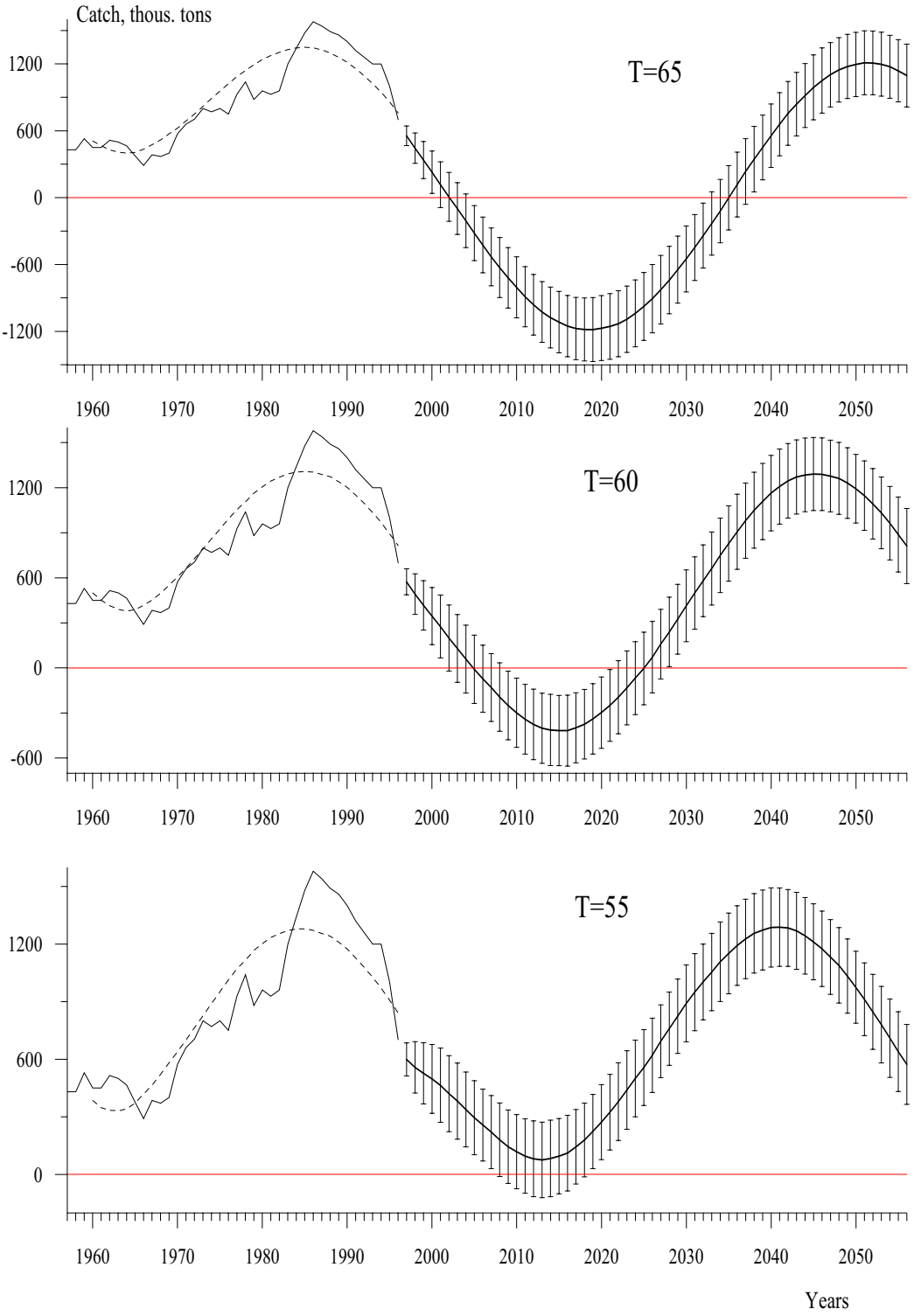

Figure 9.12 Thin solid line - European sardine catch, 1957-1996, thick solid lines with standard deviations error bars - mean value for 1000 bootstrap realizations for 1997-2056 for different periods T (years) of cyclic trend, dashed line - mean value for 1000 bootstrap realizations for 1960-1996.

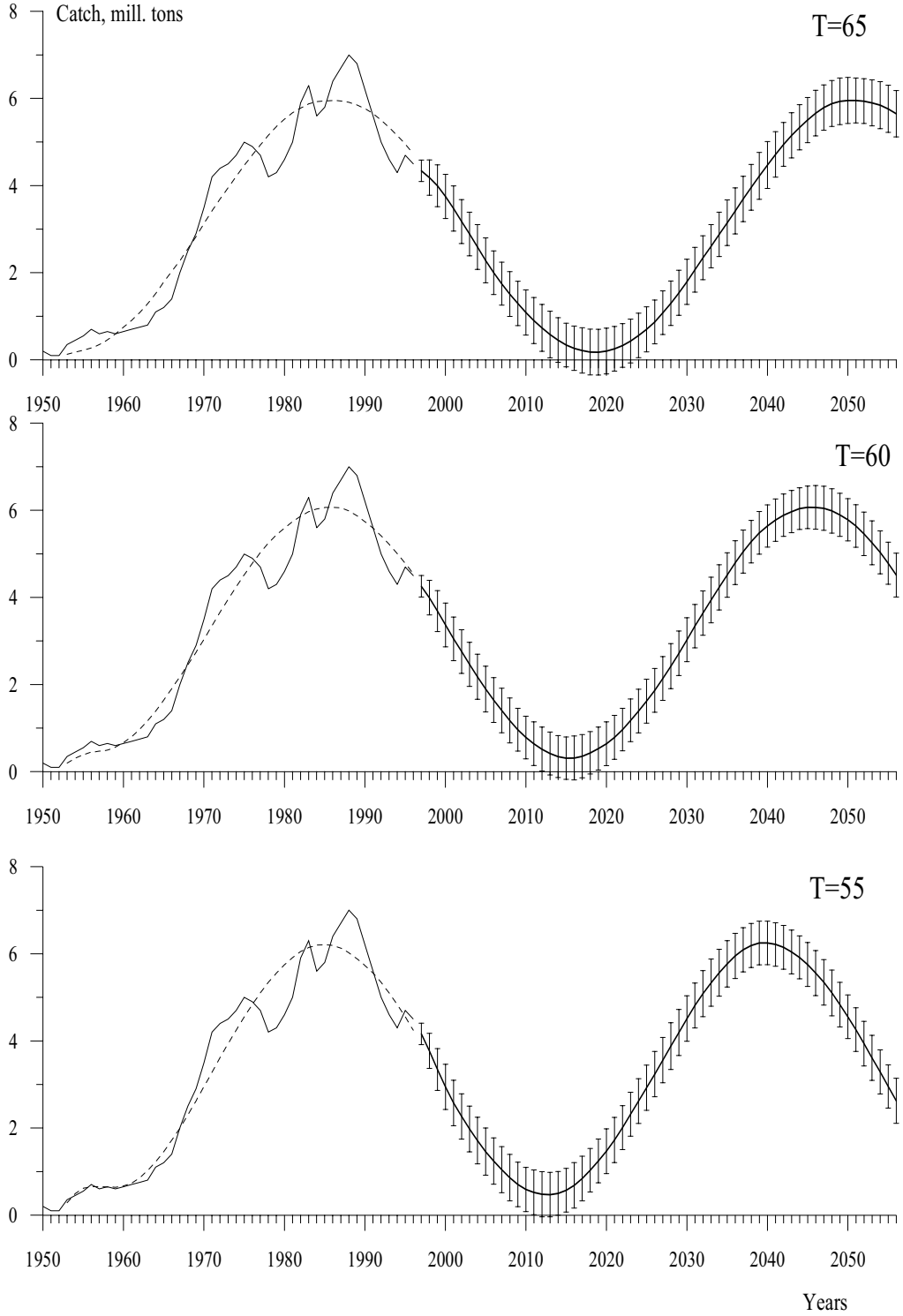

Figure 9.13 Thin solid line - Alaska pollock catch, 1950-1996, thick solid lines with standard deviations error bars - mean value for 1000 bootstrap realizations for 1997-2056 for different periods T (years) of cyclic trend, dashed line - mean value for 1000 bootstrap realizations for 1953-1996.

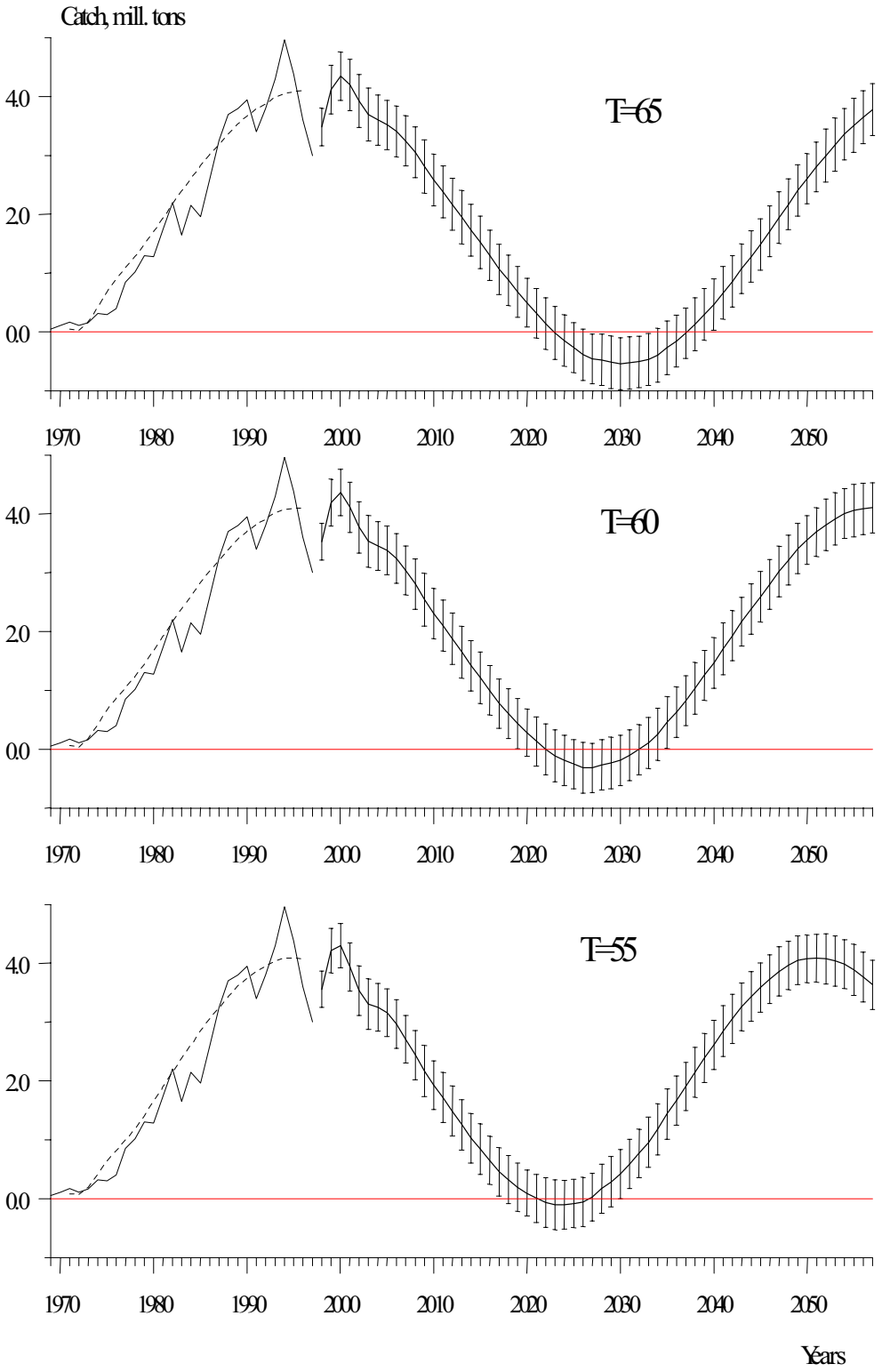

Figure 9.14 Thin solid line - Chilean jack mackerel catch, 1969-1997, thick solid lines with standard deviations error bars - mean value for 1000 bootstrap realizations for 1998-2057 for different periods T (years) of cyclic trend, dashed line - mean value for 1000 bootstrap realizations for 1971-1997.

10. PECULIARITIES OF THE CATCH DYNAMICS OF PERUVIAN AND JAPANESE ANCHOVY AND SARDINE

10.1 ANCHOVETA

Total biomass and commercial catch of Peruvian anchoveta during its maximum production (outbursts) may reach 20 and 13 million tons, respectively. Stock fluctuations of Peruvian anchoveta are not as closely correlated with the dynamics of "meridional" atmospheric circulation as other "meridional-dependent" fish species (Atlantic and Pacific herring, and Atlantic cod). In addition, the population of Peruvian anchoveta undergoes catastrophic declines because of the strong El Niño events (Mysak 1986). These events complicate forecasting of Peruvian anchoveta and requires special discussion.

Figure 10.1 presents the dynamics of Peruvian anchoveta catches and biomass (Pauly *et al.*1987). The anchoveta biomass estimated using a Virtual Population Analysis (VPA) model is very close to the corresponding estimates from the independent sources (i.e., acoustic surveys, c.f. Johannesson and Vilchez 1980). However, the dynamics of Peruvian anchoveta catches and biomass are rather different.

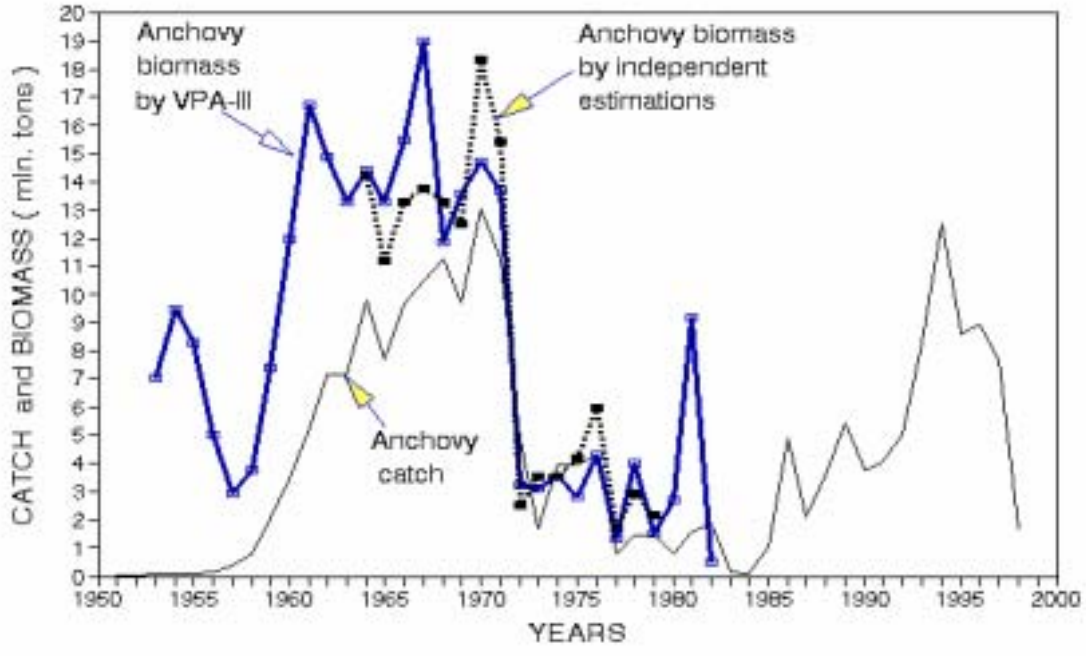

Figure 10.1 A comparison of Peruvian anchoveta catches and biomass obtained through the VPA model and independent estimates.

The effect of strong El Niño events on both the anchoveta biomass and catch dynamics is shown in Figure 10.2.

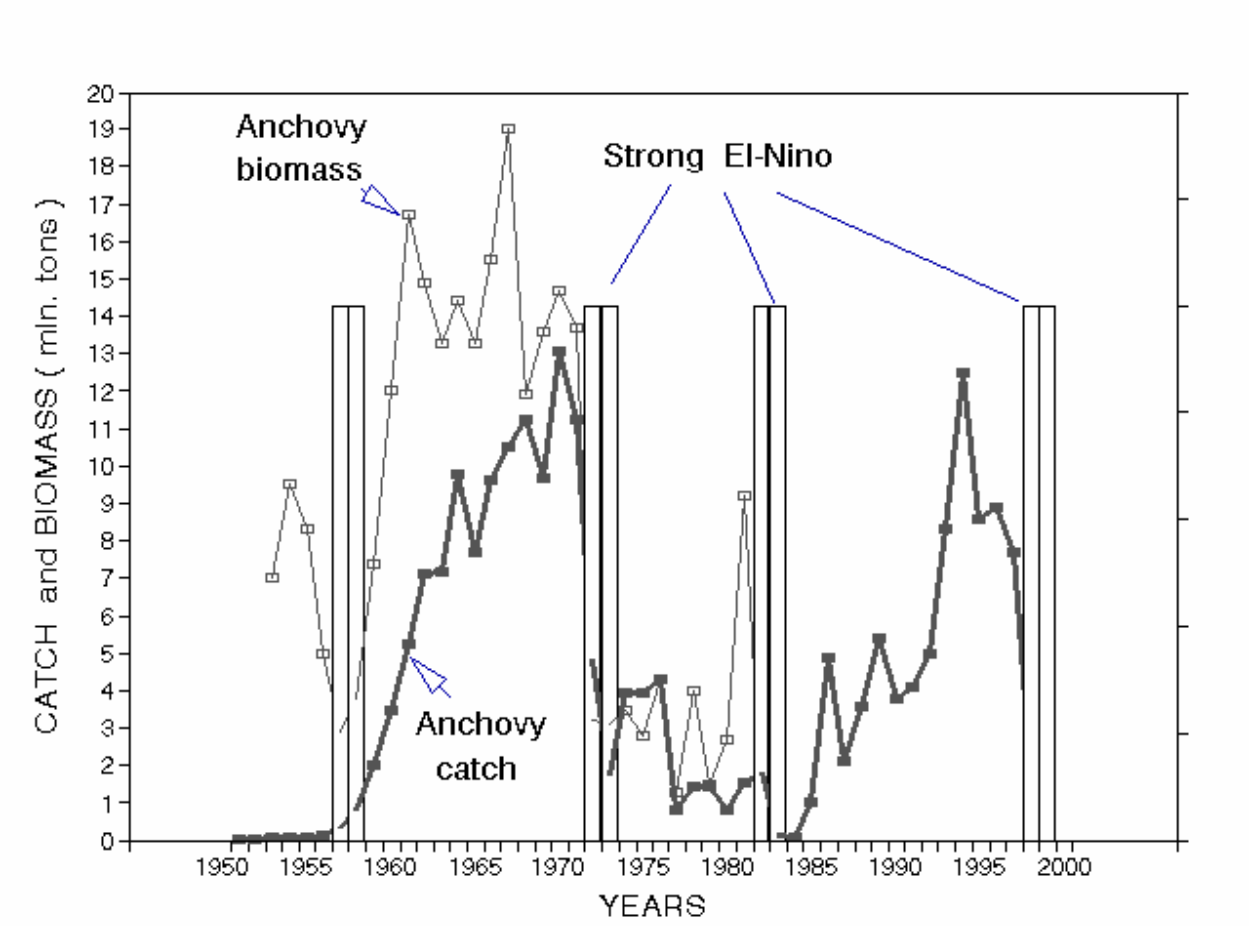

Figure 10.2 Dynamics of Peruvian anchoveta biomass, commercial catch and strong El Niño events for 1950-1998.

The strong El Niño event of 1957-58 severely reduced the anchoveta population. The anchoveta biomass dropped sharply after 1971 (the year preceding the strong El Niño of 1972-1973) by 80%. The strongest El Niño event in the century occurred in 1982-1983, causing a catastrophic collapse in the anchoveta population. Anchoveta catches dropped to the century's lowest level of 0.1 million tons. Another of the century's strongest El Niño events, that of 1997-98, also caused a sharp decrease in the anchoveta catches (to 1.7 million tons). However, preliminary data suggest that the expected anchoveta catch in 2000 to be about 7-8 million tons.

In contrast to anchoveta, Peruvian sardine did not respond much to the strongest El Niño event of 1982-83, and sardine catches reached their maximum (6.5 million tons) in 1985.

Figure 10.3 shows that the anchoveta and sardine outbursts are out of phase. The sardine outbursts are attributed to the "zonal" ACI epochs (Fig. 3.3), and Peruvian anchoveta increase considerably during the "meridional" ACI epochs.

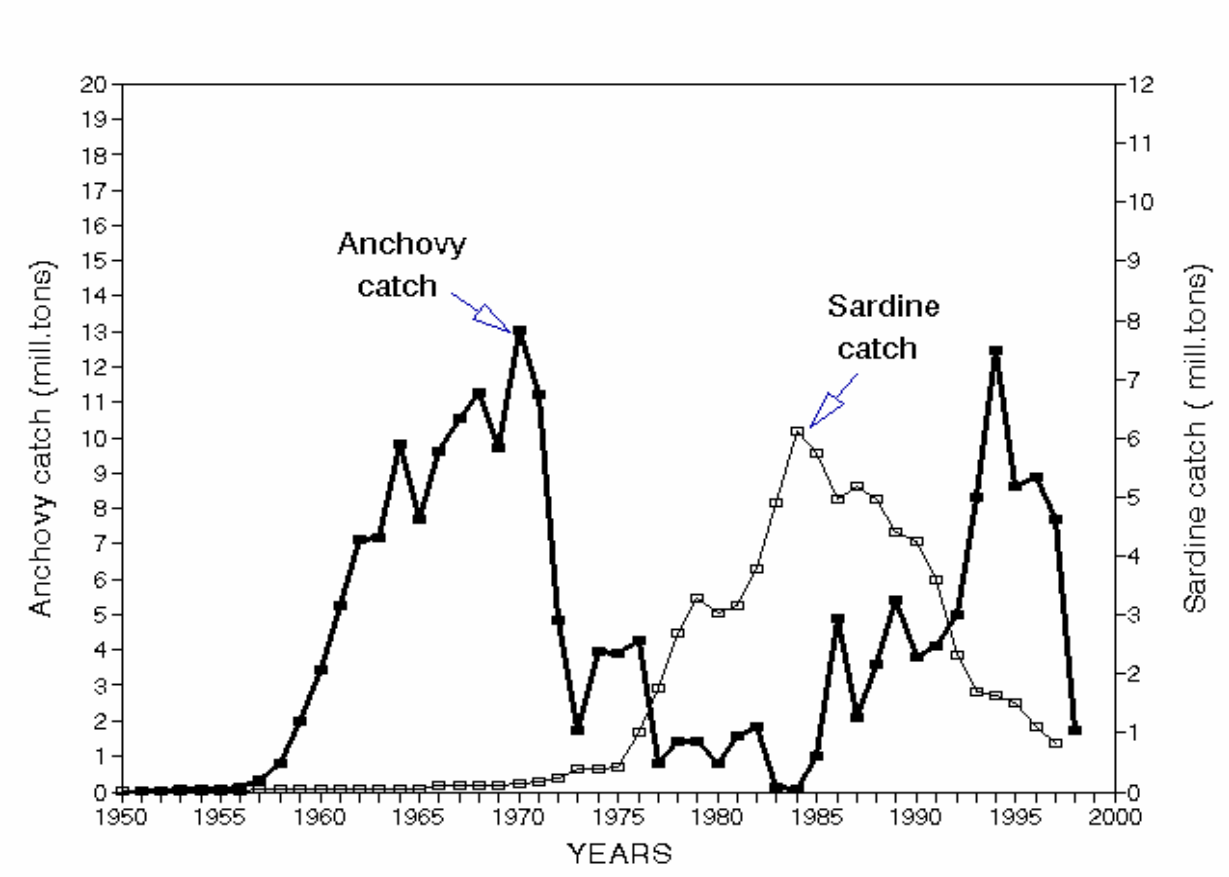

Figure 10.3 Dynamics of Peruvian anchoveta and Peruvian sardine catch 1950-1998

Strong El Niño events cause gaps in the time series of Peruvian anchoveta catch and biomass, obscuring the effect of the climate-governed dynamics of this species. That is why it is easier in the first instance to start with the dynamics of other “meridional-dependent" species (Japanese anchovy, Pacific and Atlantic herring), whose populations are not (immediately) affected by El Niño events.

Total catches of Japanese anchovy have been recorded since the early 20th century. Yet the total catch may hardly reflect the population dynamics of this species, particularly because the distribution of fishing effort has changed considerably in the recent 10-15 years, a result of the broad extension of fisheries for Japanese anchovy (Fig. 10.4a). For example, from the early 1960s, the number of fishing boats in South Korea has risen (particularly in 1980), and total catch increased six-fold (from 40 to 250 thousand tons). China's Japanese anchovy fishery started in 1990, and has expanded 25-fold (up to 1.28 million tons) in only 8 years, from 1990 to 1998. At the same time, the anchovy fisheries in Japan remained on more or less stable level. The number and tonnage of fishing boats have changed relatively insignificantly (by 10-15%) since the early 1960s (Fisheries of Japan, 1996).

Given these changing circumstances, the long-term changes in the population of Japanese anchovy are likely better reflected in the long-term statistics of net Japanese catch than in the total catch. The Japanese catch of Japanese anchovy versus Japanese sardine are presented in Figure 10.4b.

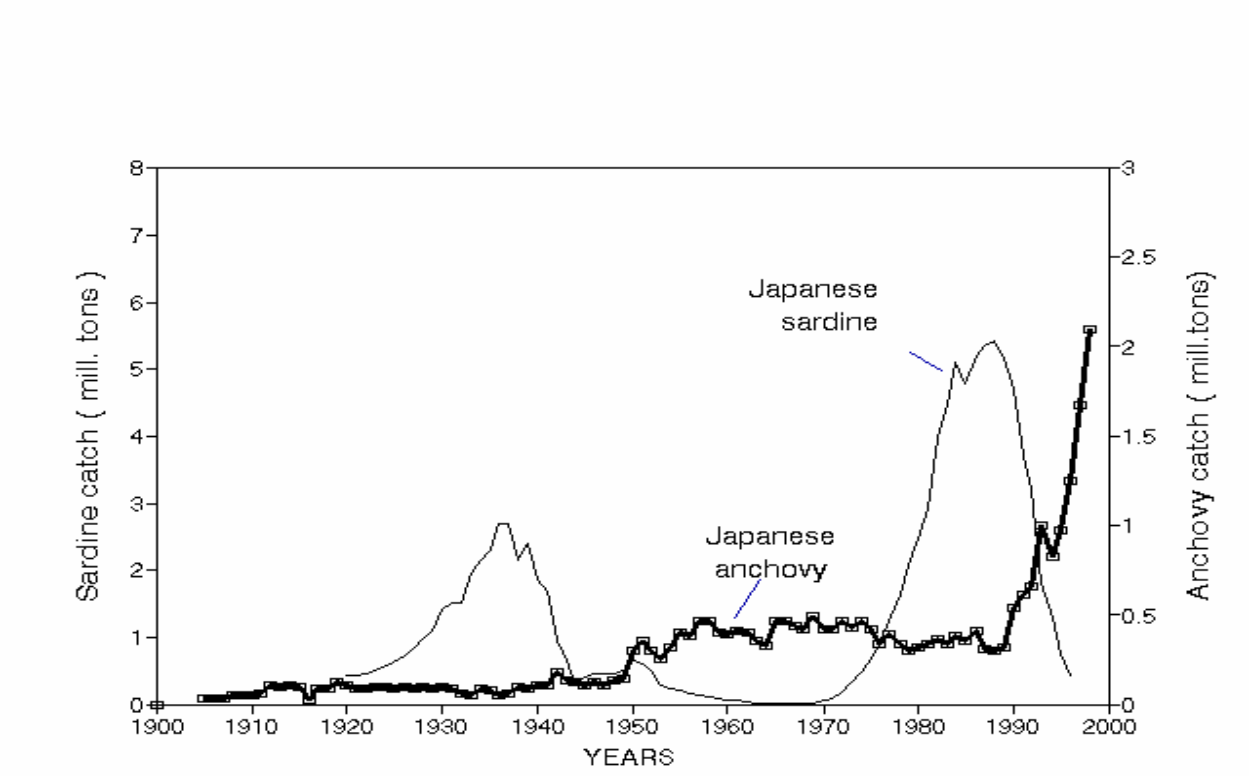

Fig.10.4a Total catch of Japanese anchovy and sardine by all countries.

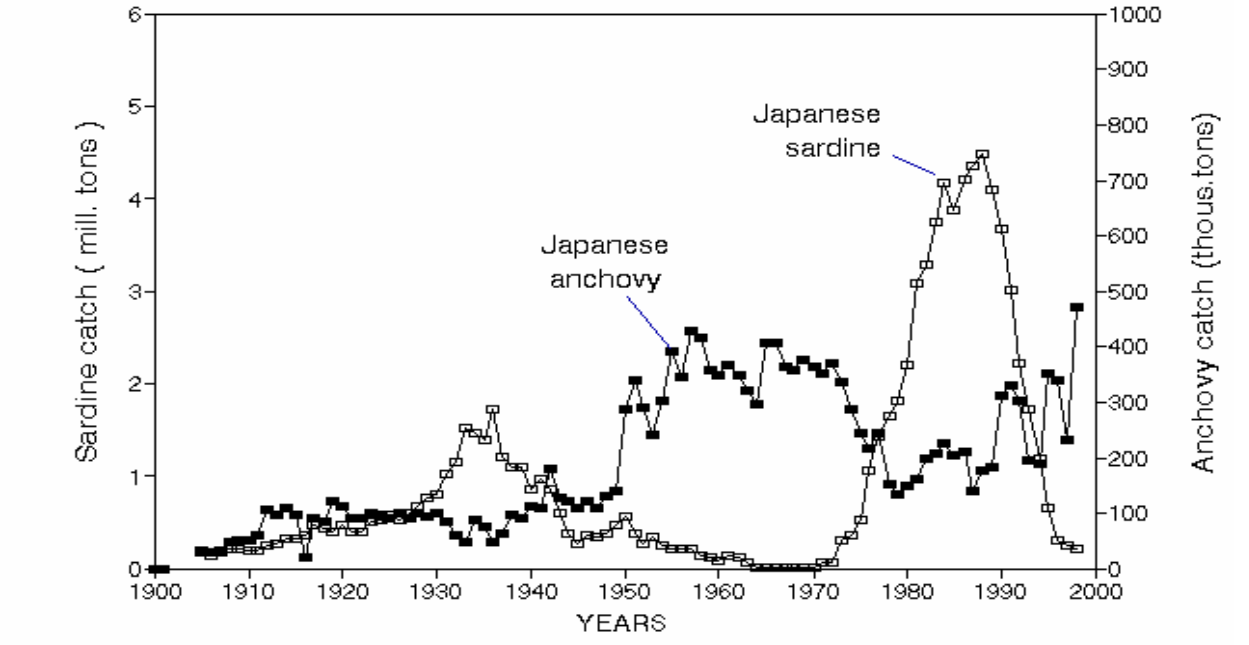

Fig.10.4b Catch trends of Japanese anchoveta by Japanese fishery fleet as compared with Japanese sardine (1905 – 1998). From 1905 to 1998, the anchovy catches were opposite in phase to Japanese sardine catches. This opposite phase relationship between sardine and anchovy catches has been most obvious since the early 1950s, when the anchovy catches in Japan exceeded 200 000 tons.

Japanese anchovy catch appears to be in phase with the dynamics of other “meridional-dependent” species. The catch series for Japanese anchovy, and Pacific and Atlantic herring suggest tentatively that the population dynamics of all these species are generally in phase (Fig. 10.5). Figure 10.6 shows that the catch dynamics of Pacific herring, and Japanese and Peruvian anchovy are in reasonably good agreement with the dynamics of “meridional” Atmospheric Circulation Index. This is supporting evidence for the dependence of these species on the dynamics of global climatic indices (See Chapter 2).

It must be mentioned that the biomass curve of Peruvian anchoveta is in somewhat better agreement with climate dynamics compared to the catch curve, since the anchoveta biomass began to rise during the early 1950s, but Peru's large-scale anchoveta fisheries started almost 10 years later (see the beginning of the this chapter).

Unfortunately the time series for commercial catch of Peruvian anchoveta are rather short. Some additional information on the long-term dynamics of this species can be obtained from scale deposition in bottom sediments at a site on the shelf off Callao (Baumgartner *et al.* (b) in prep., cited by Schwartzlose *et al.* 1999; Fig. 10.7).

We need to emphasize some important points concerning the reconstructed series:

a) The "gaps" caused by strong El Niño events are absent in the reconstruction. Despite the size of the effect, short-term fluctuations due to El Niño are likely to be smoothed in the course of fish scale accumulation in the bottom sediments.

b) It is clear that the time period between the anchoveta maxima are about 65 years, which corresponds to the fluctuation period of global climatic indices (See Chapters 1, 3, and 5-9).

c) The reconstruct series also suggests that the amplitude and periodicity of anchoveta abundance are similar to those observed recently, although they took place long before the industrial fishery began. Therefore these longer-term fluctuations depend on some unidentified natural factors only.

Similar data were obtained in the Californian upwelling where sardine and anchovy abundance series have exhibited a period of 50-70 years over the last 1700 years. As with the Peruvian data, both period and amplitude of these fluctuations are similar to the period and amplitude of the present century's directly observed fluctuations, although those occurring in the sediment record could only be the result of natural factors (Baumgartner *et al.*1992).

At the same time, the anchovy abundance maxima in the reconstructed series do not coincide with the corresponding maxima in the biomass (Fig.10.7). In the reconstructed series, the maximum falls on the 1940-1950s, while in the "measured" biomass, the maximum falls on the middle and late 1960s (i.e. the curve of actual data are ahead of the reconstructed one by 10-15 years).

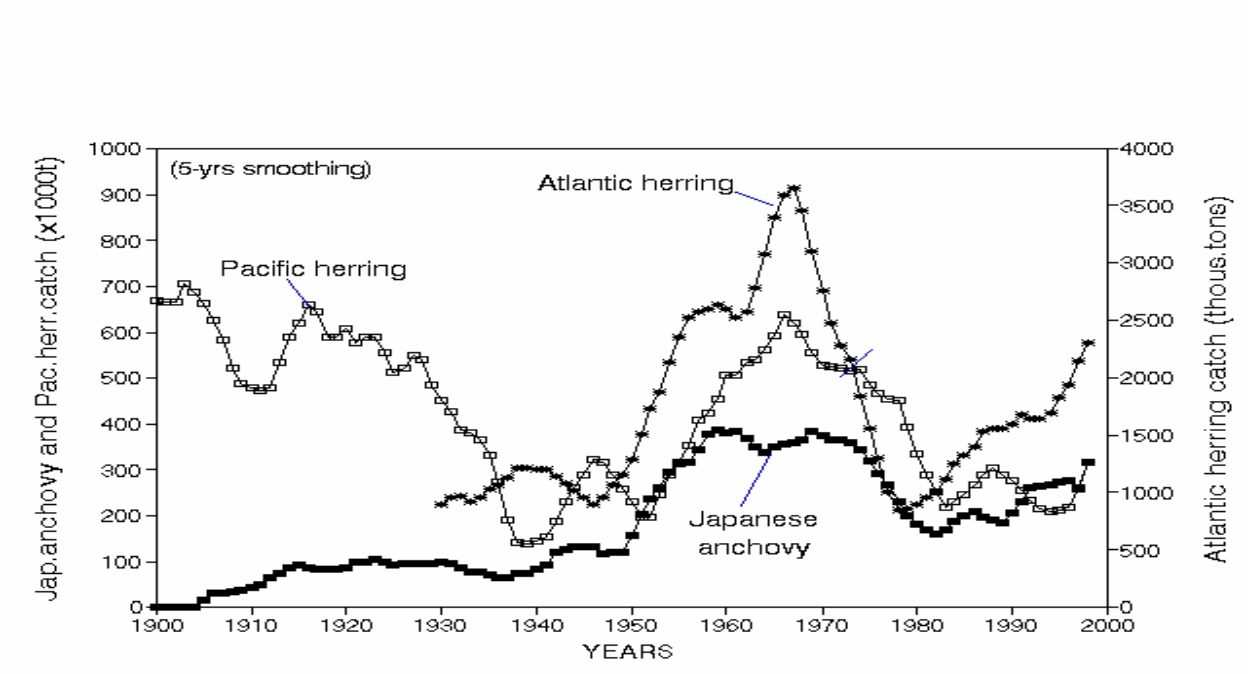

Figure 10.5. Catch dynamics of "meridional" group species: Pacific and Atlantic herring and Japanese anchovy (by only Japanese fleet).

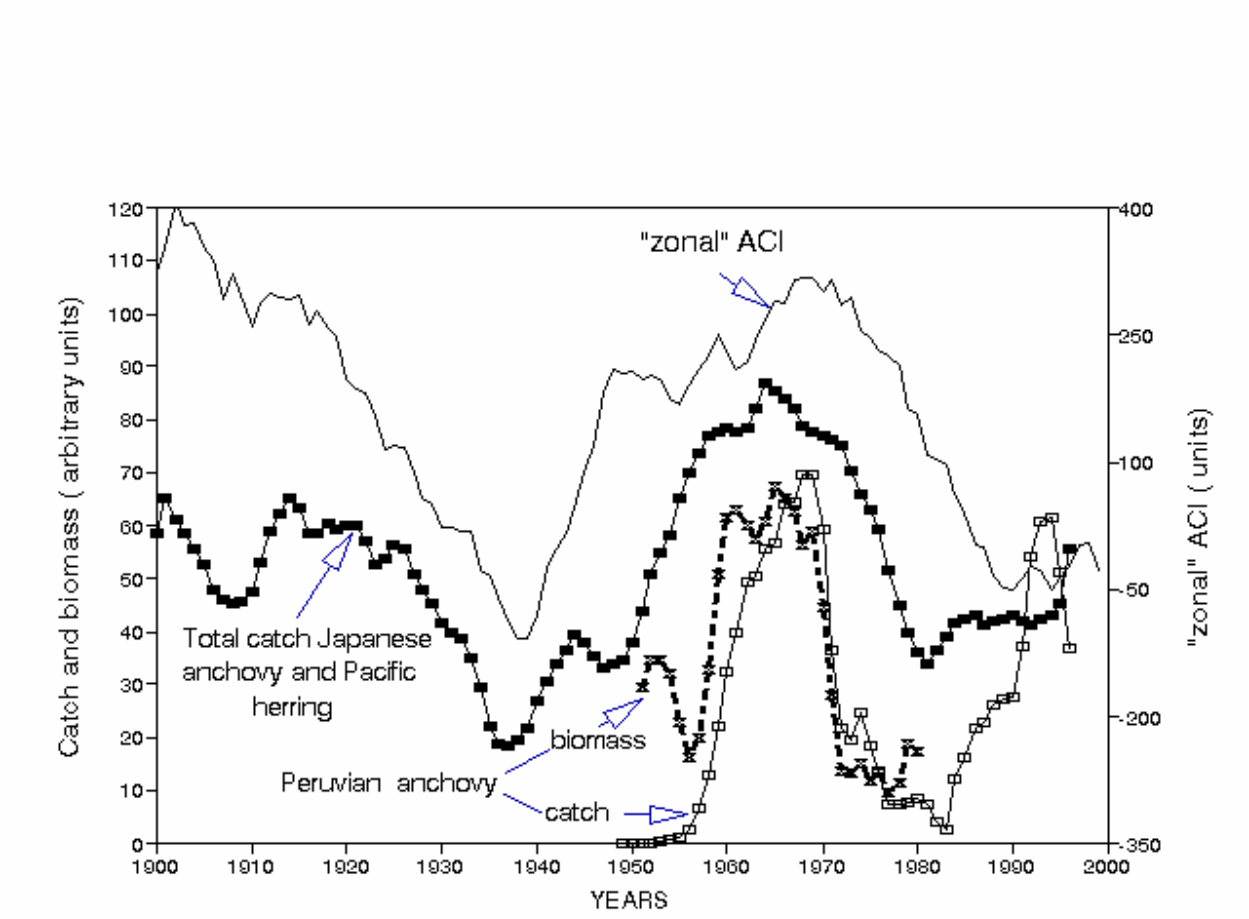

Figure10.6 Catch dynamics of "meridional" dependent species in the Pacific Ocean: Japanese anchovy, Pacific herring and Peruvian anchoveta (catch and biomass) compared with "meridional" ACI trend 1900-1998.

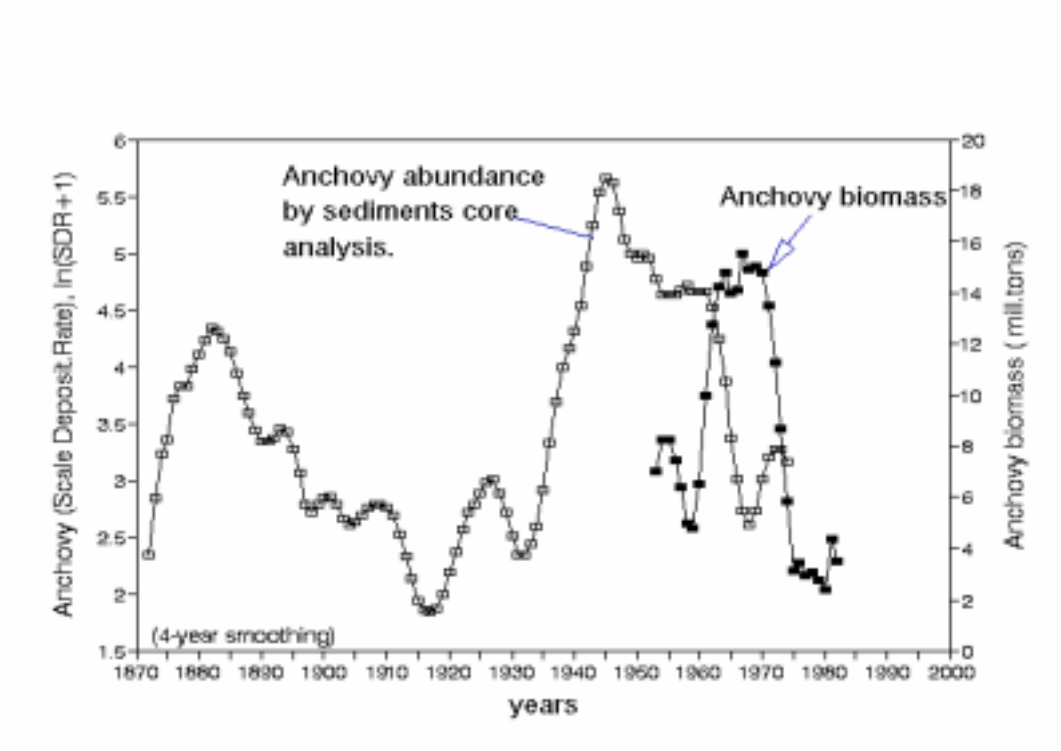

Figure 10.7 Comparison of reconstructed curve of Peruvian anchoveta obtained by scale deposition rates and anchoveta biomass obtained from VPA.

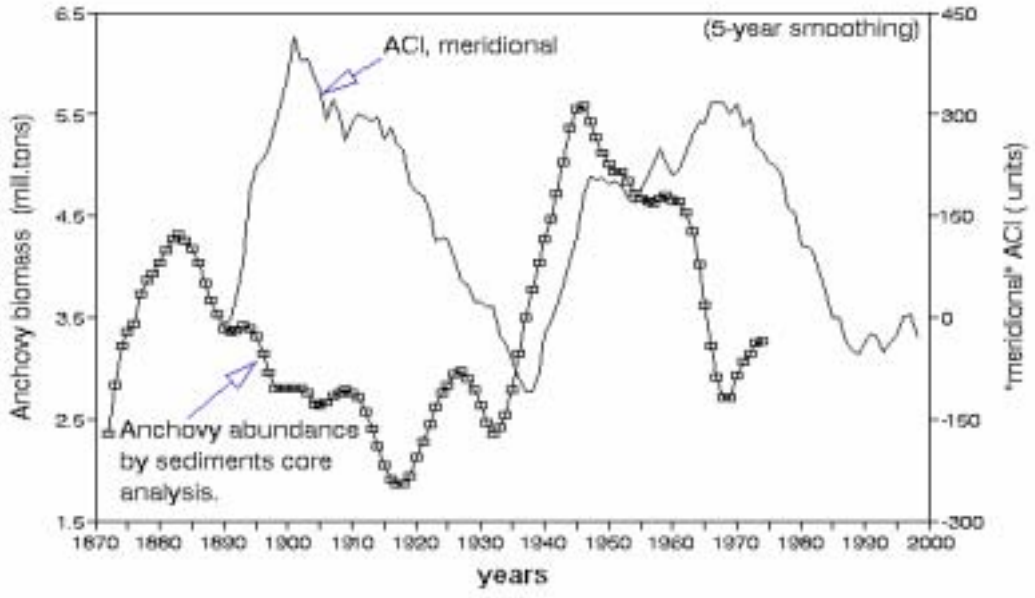

Figure 10.8 Comparison of the "meridional" ACI trend and the reconstructed Peruvian anchoveta abundance from scale deposition rate.

The same discrepancy is present between the anchovy reconstructed series and the “meridional” ACI (Fig.10.8). Both curves are similar in shape and period (about 65 years), but the ACI curve is ahead of the reconstructed population curve by 10-15 years. This inconsistency could be the result of problems with dating procedures for sediment cores.

Accurate dating of fossil structures in bottom sediments is a difficult task. Earlier attempts to reconstruct the Peruvian anchoveta population using scale deposition in bottom sediment cores (DeVries and Pearcy 1982) were not completely successful. There were considerable difficulties in constructing a continuous chronology of deposition from a 3-m long core from the upper slope off Peru (Schwartzlose *et al.*1999). Shackelton (1987), sampling along the Namibian continental shelf, also tried to reconstruct the dynamics of anchovy and sardine populations from scale deposition in bottom sediment cores. The sediments were difficult to date due to the discontinuous nature of the varved (annually layered) sediment formation. Consequently, the author was unable to provide a chronology of fish-scale deposition that could be used to reconstruct the history of the Namibian anchovy population.

The reconstructed series of the Peruvian anchoveta abundance (Baumgartner *et al.* in prep) was developed using a sediment core taken at 194 m water depth on the shelf off Callao. This core also did not exhibit continuous annual layers (varves). However, the chronology of deposition has been undisturbed by biological or physical disruption and therefore can be reconstructed using radiometric dating from the decay rates of isotopes ^{210}Pb and ^{228}Th/^{232}Th (Schwartzlose *et al.*1999). Even though minor uncertainties using these isotopic methods may result in a shift in the absolute (calendar) benchmark when analyzing the sediment core, relative dating remains accurate. Since both reconstructed and measured series of anchoveta abundance and biomass reflect the same processes, their maxima should coincide.

The recent biomass estimates from the VPA-III model (using the data from fishery statistics and independent acoustic methods), should be more reliable than abundance estimates from varved sediment cores. Given the uncertainties over dating procedures, the whole varve-based reconstructed series was shifted 15 years ahead to match up these two curves (Fig. 10.7, 10. 8 and 10.9). Figure 10.9 shows that the shifted reconstructed series and stock assessment estimates are in good agreement with the dynamics of “meridional” ACI.

Figure 10.9 superposes the global climatic indices, and catches and abundance of “meridional-dependent” fish species. It is clear that the dynamics of "meridional" ACI; Peruvian anchoveta biomass (VPA-III), abundance (shifted reconstructed series), and catch, Japanese anchovy catch; and Pacific herring catch are all temporally related.

In summary, unlike most fish species shown in Figure 10.9, the long-term dynamics of the Peruvian anchoveta biomass and catches is complicated by El Niño events. The most strongly manifested El Niño events in the 20th century occurred in the 1911-12, 1918-19, 1925-26, 1940-41, 1957-58,1972-73,1982-83 and 1997-98. The events are not regular, since the corresponding interludes have lasted from 7 to 17 years. In the 20th century, the average recurrence interval for the strongest El Niño events was 10.5 ± 2 years. This means that on average every 10 years, the population of Peruvian anchoveta undergoes catastrophic collapses.

The capability of anchoveta populations for quick recovery after strong El Niño events is astonishing. For example, the anchoveta biomass reached 12.5 million tons in only four years after the strong El Niño event of 1957-58. After the strongest El Niño event in the 20th century of 1982-1983 anchoveta catches dropped catastrophically to 0.1 million tons. However, three years later, the catches increased back to 5 million tons.

The very strong El Niño event of 1997-98 led to a severe decrease in anchoveta catches (1.7 million tons), but in 2000 the anchoveta catch is expected to be about 7-8 million tons. However, the population recovery took place much more slowly after a strong El Niño event of the 1972-73, when the catches were low for 8 years afterwards.

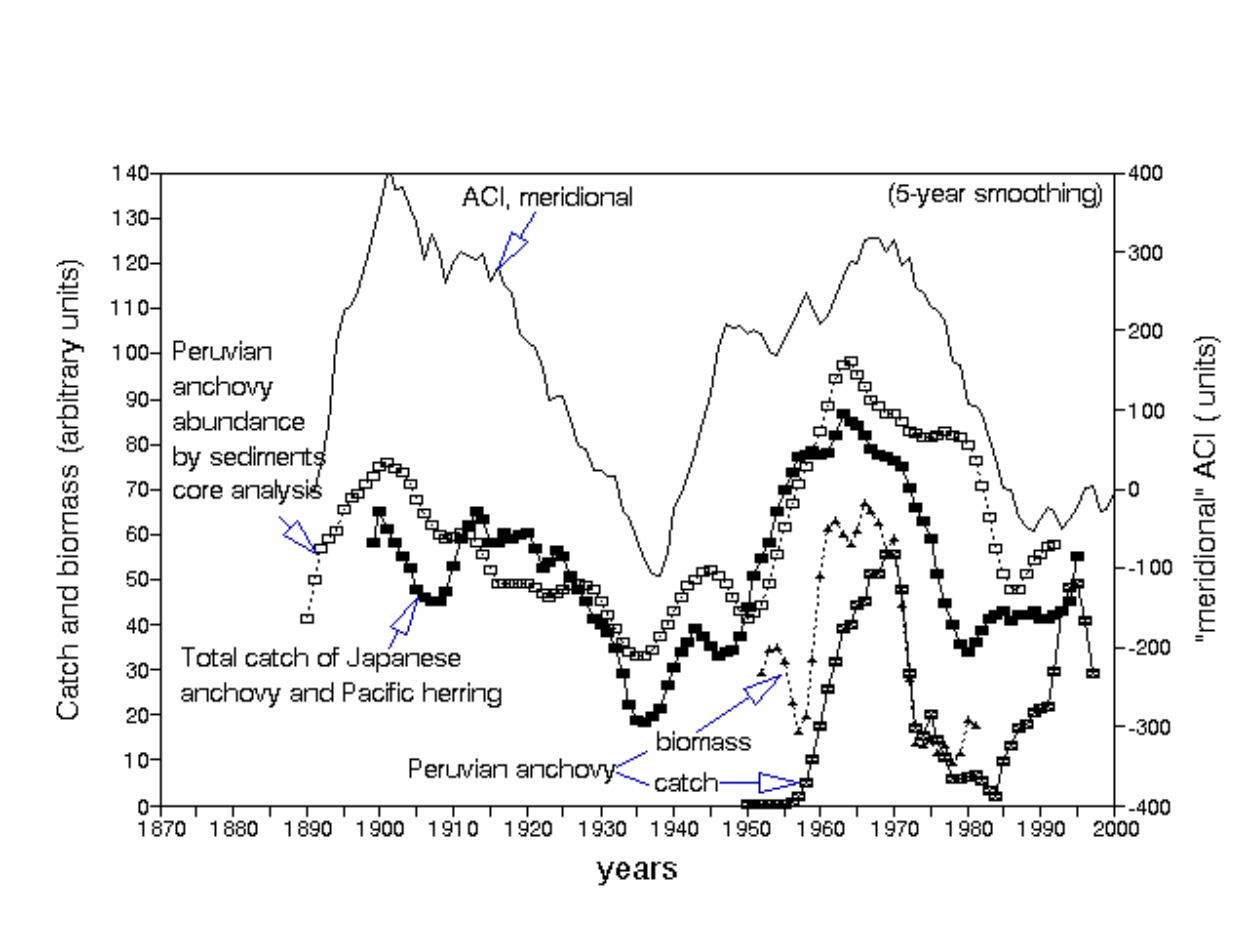

Figure 10.9 Comparison of trends: Peruvian anchoveta biomass and catch, Japanese anchovy (catch by Japanese fleet), Pacific herring, reconstructed Peruvian anchoveta abundance by scale-deposition rate (shifted 15 years to the right) and the “meridional” ACI curve.

Can we predict the long-term changes in the Peruvian anchoveta population for the future 10-20 years? According to the results discussed in Chapter 3, the present "zonal" circulation epoch comes now to its end. The next "meridional" circulation epoch is starting to dominate in the 2005-2030s. The forecasts of main trends of both “zonal” and “meridional” epochs discussed in Chapter 9 enables to us to estimate a probable future dynamics of the “meridional” ACI (Fig.10.10).

10.2 THE FORECAST

Based on the trends presented in Figures 10.9 and 10.10, it may be supposed that the abundance and catches of "meridional dependent" species (Japanese anchovy, Pacific herring, Atlantic herring and Peruvian anchoveta) will increase in line with the development of the present “meridional” epoch up to the middle 2020s, followed by a gradual decrease. However, unlike the first three species, the population of Peruvian anchoveta may be affected by strong El Niño events, which will result in “gaps” in abundance and catches and interfere with the “smooth” climate-governed dynamics of the population as portrayed below.

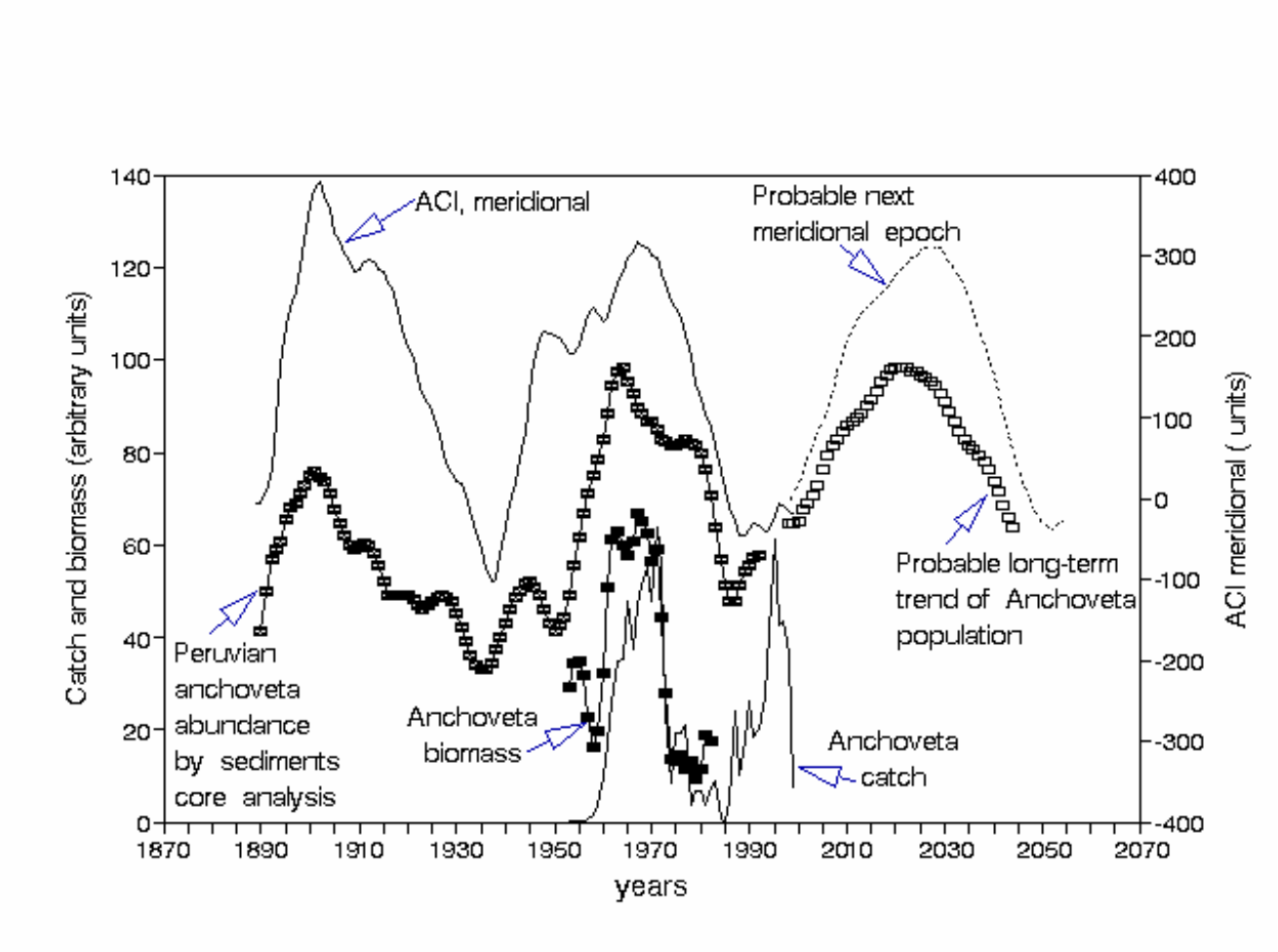

Figure 10.10 Relative trends of catch, biomass and reconstructed anchoveta abundance by scale-deposition rate as compared with "meridional" ACI trends and the probable forecasted anchoveta population. (Reconstructed anchoveta abundance curve shifted 15 years to the right; see text for details).

The model generated (Chapter 9) forecast of probable anchovy catch in the Pacific is presented in Table 10.1 and Figure 10.11.

Table 10.1. Model-generated forecast of anchovy catch (million tons) in the Pacific region for 2005–2040s.

Years	Peruvian anchovy	Japanese Anchovy	Total
2005	6. 7	2. 5	9. 2
2010	8. 6	3. 0	11. 6
2015	10. 5	3. 1	13. 6
2020	8. 5	2. 6	10. 5
2025	6. 8	2. 0	8. 8
2030	4. 6	1. 0	5. 6
2035	2. 6	0. 7	3. 3
2040	2. 4	0. 4	2. 8

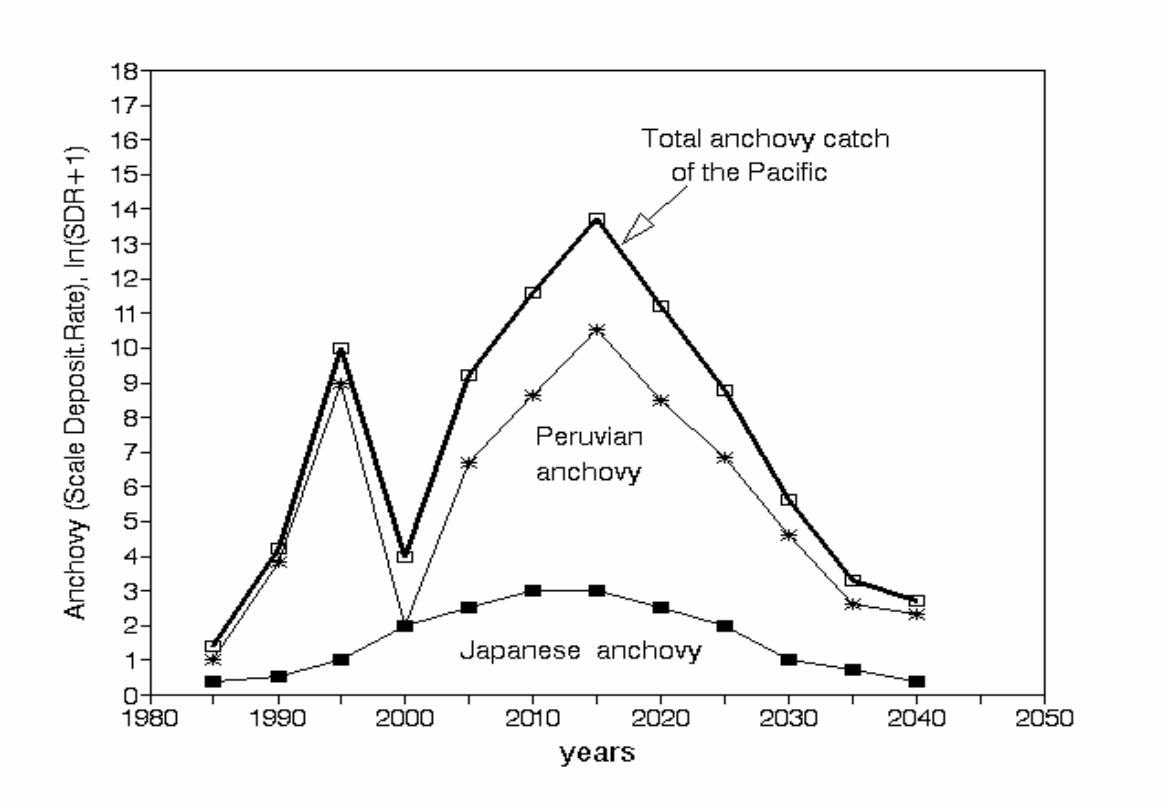

Figure 10.11 Forecasted changes of Peruvian and Japanese anchovy catches for the period of 2000-2040s

10.3 SUMMARY

Our approach makes it possible to forecast general trends of anchoveta catch for 30–40 years ahead. This is based on the following assumptions:

(1) General stock fluctuations of Peruvian and Japanese anchovies correspond to the dynamics of "meridional" ACI. This means that there should be a steady increase until the middle of 2020s.

(2) Unlike other pelagic commercial species, the climate-dependent dynamics of Peruvian anchoveta is affected by strong El Niño events, so that the future dynamics of this species are not expected to follow a smooth curve, but should be punctuated by sharp, unexpected declines in abundance;

(3) Total anchovy catch in the Pacific Ocean is dominated by Peruvian anchoveta (e.g. 70-75% during peaks), therefore the forecast of total anchovy catch presented below (Table. 10. 1 and Fig. 10.11) is only a rough approximation to the stock dynamics of this species group.

11. PROBABLE CHANGES IN THE CATCHES OF MAJOR COMMERCIAL SPECIES IN VARIOUS REGIONS OF THE WORLD OCEANS

The total catch dynamics of major commercial species is presented in Figure 11.1, with catches forecast from 2000. For the last 15 years (1985–2000), the total catch of the Pacific and Atlantic has decreased sharply (by almost 10 million tons). This is due to simultaneous decrease in the stock of six major commercial species (Japanese, Peruvian and European sardine, Alaska pollock, Chilean jack mackerel and Pacific salmon). The latter are in line with the dynamics of zonal atmospheric circulation (zonal ACI).

The decrease in commercial catches would be even more extreme if there was no gradual increase in the population of the meridional-dependent species: Pacific and Atlantic herring, South African sardine, and Japanese and Peruvian anchovy. After 2000, the present zonal ACI epoch will come into its final stage, and simultaneously, the new meridional epoch will start. Extrapolating from past experience (1950-1980s), commercial stock and catches of Pacific and Atlantic herring, Atlantic cod, South African sardine, and Japanese and Peruvian anchovy are likely to increase in line with the oncoming meridional epoch (2020–2030s). This will result in a gradual increase in the catches of "meridional-dependent" commercial species up to 23–24 million tons by the 2015–2020, followed by the decrease of up to 20 million tons by 2030. The stocks of zonal-dependent species will decrease gradually by the 2015–2020s, then start to increase, following the dynamics of "zonal" ACI, reaching its new maximum (about 23-25 million tons) by the 2040s. The opposite phase character of the total catch dynamics of "meridional" and "zonal" species is clear from Figure 11.2.

Changes in the catch of major commercial species in the Atlantic alone are less pronounced, and depend primarily on the dynamics of "meridional-dependent" species: Atlantic herring, Atlantic cod, South African sardine and anchovy. Hence, the catch dynamics of major commercial species in the Pacific is not very different from the corresponding dynamics of total catch summed for the Pacific and Atlantic (Figure 11.1).

Total catches of the major commercial species in the Atlantic are expected to decrease from 2020 to 2040. The contribution of zonal-dependent species to the total Atlantic catch is not high, and the expected decrease in "meridional-dependent" species is unlikely to be compensated fully by a corresponding increase in the catches of zonal-dependent species.

Differences between the total catch dynamics of the major commercial species in the Atlantic and Pacific are not well manifested (Figure 11.3). This is due to the "masking effect" of Peruvian anchoveta in the Pacific region where "zonal-dependent" species dominate.

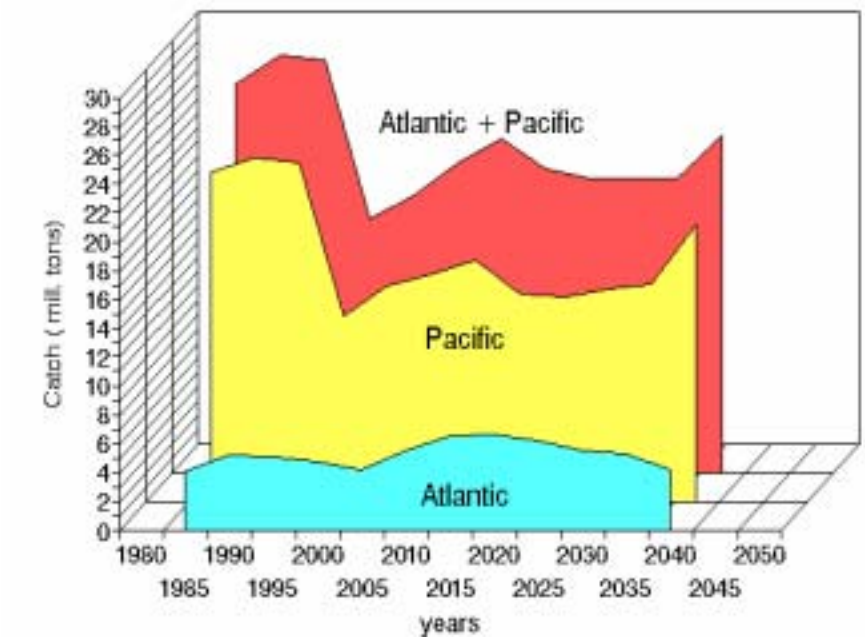

Figure 11.1 Observed and forecast total catch of major commercial species in the Atlantic and Pacific. Forecast catches are given for the period 2000-2040.

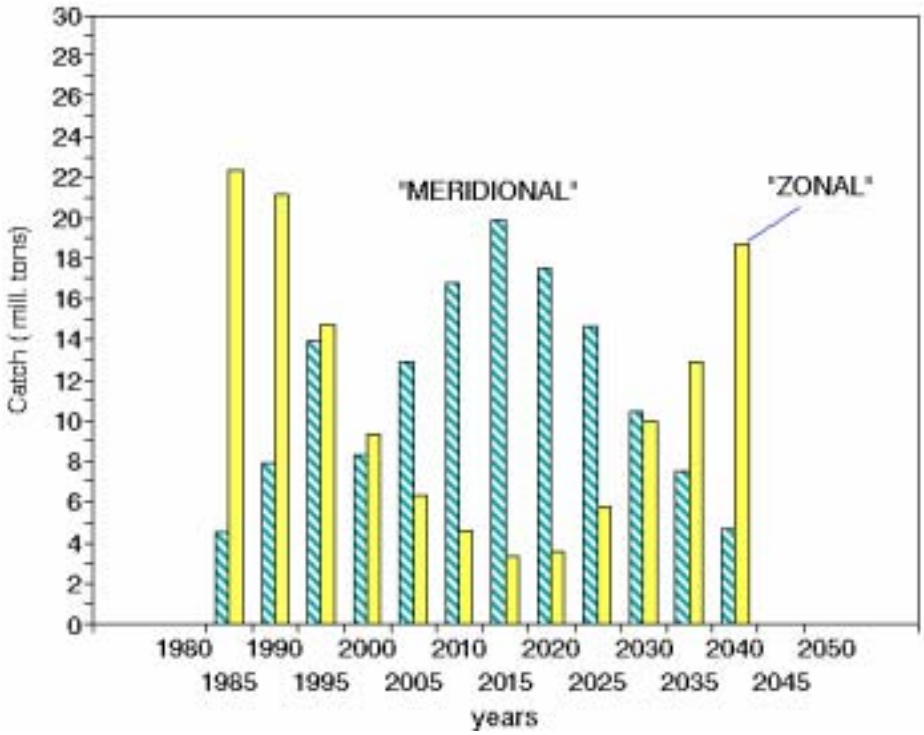

Figure 11.2 Total catch forecast for the major “meridional-dependent” (blue) and “zonal-dependent” (yellow) commercial species groups.

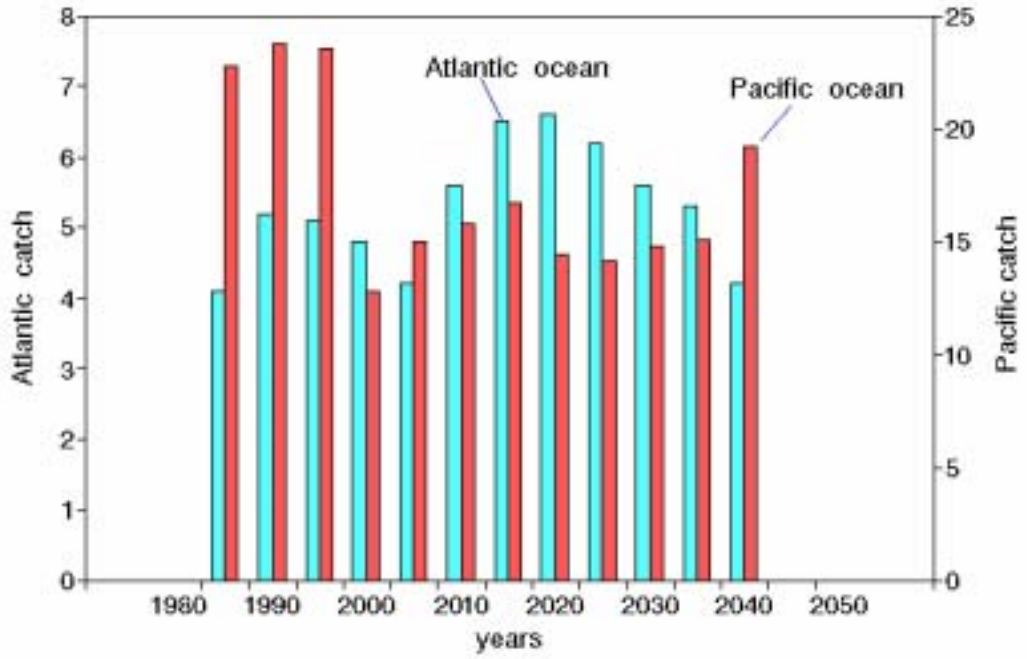

Figure 11.3 Catch changes forecast for the major commercial species in the Atlantic and Pacific.

If anchovy is withdrawn from the total Pacific catch, then the "out of phase" character of the catch dynamics in both oceans becomes clear (Figure 11.4). This "out of phase" character of the catch dynamics in the Atlantic and Pacific may be explained by the effect of the same global climatic process affecting both regions. In this system, the meridional-dependent commercial species dominate in the North Atlantic whereas zonal-dependent species dominate in the North Pacific. The total catch in these two regions fluctuates in agreement with the alternation of zonal and meridional climatic epochs. (Figure 11.5; see also Figures 3.6, 3.7)

The forecasted catch dynamics of major commercial species in the South Pacific and the South Atlantic are compared in Figure 11.6. Forecasted catch dynamics of the main commercial species in the Southern Hemisphere is to a large extent determined by the Peruvian anchovy catch, corresponding to “meridional-depending” dynamics with a maximum around 2015–2020s.

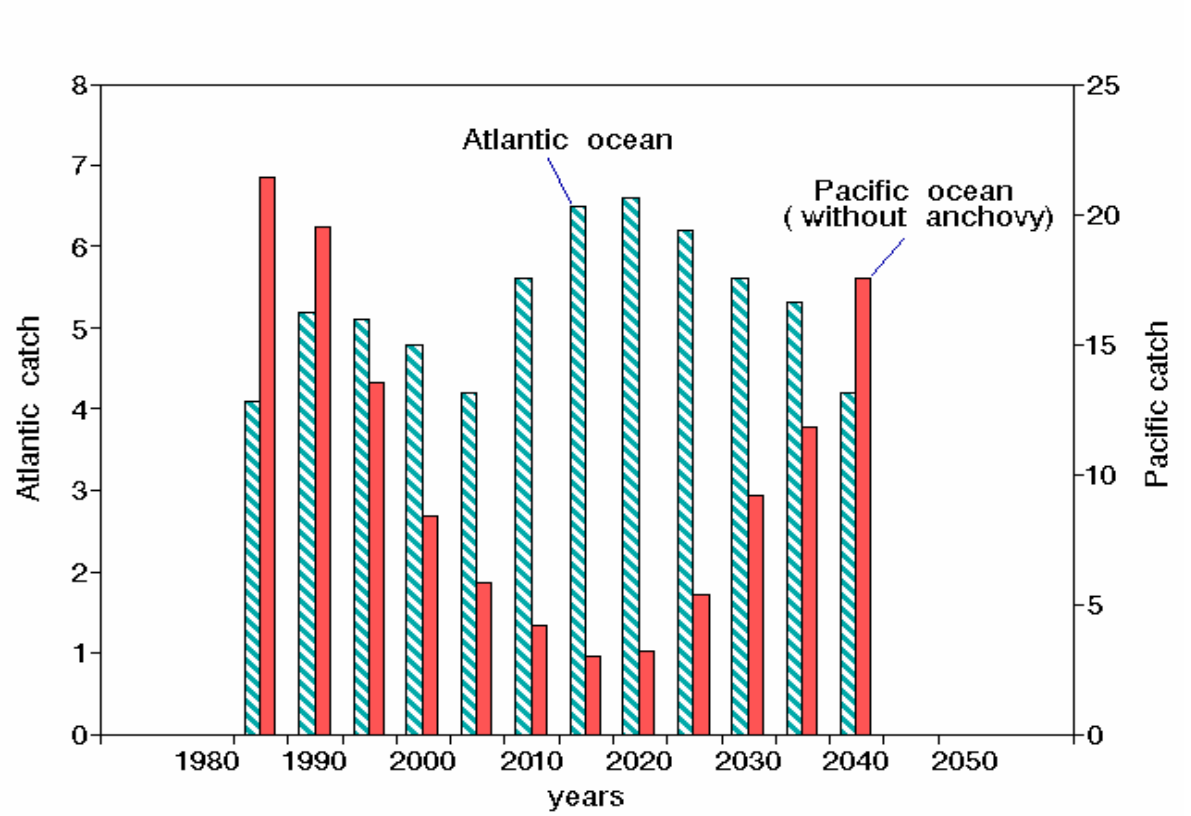

Figure 11.4 Forecasted catches of major commercial species in the Atlantic and Pacific (excluding Peruvian anchovy) for 2000-2040.

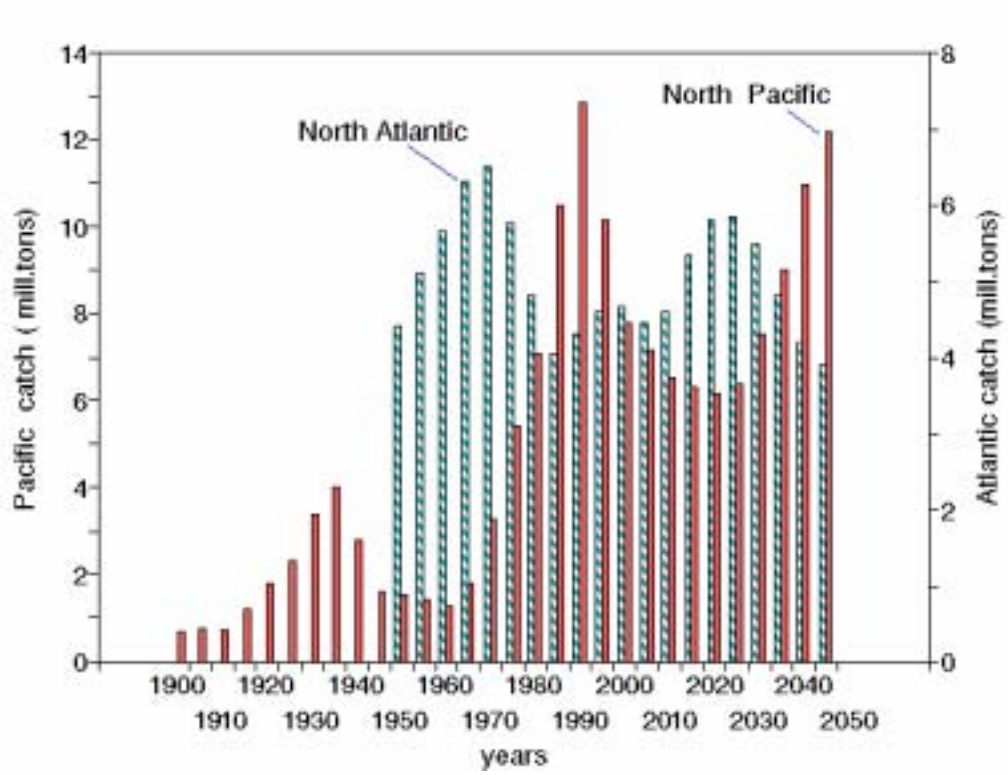

Figure 11.5 Actual (1920—1998) and forecasted (2000—2040) catches of major commercial species of North Atlantic and North Pacific.

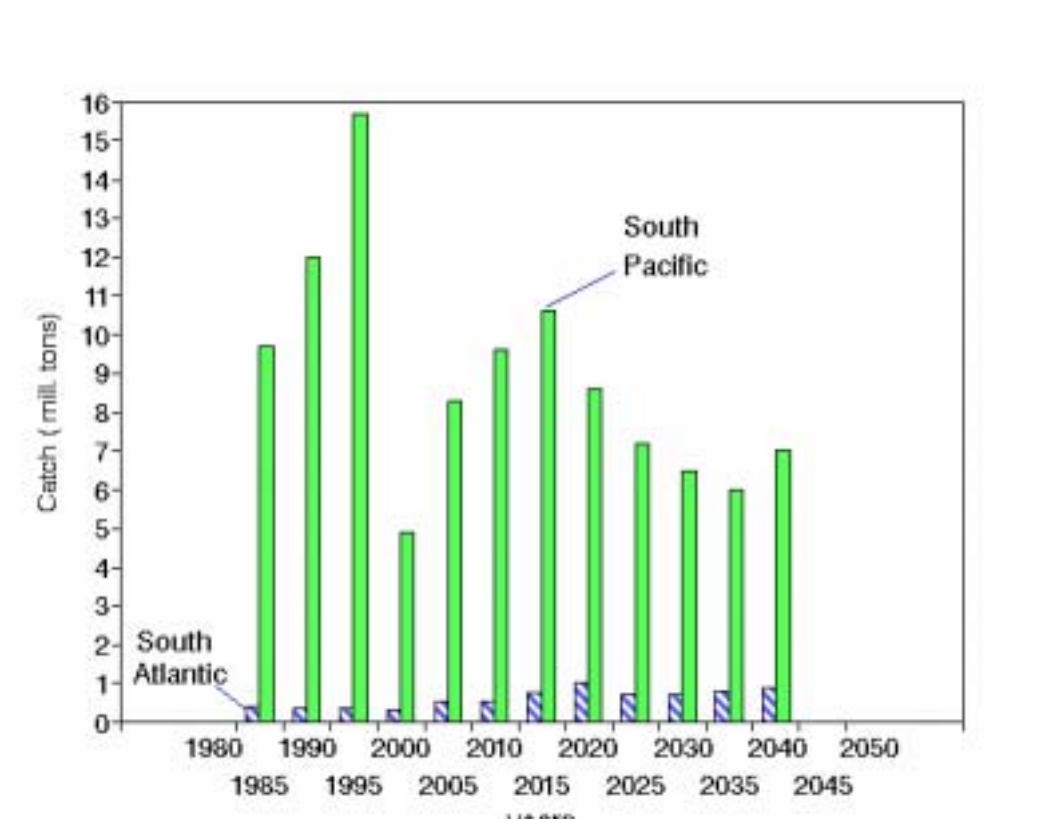

Figure 11.6 Forecasted catch dynamics of major commercial species of South Atlantic and South Pacific for 2000 – 2040.

11.1 PROBABLE CHANGES OF MAJOR COMMERCIAL SPECIES IN 2000–2040.

Table 11.1 Changes in catches (million tons) forecast for the major commercial species for 2005 - 2040 by 5 years intervals. The values indicate the change relative to the previous 5 years.

Years:	2005	2010	2015	2020	2025	2030	2035	2040
World Catch	+1.6	+2.2	+1.8	-2.2	-0. 6	0	0	+ 3.0
Atlantic Ocean	-0.6	+1.4	+0.9	+0.1	-0.4	-0.6	-0.3	-1.1
Pacific Ocean	+2.2	+0.8	+0.9	-2.3	-0.2	+0.6	+0.3	+4.1

Table 11.1 presents the forecasted catch dynamics in the Atlantic and Pacific regions calculated over 5 years intervals. For our purpose, the most interesting are the catch changes expected in the next 15 years. Estimation of the annual increment suggests that, by 2015 the catches of major commercial species are likely to change as follows (compared to 2000):

- Total world catch: +5.6 million tons
- Atlantic catch: +1.7 million tons
- Pacific catch: + 3.9 million tons

In the period of 2015–2030, the catches will change as follows (compared to 2015):

- Total world catch: - 2.8 million tons
- Atlantic catch: - 0.3 million tons
- Pacific catch: - 2.5 million tons

In general, the catches forecast for the major commercial species in both oceans will increase in the 2000-2015s and decrease in the 2015-2030s. This is due to the expected increase of the meridional-dependent catch in the Atlantic Ocean and probable increase in Peruvian anchovy catch in South Pacific. At the same time, in the most important fishery region, the North Pacific, the catch of the major commercial species is expected to decrease significantly due to a long-term decline in zonal-dependent species abundance.

The long-term catch fluctuations depend primarily on the variation of only 12 major commercial species, which are strongly influenced by climatic effects. The total world marine catch includes many more species. Around 550 fish species are caught commercially. The catch of these species has remained relatively stable (about 35 million tons) for the last 20-25 years is not expected to be so influenced by climate. Therefore, changes in total catches will reflect changes in the 12 major commercial species only.

12. CONCLUSION

This study establishes the concept of 60-year climate oscillations corresponding to the regular fluctuations of the populations and catches of the main commercial fish species. Analysing roughly 30-year alternation of the so-called "climatic epochs" characterised by the variation in the Atmospheric Circulation Index (ACI), the study revealed two ACI-dependent groups of major commercial species correlated positively with either "meridional" or "zonal" air mass transport on the hemispheric scale.

Climate periodicity serves as a basis for a predictive model of the population and catches of major commercial fish species. The model has two basic limitations.

(1) It is applicable to the abundant fish species only (commercial catch > 1.0 - 1.5 million tons) yielded over large areas, such as North Pacific or North Atlantic as a whole;

(2) The model is intended to analyse and forecast the long-term trends in the population of major commercial species with the assumption that general intensity of commercial fisheries will stay at its average level over the last 20 - 25 years.

The concept of generating forecasts of anthropogenic climate change and consequent changes in fish production is beyond the scope of this study. However, there is a clear link between fish production and climate, so projecting future climate changes is of importance. Not only can climate be used to forecast commercial fish yields, but also it may be possible to estimate general changes in biological production on the global scale. It is therefore important to maintain databases on routine fisheries data and climate indices in the long term, in order to track these critical processes.

Acknowledgements

I am very grateful to all my colleagues, with whom I repeatedly discussed the climate-and-fishery and many related issues while working on this paper. I address my special gratitude to Dr. A. Lubushin, a senior scientist in the Institute of the Earth Physics, Russian Academy of Sciences, for his excellent job in modelling (see Chapter 8), and to my son Alexy Klyashtorin who has kindly translated the manuscript into English.

13. REFERENCES

Aguero, V. (1987) A Bioeconomic Model of the Peruvian Pelagic Fishery. pp307-324. In: Pauly, D., Tsukayama, I. (ed.) *The Peruvian Anchoveta and its Upwelling Ecosystem: Three Decades of Change.* ICLARM Studies and Reviews No. 15. Callao, Peru, IMARPE. 351p.

Anderson, T. W. (1971) The statistical analysis of time series. New York, John Wiley & Sons, Inc.

Anisimov, V., Polyakov, O. (1999) On the prognosis of air temperature change for the first quarter of 21st century. *Meteorology and Hydrology.* 2: 25-31. (in Russian, English summary)

Bakun, A. (1990) Global Climate Change and Intensification of. Coastal Ocean Upwelling, Science. 247: 198-200.

Bakun, A.(1996) *Ocean Processes and Marine Population Dynamics,* California Sea Grant and Centro de Inesigationes Biologicas, La Paz , Mexico, 323p.

Barnes, R. T. H., Hide, R., White, A. A., Wilson, C. A. (1983) Atmospheric angular momentum fluctuations, length-of-day changes and polar motion. *Proc. Royal Soc. London* 334:55-92.

Battan, L. J. (1983) Weather in your life. San Francisco, Freeman and Co. 223p.

Baumgartner, T. R., Soutar, A, Ferreira-Bartrina, V. (in preparation) Comparative history of sardine and anchovy populations in the California and Peru-Chile ecosystems from fish scale deposition records.

Baumgartner, T. R., Soutar, A., and Ferreira-Bartrina V. (1992) Reconstruction of the history of Pacific sardine and Northern Pacific anchovy populations over the past two millennia from sediments of the Santa Barbara basin. CalCOFI Report, 33: 24-40.

Beamish, R. J. and Bouillon, D. R. (1993) Pacific salmon production trends in relation to climate. *Can. J. Fish. Aqua. Sci.* 50: 1002-1016.

Beamish, R. J. D., Noakes, J., McFarlane, G. A., Klyashtorin, L., Ivanov, V. V., Kurashov, V. (1999) The regime concept and natural trends in the production of Pacific salmon*Can.J.Fish.Aqua.Sci* 56: 516-526

Bell, G. D., Halpert, M. S., Cosky, V. E., Gelman, M. E., Roplewski, Ch. E., Douglas, A. V., Shnell, R. C. (2000) Climate assessment for 1998. *Bull. Am. Meteorol. Soc.* 80, No 5:1040-1140.

Box, G. E. P., Jenkins, G. M. (1970) *Time series analysis. Forecasting and control.* San Francisco, Holden-Day.

Briffa, K. R., Bartholin, T. S., Eckstein, D., Jones, P. D., Karlen, W., Schweingruber, F. W., Zetterberg, P. (1990) A 1400 year tree-ring record of summer temperatures in Fennoscandia. *Nature* 346: 434-439.

Brodeur, R. D. and Ware, D. M. (1995) Interdecadal variability in distribution and catch rates of epipelagic nekton in the Northeast Pacific ocean. In: Beamish, R. J. (ed.) *Climate and Northern Fish Populations.* Can. Spec. Publ. Fish. Aquat. Sci. 121: 329-356.

Brodeur, R. D., (1993) Long-term variability in zooplankton biomass in the subarctic Pacific Ocean. *Fisheries Oceanography* 1: 32-38.

Csirke, J. (1980) Recruitment in the Peruvuian anchoveta and its dependence on the adult population. p307-313. In: Saville, A. (ed.) *The assessment and management of pelagic fish stocks.* Rapp. P.V. Réun. CIEM. 177.

Csirke, J. 1995. Fluctuations in abundance of small and mid-sized pelagics. *Scientia Marina* 59(3-4): 481-490.

Csirke, J. Sharp, G.D. (ed.) (1984) Reports of the Expert Consultation to Examine the Changes in Abundance and Species Composition of Neritic Fish Resources, San Jose, Costa Rica, 18-29 April 1983. *FAO Fish. Rep. Ser.* No.291 (1). 102p.

Dansgaard, W., Johnsen, S. J., Reeh, N., Gundestrup, N., Clausen, H. B., Hammer, C. U. (1975) Climatic changes, Norsemen and modern man. *Nature* 255: 24-28.

DeVries, T.J. and Pearcy, W.G. (1982) Fish debris in sediments of the upwelling zone off central Peru. A late quaternary record. Deep Sea Res. 28(1A): 87-109

Dickey, J. O., Marcus, S. L., Hide, R. (1992a) Global propagation of international fluctuations in atmospheric angular momentum. *Nature* 334: 115-119.

Dickey, J. O., Steppe, J. A., Hide, R. (1992b) The earth's angular momentum budget on seasonal time scales. *Science* 255: 321-324.

Dzerdzeevski, B. L. (1969) Climate epochs in the twentieth century and some comments on the analysis of past climates. In: Wright, H. W. (ed.) *Quaternary geology and climates*. InternAss. Quoternary Res 16: 49-60, Washington.

Efron B., Tibshirani, R. (1986) Bootstrap methods for standard errors, confidence intervals and other measures of statistical accuracy, Statistical Sciences, vol. 1: 54-77.

FAO (1994) Bulletin of Fishery Statistics, No. 34 Fishery fleet statistics: 1970, 1975, 1980, 1984-1992. Rome, Food and Agriculture Organization of the United Nations. 1994. 448p.

FAO (1994) FAO Expert Consultation on Fisheries Research, Rome, 12-15 April 1994. *Fisheries Circular* 877. , Rome, Food and Agriculture Organization of the United Nations. 105p.

FAO (1996) Chronicles of Marine fishery landings (1950-1994) Trend analysis and fisheries potential. Grainger, R. J. R. and Garcia, S. M. *Fisheries Technical Paper* 359. Rome, Food and Agriculture Organization of the United Nations. 48p.

FAO (1997a) Review of the state of world fishery resources: Marine fisheries (by Marine Resources Service, Fishery resources Division, Fisheries Department). *Fisheries Circular* 920. Rome, Food and Agriculture Organization of the United Nations. 105p.

FAO (1997b) Empirical Investigation on the Relationship between climate and small pelagic Global Regimes and El Nino- Southern oscillation (ENSO). Lluch-Cota, D., Hernandez-Vazquez, S., Lluch-Cota, S. *Fisheries Circular* 934. Rome, Food and Agriculture Organization of the United Nations. 48p.

FAO (2000) Yearbook of Fishery Statistics - Capture Production 1998. Vol. 86/1. Rome, Italy: FAO. Downloadable at: http://www.fao.org/fi/statist/FISOFT/FISHPLUS.asp

Fishery statistics of Japan 1996. Statistics and Information Department Ministry of Agriculture Forestry and Fisheries.

Francis, R. C. (1990) Climate change and marine fisheries. *Fisheries (Bull. Amer. Fish. Soc.)* 15(6): 7-10.

Garrod, D. J. Schumacher, A. (1994) North -Atlantic Cod: the broad canvas. *ICES mar. Sci. Symposium* 198: 59-76.

Girs, A. A. (1971) Macrocirculation method for long-term meteorological prognosis. Leningrad, Hydrometizdat Publ. 480p. (in Russian)

Glantz, M. H. (1990) Does History have a Future? Forecasting Climate Change Effects on Fisheries by Analogy *Fisheries (Bull. Amer. Fish. Soc)* 15(6): 39-45.

Hide, R., Dickey, J. O. (1991) Earth 's variable rotation. *Science* 253: 629-637.

Huber, P. J. (1981) *Robust statistics*. New York, John Wiley and Sons Inc.

IFOP (1985) Taller Nacional: fenomeno El Niño 1982-83. Invest. Pesq. (Chile) 32. Numero especial. 256p.

Johannesson, K., and R. Vilchez (1980) Note on hydroacoustic observations of changes in distribution and abundance of some common pelagic fish species in the coastal waters of Peru, with special emphasis on anchoveta. Pp.287-323 In: *Workshop on the Effects of Environmental Variation on the Survival of Larval Pelagic Fishes*. (G.D. Sharp, ed.) IOC Workshop Report No.28. Unesco, Paris.

Jonsson, J. (1994) Fisheries off Iceland, 1600-1900. *ICES mar. Sci. Symposium* 198: 3-16.

Kashyap, R. L., Rao, A. R. (1976) Dynamic stochastic models from empirical data. New York, Academic Press.

Kawasaki, T. (1992a) Climate-dependent fluctuations in Far Eastern Sardine Population and their impacts on fisheries and society. pp.325-355. In: Glantz, M. (ed.) *Climate Variability, Climate Change and Fisheries*. Cambridge Univ. Press.

Kawasaki, T. (1992b) Mechanisms governing fluctuations in pelagic fish populations. In: Paine, A., *et al*. (ed.) *Benguela trophic Functioning. South African Journal of marine Sciences* 12: 873-879.

Kawasaki, T. (1994) A decade of the regime shift of small pelagics. FAO expert consultation (1983) to the PICES III (1994). *Bulletin of the Japanese Society of Fisheries Oceanography* 58: 321-333.

Klyashtorin, L. (1998) Cyclic climate changes and Pacific salmon stock fluctuations. A possibility for long-term forecasting. NPAFC (North Pacific Anadromous Fish Commission). Technical Report. Workshop on Climate Change and salmon Production Vancouver, March 26-27, 1998 (Canada). pp.6-7.

Klyashtorin, L. B. (1997) Pacific salmon: climate–linked long-term stock fluctuations. *PICES Press* (Newsletter of North Pacific Science Organization) 5:2-34.

Klyashtorin, L. B. (1998) Long-term climate change and main commercial fish production in the Atlantic and Pacific. *Fisheries Res*. 37: 115-125

Klyashtorin, L. B. (1999) Global and regional characteristics of climate change in the Pacific. The agreement with the Southern Oscillation Index. Beyond El Nino Conference on Pacific Climate Variability and Marine Ecosystem Impacts from the Tropics to the Arctic, La Jolla, California, U. S. A., March 23-26, 2000. 54p.

Klyashtorin, L., Nikolaev A., Klige, R. (1998) Variation of global climate indices and Earth rotation velocity. In: *Book of Abstracts GLOBEC First Open Science Meeting*, Paris, 17-20 March 1998. 55p.

Klyashtorin, L., Sidorenkov, N. (1996) Long-term climatic change and pelagic fish stock fluctuations in the Pacific. Reports of Pacific Research Instuite of Fisheries and Oceanography (Vladivostok) 119: 33-54. [Dolgoperiodny klimaticheskii izmenenija i fluktuatzii zapasov pelagicheskikh ryb v Pacifike] (in Russian, English summary).

Klyashtorin, L., Smirnov, B. (1995) Climate-dependent salmon and sardine stock fluctuations in the North Pacific. In: Beamish, R., (ed.) *Climate change and northern fish fluctuations.* Can. Spec. Publ. Fish. Aquat. Sci. 121: 687-689.

Korelsky, V. (ed.) (1996) Fisheries of Japan*,* Expeditor publ., Moscow. 160pp, (in Russian).

Lamb, H. H. (1972) *Climate, present, past and future*. London, Methuen and Co. 613p.

Lambeck, K. (1980) *The Earth Variable Rotation*. Cambridge Univ. Press.

Lambeck, K. Cazenave, A. (1976) Long Term Variations in the Length of Day and Climatic Change. *Geophys. J. R. astr. Soc*. 46: 555-573

Langley, R. B., King, R. W., Shapiro, I. I., Rosen, R. O., Salstein, D. A. (1981) Atmospheric angular momentum and the length of day: A common fluctuation with a period near 50 days. *Nature* 294: 730-732.

Leroux, M. (1998) *Dynamic Analysis of Weather and Climate*. Chichester, John Wiley and Sons Inc. in association with Praxis Publishing. 363pp.

Lluch-Belda, D., Crawford, R., Kawasaki, T., MacCall, A., Parrish, R., Shwartzlose, R., Smith, P. (1989) World-wide fluctuations of sardine and anchovy stock. The regime problem. *S. Afri. J. Mar. Sci.* 8: 195-205.

Lluch-Belda, D., Hernandez-Vazquez, S., Hernandez-Vazquez, S., Salinas-Zavala, C., Shwartzlose, R. (1992) The Recovery of the California sardine as related to global change. *Calif. Coop. Oceanic Fish. Invest. Rep*. 33: 50-59.

Lluch-Belda, D., Schwartzlose, R.A., Serra, R., Parrish, R., Kawasaki, T., Hedgecock, D. Crawford, R.J.M. (1993) Sardine and anchovy regime fluctuations of abundance in four regions of the world oceans: a workshop report. *Fisheries Oceanogaphy* 1(4): 339-347.

Lluch-Belda, D., Shwartzlose, R., Serra, R., Parrish, R., Kawasaki, T., Hedgecock, D., Crawford, R. (1993) Sardine and anchovy regime fluctuations of abundance in four regions of the World Ocean: a workshop report. *Fisheries Oceanography* 2: 339-343.

Loeb, V., Rojas, O. (1988) Interannual variation of ichthyo-plankton composition and abundance relations off northern Chile. *Fish. Bull., U.S.* 86(1): 1-24.

Manthua, N. J., Hare, S. R., Zhang, Y., Wallace J. M., Francis, R. C. (1997) A Pacific inter-decadal climate oscillation with impacts on salmon production. *Bull. Am. Meteorol. Soc*. 78: 1069-1079.

Marple, S. L. Jr. (1987) *Digital spectral analysis with applications.* New Jersey, Prentice-Hall, Inc.

Minobe, S. (1997) A 50-70 year climatic oscillation over the North Pacific and North America. *Geophys. Res. Lett*. 24: 683-686.

Minobe, S. (1999) Resonance in bi-decadal and penta-decadal climate oscillations over the North Pacific: Role in climatic regime shifts. *Geophys. Res. Lett.* 26: 855-858.

Moiseev, P. A. (1995) The present state, trends and future of world fishery and aquaculture. A review information no. 2, Ser: Economical problems of the world Fishery. 1-48. Moscow, ECINAS Publ. (Russian Federal Committee for Fisheries). [Sostoyanie, tendentsie i budushie mirovogo pybolovstva I akvakultury] (in Russian).

Monin ,A.S.(2000) Climate as a problem in physics. *Achievements in the Physical Sciences*,170,No4 419-445.(Climate kak problema phisiki, *Uspekhi phizicheskikh nauk*) (in Russian)

Munk, W. H., McDonald, G. J. F. (1960) *The rotation of the Earth.* Cambridge Univ. Press. 323p.

Mysak, L. A. (1986) El Nino interannual variability and Fisheries in the Northeast Pacific Ocean. *Can. J. Fish. Aquat. Sci*. 43: 464-497.

Pauly, D., Palomares, M. L., Gayanilo, F. C. (1987) VPA Estimates of the Monthly Population, Length Composition, Recruitment, Mortality, Biomass and Related Statistics of Peruvian anchoveta 1953-1981. pp142-165. In: Pauly, D., Tsukayama, I. (ed.) *The Peruvian Anchoveta and its Upwelling Ecosystem: Three Decades of Change.* ICLARM Studies and Reviews No. 15. Callao, Peru, IMARPE. 351p.

Polovina, J. J., Mitchum, G. T., Graham, N. E., Craig, M. P., Demartini, E. E., Flint, E. E. (1994) Physical and biological consequences of a climate event in the central North Pacific, Fisheries Oceanography, 3: 5-21.

Regier, H. A., Meisner, J. D. (1990) Anticipated effects of climate change on freshwater fishes and their habitat. *Fisheries (Bull. Amer. Fish. Soc)* 15(6): 10-15.

Robertson, D. S. (1991) Geophysycal applications of very-long baseline interferometry. *Rev. Mod. Phys.* 63: 899-918.

Rosen, R. D., Salstein, D. A. (1983) Variations in atmospheric angular momentum on global and regional scales and the length of day. *J. Geophys. Res.* 88: 5451-5470.

Salstein, D. A., Kann, D. M., Miller, A. J., Rosen, R. D. (1993) The sub-bureau for Atmospheric Angular Momentum of the International Earth Rotation Service: A meteorological Data Center with Geodetic Applications. *Bulletin American Meteorological Society* 74(1): 67-80.

Salstein, D. A., Rosen, R. D. (1986) Earth rotation as a proxy for inter-annual variability in atmospheric circulation. *J. Clim. Appl. Meteor.* 25: 1870-1877.

Schlesinger, M. E., Ramankutty, N. (1994) An oscillation in the global climate system of period 65-70 years. *Nature* 367: 723-726.

Schwartzlose, R. A., Alheit, J., Bakun, A., Baumgasrtner, T., Cloete, R., Crawford, R., Fletcher, W., Green-Ruiz, M. Y., Hagen, E., Kawasaki, T., Lluch-Belda, D., Lluch-Cota, S., MacGall, A., Matsuura, Y., Nevarez-Martinez, M., Parrish, R., Roy, C., Serra, R., Shust, K., Ward, M., Zuzunaga, J. (1999) Worldwide large-scale fluctuations of sardine and anchovy populations. *S. Afr. J. mar. Sci*. 21: 289-347 .

Shackelton, L.Y. (1987) A comparative study of fossil fish scales from three upwelling regions. In *The Benguela and Comparable Ecosystems*. Payne, A.I., Gulland, J.A. and K.H. Brink (Eds). *S. Afr. J. mar. Sci* **5**:79-84.

Sharp, G. D., J., Csirke (ed.) (1984) Proceedings of the Expert Consultation to Examine the Changes in Abundance and Species Composition of Neritic Fish Resources, San Jose, Costa Rica, 18-29 April 1983. *FAO Fish Rep. Ser.* 291, vols. 2-3. 1294p.

Sharp, G.D., Csirke, J., Garcia, S. (1983) Modeling Fisheries: What was the question? pp1177-1224. In: Sharp, G.D., Csirke, J. (ed.) Proceedings of the Expert Consultation to Examine the Changes in Abundance and Species Composition of Neritic Fish Resources, San Jose, Costa Rica. 18-29 April 1983. *FAO Fish. Rep. Ser*. 291, vol. 3.

Sonechkin, D. M. (1998) Climate dynamics as a non-linear Brownian motion. *International Journal of Bifurcation and Chaos* 8(4): 799-803.

Statgraphics (1988) Statistic Graphic System by Statistical Graphic Corporation. Users Guide System. STSK Inc. Publ. 440p.

Stephenson, F. R and Morrison, L. V. (1995) Long-term fluctuations in the Earth's rotation: 700 BC to AD 1990. *Phil. Trans. R. Soc. London* A 351: 165-202.

Trenberth,K.E.,and Hurrell, J.W. (1995) Decadal coupled atmosphere-ocean variation in the North Pacific Ocean. Climate change and northern fish population. In: Beamish, R., (ed.) *Climate change and northern fish fluctuations.* Can. Spec. Publ. Fish. Aquat. Sci. 121: 14-24.

Valdivia, J. (1978) Anchoveta and El Niño. *Rapports Pour-von Reunion de conseil internacionale Exploracion du Mer* 173: 196:202.